INFORMATION TO USERS

RICE UNIVERSITY

Interpretation and Modeling of Slurry Reactor Performance to Provide Monitoring Strategies for the Aerobic Bioremediation of Dinitrotoluene Contaminated Soils

by

Rebecca C. Daprato

A THESIS SUBMITTED
IN PARTIAL FULFILLMENT OF THE
REQUIREMENTS FOR THE DEGREE

Master of Science

APPROVED, THESIS COMMITTEE

Joseph B. Hughes, Chair, Professor
Environmental Science and Engineering

C. Herb Ward, Foyt Family Chair
Environmental Science and Engineering

Phillip B. Bedient, Professor
Environmental Science and Engineering

Houston, Texas

March, 2001

UMI Number: 1405657

UMI®

ABSTRACT

Interpretation and Modeling of Slurry Reactor Performance to Provide Monitoring
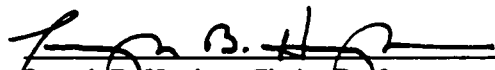Strategies for the Aerobic Bioremediation of Dinitrotoluene Contaminated Soils

By

Rebecca C. Daprato

In a previous study, pilot-scale bioslurry reactors were used to treat soils highly

contaminated with 2,4-dinitrotoluene (2,4-DNT) and 2,6-dinitrotoluene (2,6-DNT). The

treatment scheme involved a soil washing process followed by two sequential aerobic

slurry reactors augmented with DNT mineralizing bacteria. This previous work found

that constant monitoring was necessary to avoid long lag periods upon refeeding.

In this study, it was determined that the heterogeneous distribution of soil in the

reactor deleteriously impacted direct monitoring of DNT concentrations. Instead, the use

of nitrite production or NaOH consumption as surrogate monitoring parameters proved to

be more accurate predictors of reactor performance.

A model was developed to predict the distribution and biodegradation of DNT in

the reactors. Analysis of model results showed that the maximum substrate utilization

rate controlled DNT degradation rates in the reactor, a population shift occurred after

approximately 26 days, and phosphorous was limiting at high solids loading rates.

ACKNOWLEDGEMENTS

I would first like to thank my advisor, Joe Hughes, for his guidance and insights on this project and for knowing how to handle my "anxiousness" during times of stress. Special thanks to Dr. Herb Ward and Dr. Phil Bedient for their service on my committee.

I owe a debt of gratitude to Dr. Chunlong Zhang. Without his assistance and contributions, I could have never completed this work.

I would also like to thank Anthony Holder for increasing my MATLAB knowledge.

The friends that I have made in this department are part of the reason I made it through this agonizing yet wonderful experience. I especially have to thank Stephanie, Jude and Sarah for always knowing when I needed to go and have a beer!

I cannot forget to thank Patrick who has endured the brunt of my stress throughout this process. Know that I would not have made it through this experience without you: thank you.

Last, but not least, I have to thank my family. I would have never made it this far without the love and support of my parents. Thank you for always believing in me and for always being there when I needed you.

TABLE OF CONTENTS

LIST OF FIGURES

LIST OF TABLES

NOTATION AND ABBREVIATIONS USED IN TEXT

Chemical Compounds

2,4-DNT   2,4-dinitrotoluene

2,6-DNT   2,6-dinitrotoluene

TNT   trinitrotoluene

Biological and Engineering Notation

X	biomass concentration (μM)
S	substrate concentration (μM)
K_s	saturation constant ($\mu mol\ S/L$)
k	maximum substrate utilization rate ($\mu mol\ S/\mu mol\ X\ d$)
Y	yield coefficient ($\mu mol\ X/\mu mol\ S$)
k_d	bacterial decay coefficient (d^{-1})
ΔG^0_f	Gibbs free energy of formation
ΔG_n	energy required by bacteria to convert nitrogen source to NH_3 (kcal/eq.)
ΔG_p	energy required by bacteria to convert carbon source to pyruvate (kcal/eq.)
ΔG_c	energy required by bacteria to convert pyruvate and NH_3 to cellular material (kcal/eq.)
ΔG_r	change in Gibbs free energy for the reaction of electron donor and electron acceptor (kcal energy avaliable /eq. electron donor used for energy)
ΔG_s	energy required for cell synthesis (kcal/eq. cells synthesized)
ε	bacterial metabolic efficiency
a_e	cell yield coefficient (eq. cells/eq electron donor)
f_e	fraction of electron donor used for energy
f_s	fraction of electron donor used for cell synthesis

K_{om}	organic matter- water partition coefficient (L/kg OM)
C_{om}	concentration of the chemical associated with the natural organic matter (mol/kg OM)
f_{om}	fraction of the organic matter (kg OM/kg solid)
C_{min}	concentration of the chemical associated with the mineral surface (mol/m^2)
A	area of the mineral surface per mass of solid (m^2/kg solid)
C_{ie}	concentration of ionized chemical associated with charged sites on the solid surface (mol/mol surface charges)
σ_{ie}	net concentration of charged sites on the solid surface (mol surface charges/m^2)
C_{rxn}	concentration of the chemical bonded by reversible reaction to the solid surface (mol/mol rxn sites)
σ_{rxn}	concentration of reactive sites on the solid surface (mol rxn sites/m^2)
$C_{w.neutral}$	concentration of the neutral chemical in solution (mol/L)
$C_{w.ionic}$	concentration of the charged chemical in solution (mol/L)
K_d	soil to water partition coefficient (L/kg soil)

Other

VAAP	Volunteer Army Ammunition Plant
BAAP	Badger Army Ammunition Plant

CHAPTER ONE

INTRODUCTION

Dinitrotoluenes (DNT) are intermediates in the production of the explosive 2,4,6-trinitrotoluene (TNT) and precursors of toluene diisocyanate used for the manufacturing of polyurethane foams. In 1982, the United States accounted for 31% of the worldwide DNT production of 2.3 billion pounds, and in 1999 the largest producer of DNT in the United States expanded its production capacity by 50% to 1.5 billion pounds [1]. Improper handling and disposal techniques of DNT have resulted in contamination of soils and groundwater. Twenty years ago the production of TNT was terminated, but 2,4-DNT and 2,6-DNT remain common contaminants at TNT production facilities [2]. Both 2,4-DNT and 2,6-DNT exhibit acute toxicity and low-level carcinogenicity. The EPA has classified these chemicals as priority pollutants because of their toxicity and abundance in the environment [3, 4]. Therefore, remediation of the contaminated material is required.

Research has been conducted on the metabolism of DNT under both aerobic and anaerobic conditions to determine the potential for bioremediation as a treatment option [2]. These studies have shown that DNT is cometabolized and that mineralization does not occur under anaerobic conditions [5,6,7]. Under aerobic conditions, it has been shown that DNT can serve as a carbon and energy source for microbial growth and complete mineralization occurs [8,9,10,11]. Therefore, the focus of remediation technologies using bioremediation has been under aerobic conditions. Applications of bioremediation to contaminated soils include aerobic fluidized bed biofilm reactors [12,13], fixed-bed reactors [14] and slurry-phase bioreactors [15].

The work that forms the foundation of this research is the study performed by Zhang et. al. [15],which used a pilot scale aerobic bioslurry reactor to treat soils highly contaminated with 2,4-DNT and 2,6-DNT. The test soils used in this work were obtained from two former army ammunition plants, the Volunteer Army Ammunition Plant (VAAP) and the Badger Army Ammunition Plant (BAAP). The treatment scheme involved a soil-washing process followed by two sequential aerobic slurry reactors augmented with DNT-degrading bacteria. This study demonstrated that high concentrations of 2,4-DNT and 2,6-DNT could be rapidly degraded in sequential aerobic slurry reactors. This study also established that constant monitoring of this type of reactor system is necessary to avoid long lag phases caused when the reactors were allowed to fully deplete DNT.

Current research is focused on determining monitoring parameters that are accurate in predicting microbial activity in the bioslurry reactor and mathematical modeling DNT partitioning and biodegradation in the aerobic slurry bioreactor. Accurate monitoring parameters are necessary to prevent loss of bacterial activity in the reactor, which can result in long periods of down time for the system and reinoculation of the reactor. Modeling the fate of DNT in the reactor system should allow for quantitative prediction of process performance needed for full-scale implementation of this technology. Currently, there is a full-scale bioreactor designed for us at the Badger Army Ammunition Plant in Baraboo, Wisconsin to treat 2,4-DNT and 2,6-DNT contaminated soils. This research will aid in the design of full-scale remediation systems by providing a tested decision making tool. Specifically the objectives of this work were:

1. Determine the effectiveness of the soil washing procedure.

2. Evaluate the use of DNT concentrations in the bioslurry reactor as accurate monitoring parameters for the aerobic bioslurry reactors.

3. Compare other surrogate monitoring parameters for the aerobic bioslurry reactors that could be accurate in predicting microbial activity and DNT degradation.

4. Use thermodynamic calculations to determine the biological stoichiometry of DNT biodegradation.

5. Determine the bacterial kinetic coefficients for the DNT-degraders used in the bioslurry reactors.

6. Develop a model that accurately predicts the partitioning and biodegradation of DNT in the bioslurry reactor.

The format of this thesis is as follows: background information necessary to this research and a review of related work is presented in Chapter 2; Chapter 3 details the materials and methods used in this research; a detailed summary of the work that forms the basis for this study is given in Chapter 4; Chapter 5 outlines the model development; presented in Chapter 6 is a manuscript submitted to the *Journal of Hazardous Materials* (January 2001); the results from the modeling are shown in Chapter 7; Chapter 8 summarizes the general conclusions drawn from this work; and engineering significance and suggestions for further research are offered in Chapter 9 and 10, respectively.

References

1. Nishino, S.F., J.C. Spain, and Z. He, *Strategies for Aerobic Degradation of Nitroaromatic Compounds by Bacteria: Process Discovery to Field Application*, in *Biodegradation of Nitroaromatic Compounds and Explosives*, J.C. Spain, J.B. Hughes, and H.-J. Knackmuss, Editors. 2000, Lewis: Boca Raton. p. 7-61.

2. Spain, J.C., *Bacterial Degradation of Nitroaromatic Compounds Under Aerobic Conditions*, in *Biodegradation of Nitroaromatic Compounds*, J.C. Spain, Editor. 1995, Plenum Press: New York. p. 19-35.

3. Keith, L.H. and W.A. Telliard, Priority pollutants: I. A perspective view. *Environ. Sci. Technol.*, 1979. **13**: p. 416-423.

4. Rickert, D.E., B.E. Butterworth, and J.A. Popp, *Dinitrotoluene: Acute toxicity, oncogenicity, genotoxicity, and metabolism.* 1984, Washington, DC: Hemisphere. 53-60.

5. Hughes, J.B., C.Y. Wang, and C. Zhang, Anaerobic biotransformation of 2,4-dinitrotoluene and 2,6-dinitrotoluene by Clostridium acetobutylicum: a pathway through dihydroxylamino intermediates. *Environ. Sci. Technol.*, 1999. **33**: p. 1065-1070.

6. Noguera, D.R. and D.L. Freedman, Reduction and Acetylation of 2,4-Dinitrotoluene by a Pseudomonas aeruginosa Strain. *Appl. Environ. Microbiol.*, 1997. **62**: p. 2257-2263.

7. Bradley, P.M., *et al.*, Microbial Transformation of Nitroaromatics in Surface Soils and Aquifer Materials. *Appl. Environ. Microbiol.*, 1994. **60**: p. 2170-2175.

8. Nishino, S.F., G.C. Paoli, and J.C. Spain, Aerobic Degradation of Dinitrotoluenes and Pathway for Bacterial Degradation of 2,6-Dinitrotoluene. *Appl. Environ. Microbiol.*, 2000. **66**(5): p. 2139-2147.

9. Spanggord, R.J., *et al.*, Biodegradation of 2,4-Dinitrotoluene by a Pseudomonas sp. *Appl. Environ. Microbiol.*, 1991. **57**(11): p. 3200-3205.

10. Haigler, B.E., S.F. Nishino, and J.C. Spain, Biodegradation of 4-Methyl-5-Nitrocatechol by Pseudomonas sp. Strain DNT. *J. Bacteriol.*, 1994. **176**(11): p. 3433-3437.

11. Nishino, S.F., *et al.*, Mineralization of 2,4- and 2,6-Dinitrotoluene in Soil Slurries. *Environ. Sci. Technol.*, 1999. **33**: p. 1060-1064.

12. Lendenmann, U., J.C. Spain, and B.F. Smets, Simultaneous Biodegradation of 2,4-Dinitrotoluene and 2,6-Dinitrotoluene in an Aerobic Fluidized-Bed Biofilm Reactor. *Environ. Sci. Technol.*, 1998. **32**: p. 82-87.

13. Smets, B.F., *et al.*, Kinetic Analysis of Simultaneous 2,4-Dinitrotoluene (DNT) and 2,6-DNT Biodegradation in an Aerobic Fluidized-Bed Biofilm Reactor. *Biotechnol. Bioeng.*, 1999. **63**(6): p. 642-653.

14. Heinze, L., M. Brosius, and U. Wiesmann, Biological Degradation of 2,4-Dinitrotoluene in a Continuous Bioreactor and Kinetic Studies. *Acta Hydrochim. Hydrobio.*, 1995. **23**(6): p. 254-263.

15. Zhang, C., *et al.*, Slurry-Phase Biological Treatment of 2,4-Dinitrotoluene and 2,6-Dinitrotoluene: Role of Bioaugmentation and Effects of High Dinitrotoluene Concentrations. *Environ. Sci. Technol.*, 2000. **34**(13): p. 2810-2816.

CHAPTER TWO

BACKGROUND AND LITERATURE REVIEW

This chapter is organized into two sections: background information and literature review. The purpose of the background information is to provide details on the production of dinitrotoluenes, specifically 2,4-dinitrotoluene (2,4-DNT) and 2,6-dinitrotoluene (2,6-DNT), and on the properties of these substances that are important to this research. The background section of this chapter begins with a description of the synthesis of 2,4-DNT and 2,6-DNT and then shows the extent of contamination in the United States. The next section provides details on some of the bacteria that are capable of degrading 2,4-DNT and 2,6-DNT and shows the metabolic pathways by which 2,4-DNT and 2,6-DNT are degraded. The literature review section begins with a discussion of the concept of biological kinetics and stoichiometry, which is applied to the bacteria used in this work. The final section of the literature review chapter gives an overview of the sorption characteristics of dinitrotoluenes. The kinetics and biological stoichiometry for the bacteria and the sorption characteristics of DNTs are important when modeling the fate and transport of DNT in a bioslurry reactor.

2.0.0 Background

2.0.1 Synthesis of 2,4-dinitrotoluene and 2,6-dinitrotoluene

Dinitrotoluenes are intermediates in the production of trinitrotoluene (TNT). TNT is synthesized from toluene in a step nitration process, depicted in Figure 2.1. The first nitration produces 2-nitrotoluene and 4-nitrotoluene in equal amounts. The second nitration produces 76% 2,4-DNT, 19% 2,6-DNT [1], and 5% other
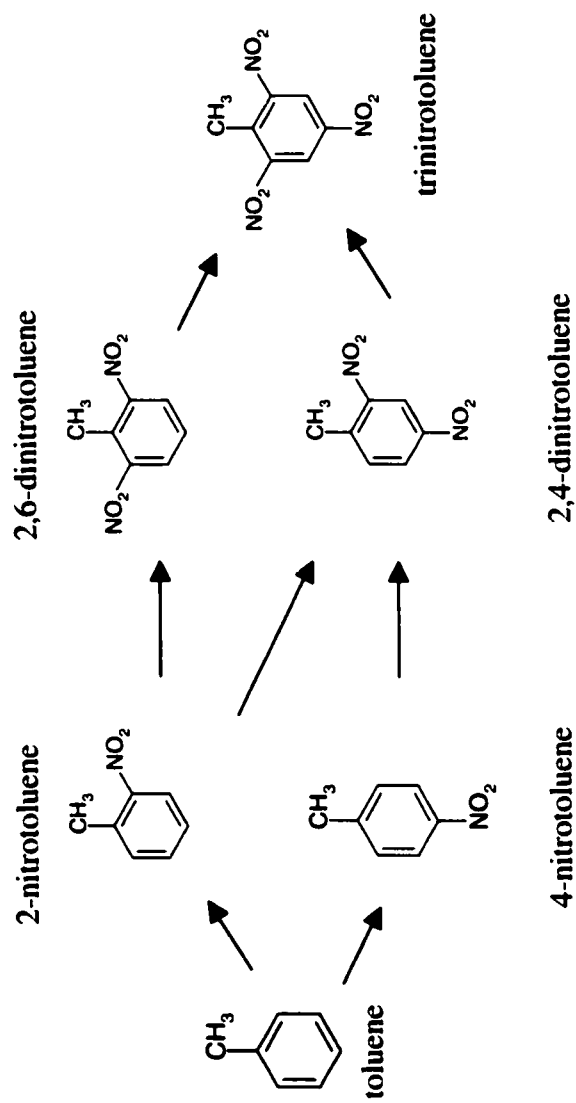
Figure 2.1. TNT production by a three step nitration of toluene[1].

isomers. The third nitration produces TNT, from 2,4-DNT and 2,6-DNT[2].

Due to safety considerations, TNT manufacturing facilities were placed in remote areas with each nitration step occurring in separate buildings. TNT is no longer manufactured in the United States, but because it was manufactured for more than 65 years, DNT contamination is wide spread. Figure 2.2 shows a map with most of the explosive-contaminated manufacturing, processing, and storage sites in the United States [3]. Today, DNT is an important industrial chemical that is used as a precursor to toluene diisocyanate used in the production of polyurethane foams[1]. However, environmental release of DNT is rare in current industrial processes[2].

2.0.2 Aerobic degradation of 2,4-dinitrotoluene and 2,6-dinitrotoluene

The study of the degradation of DNT has been ongoing for more than 20 years, but only recently have bacteria capable of degrading 2,4-DNT and 2,6-DNT been isolated. Strains that grow on single DNT isomers have been isolated from contaminated systems worldwide, and strains capable of using 2,4-DNT and 2,6-DNT as sole carbon, nitrogen, and energy sources have been isolated from bioreactors receiving mixtures of DNT isomers[4, 5]. Select bacterial strains that degrade either 2,4-DNT or 2,6-DNT are listed in Table 2.1 [5].

Burkholderia sp. strain DNT was one of the first 2,4-DNT-degrading bacteria isolated [6]. Since that time, more than 30 strains that degrade 2,4-DNT have been isolated from soils and surface water that are contaminated with DNT[5]. All of the new strains isolated use the same pathway as
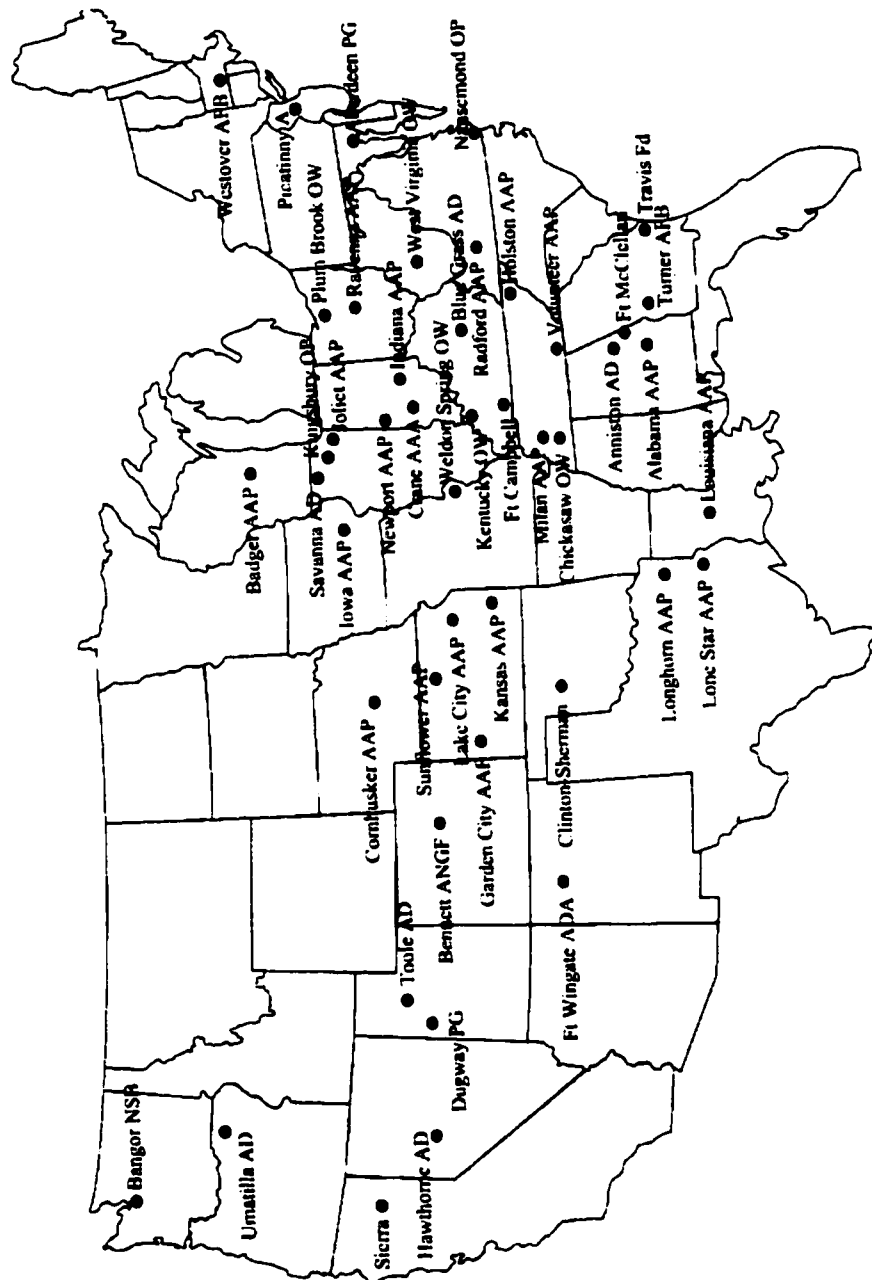
Figure 2.2. Explosive-contaminated manufacturing, processing, and storage sites in the United States of America: A, Arsenal; AAP, Army Ammunition Plant; AD, Army Depot; AFB, Air Force Base; ANGF, Air National Guard Field; NSB, Naval Submarine Base; OW, Ordnance Works, and PG, Proving Ground [3].

TABLE 2.1. Identification of selected DNT-degrading strains [5].

Strain	Identification		Source[a]; yr isolated	DNT isomer degraded
	16S rDNA	Biolog		
R34	*Burkholderia cepacia*	*Psudeomonas sp*	1;1992	2,4
PR7	*Burkholderia cepacia*	*Psudeomonas sp*	1;1992	2,4
JS850	*Burkholderia cepacia*	None	3;1995	2,6
JS863	*Hydrogenophaga palleronii*	None	2;1995	2,6
JS867	*Alcaligenes sp.*	*Alcaligenes denitrificans*	2;1995	2,4
JS871	*Alcaligenes sp.*	*Alcaligenes xylosoxidans*	2;1995	2,4
JS872	*Burkholderia cepacia*	*Psudeomonas cepacia*	2;1995	2,4
JS881	*Psudeomonas putida*	*Psudeomonas sp*	1;1992	2,6

[a] Source: 1, Radford Army Ammunition Plant, soil and surface water; 2, Volunteer Army Ammunition Plant, soil and surface water; 3, West Virginia, activated sludge

Burkholderia sp. strain DNT, but the lag phase for the pathway is much shorter in strains JS872, PR7, and R34. None of the 2,4-DNT isolates are capable of growth on 2,6-DNT, and none of the 2,6-DNT isolates are capable of growth on 2,4-DNT[5].

The 2,4-DNT degradative pathway was determined in *Burkholderia* sp. Strain DNT and is shown in Figure 2.3a [7]. An initial dioxygenase attack at the 4-nitro position converts 2,4-DNT to 4-methyl-5-nitrocatechol with the release of nitrite[6]. A monooxygensase attack at the remaining nitro position converts 4-methyl-5-nitrocatechol to 2-hydroxy-5-methylquinone with the release of nitrite[7]. 2-hydroxy-5-methylquinone is then converted to 2,4,5-trihydroxytoluene by a quinone reductase in a reaction requiring NADH. The product of the 2,4,5-trihydroxytoluene ring cleavage is unstable, but properties of the purified ring cleavage enzyme and genetic evidence strongly indicate that 2,4,5-trihydroxytoluene undergoes *meta*-ring fission catalyzed by an extradoil dioxygenase[8].

The 2,6-DNT and 2,4-DNT pathways are very different except for the initial step. As with the 2,4-DNT pathway, an initial diooxygenase attack transforms 2,6-DNT with the release of nitrite, but in this case, the product is 3-methyl-4-nitrocatechol (Figure 2.3b). 3-methyl-4-nitrocatechol then undergoes a *meta*-ring cleavage catalyzed by a catechol-2,3-dioxygenase to produce 2-hydroxy-5nitro-6oxohepta-2,4-dienoic acid. A partially purified hydrolayse converts 2-hydroxy-5nitro-6oxohepta-2,4-dienoic acid to 2-hydroxy-5-nitropenta-2,4-dienoic acid. The remaining nitro group is released in subsequent reactions that have not been characterized[5].
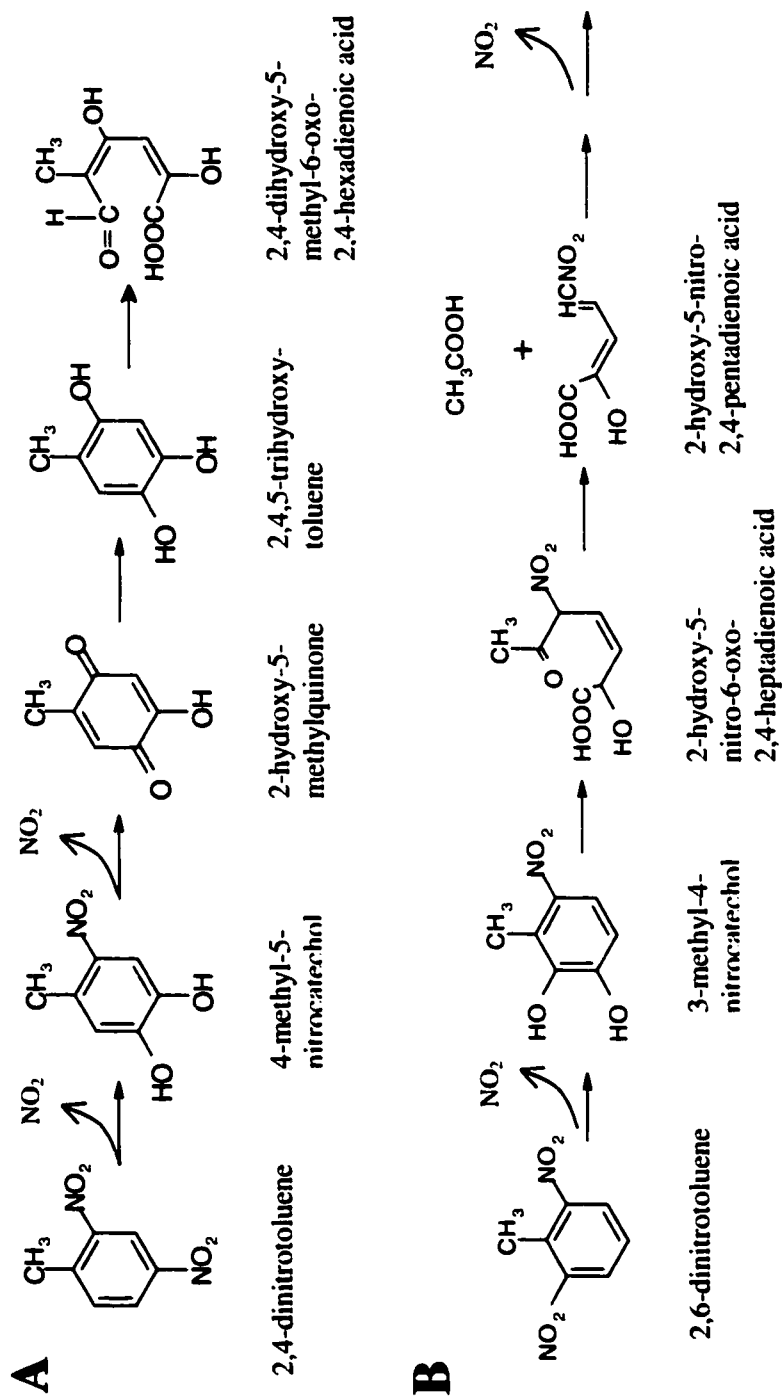
Figure 2.3. Degradation pathways for 2,4-dinitrotoluene (A) and 2,6-dinitrotoluene (B) [2].

At many TNT production facilities, DNT contamination contains both 2,4-DNT and 2,6-DNT, and the presence of both isomers of DNT can have inhibition impacts on the biodegradability of individual DNT compounds. In some strains of 2,4-DNT degrading bacteria, 2,4-DNT degradation is inhibited by 2,6-DNT concentrations as low as 100 μM [2, 5]. Conversely, 2,6-DNT degradation is inhibited only by high concentrations of 2,4-DNT [2]. Nitrite is also inhibitory to 2,4-DNT-degrading strains at concentrations above approximately 20 mM and is toxic to Burkholderia sp. Strain DNT at concentrations above 10 mM. 2,6-DNT-degrading strains appear to be unaffected by nitrite concentrations above 20 mM[2].

2.1.0 Literature Review

2.1.1 Kinetics and Biological Stoichiometry

Bacterial growth results when physicochemical conditions in an environment are favorable. The growth of bacteria under favorable conditions can be described by a growth curve as shown in Figure 2.4. The growth curve displays the distinct stages of a growth cycle: 1) lag phase, 2) exponential growth phase, 3) stationary phase, and 4) decay phase.

The lag phase occurs directly after inoculation or after a change in environmental conditions and is a period of acclamation of the cells to their new environment. In the exponential phase, the cells have adjusted to their new environment, and are multiplying rapidly. The stationary phase occurs when the cells have exhausted substrate or nutrients, and the net growth of the cells is zero. Finally, the decay phase is a period of cell death that occurs directly after the stationary phase [9].
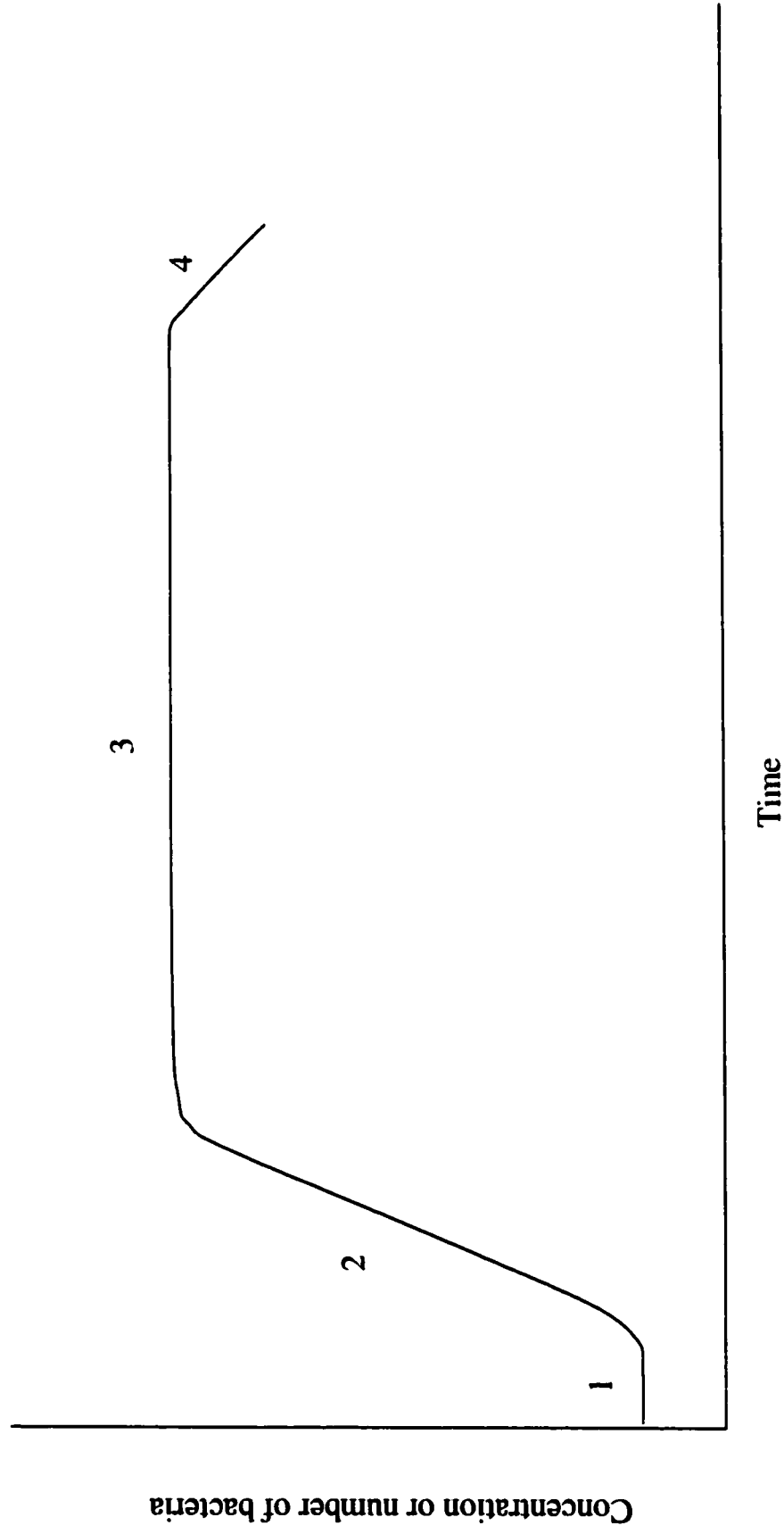
Figure 2.4. Bacterial growth curve with distinct stages of a growth cycle: 1) lag phase 2) exponential phase, 3) stationary phase, 4) decay phase.

This type of cell growth is best described by Monod kinetics. The Monod equation is shown below in Equation 2.1.

$$\frac{d[S]}{dt} = -\frac{k[S][X]}{K_s + [S]} \qquad (2.1)$$

The Monod equation is semi-empirical and is derived from the assumption that the amount of enzyme or its catalytic activity is sufficiently low to be growth rate limiting, and that a single enzyme system with Michaelis-Menten kinetics is responsible for the uptake of the substrate[9]. Combining the Monod equation with a growth equation gives Equation 2.2.

$$\frac{d[X]}{dt} = Y\left(\frac{k[S][X]}{K_s + [S]}\right) - k_d[X] \qquad (2.2)$$

This equation is only valid for batch systems and does not describe the lag phase.

In the equations above, S is the substrate concentration (μM), X is the biomass concentration (μM), and K_s, k, Y, and k_d are all kinetic coefficients. The coefficient K_s is known as the saturation constant and is equal to the concentration of the rate limiting substrate when the specific growth rate is equal to one-half the maximum (μmol S/L) [9]. The coefficient k is the maximum substrate utilization rate (μmol S/μmol X d). Y is the yield coefficient for the bacteria and is defined as the amount of cells produced per amount of substrate utilized, and k_d is the decay coefficient for the cells (time^{-1}). These kinetic coefficients can be affected by several environmental factors such as temperature, pH, and amount of dissolved oxygen.

Kinetic coefficients can be determined using chemostat studies, but to date these tests have not been performed for DNT-degrading bacteria. Kinetic coefficients have been determined from two reactor studies done by Smets[10] and Heinze[11]. The first

study was performed in an aerobic fluidized-bed reactor, where k and K_s were determined

for both 2,4-DNT and 2,6-DNT using a mechanistic mathematical biofilm model[10].

The reported values for k were 0.83 to 0.98 g DNT/g X•COD•d for 2,4 –DNT removal

and 0.14 to 0.33 g DNT/g X•COD•d for 2,6-DNT removal. K_s values for 2,4-DNT

removal were 0.029 to 0.36 g DNT/m^3 and for 2,6-DNT removal were 0.21 to 0.84 g

DNT/m^3[10].

The second study examined a batch culture to determine the kinetic coefficients

[11]. From these batch experiments, a yield coefficient of 0.30 ± 0.05 g X/g DNT was

reported. Experimental data from the batch experiments were fitted to the Monod

equation, which produced K_s = 0.01 to 0.03 mmol/L [11].

Kinetic coefficients can also be predicted using thermodynamics. Rittman and

McCarty [12] describes a method that uses the change in Gibbs Free Energy (ΔG) for

given biological reactions to predict the true yield coefficient. In order to determine the

change in the Gibbs Free Energy for biological reactions, the half reactions must be

determined.

All biological reactions consist of two components, one for synthesis and one for

energy. The synthesis reaction describes the production of cell material, while the energy

reaction is coupled with the utilization of a terminal electron acceptor. Therefore, in

order to determine the stoichiometry for a specific biological reaction, half-reactions for

the electron acceptor (R_{ea}), the electron donor (R_{ed}), and cell material (R_{bg}) are used. The

half-reactions are written on an equivalent basis and the sum of the half reactions gives

the overall stoichiometric equation (R) shown below[13].

$$R = R_{ed} - f_e R_{ea} - f_s R_{bg} \qquad (2.3)$$

where

$$f_e + f_s = 1.0 \qquad (2.4)$$

The term f_e represents the fraction of the electron donor that is used for energy, and fs represents the fraction that is used for synthesis.

For DNT, the half reactions and ΔG values are shown below.

kcal/eq

$$R_{ed} = \frac{1}{32} C_7 H_6 O_4 N_2 + \frac{7}{16} H_2 O \rightarrow \frac{7}{32} CO_2 + \frac{1}{16} NO_2^- + \frac{17}{16} H^+ + e^- \qquad \text{-0.234}$$

$$R_{ea} = \frac{1}{4} O_2 + H^+ + e^- \rightarrow \frac{1}{2} H_2 O \qquad \text{18.675}$$

$$R_{bg} = \frac{1}{26} C_5 H_7 O_2 N + \frac{10}{26} H_2 O \rightarrow \frac{1}{26} NO_2^- + \frac{5}{26} CO_2 + \frac{27}{26} H^+ + e^- \qquad \text{N/A}$$
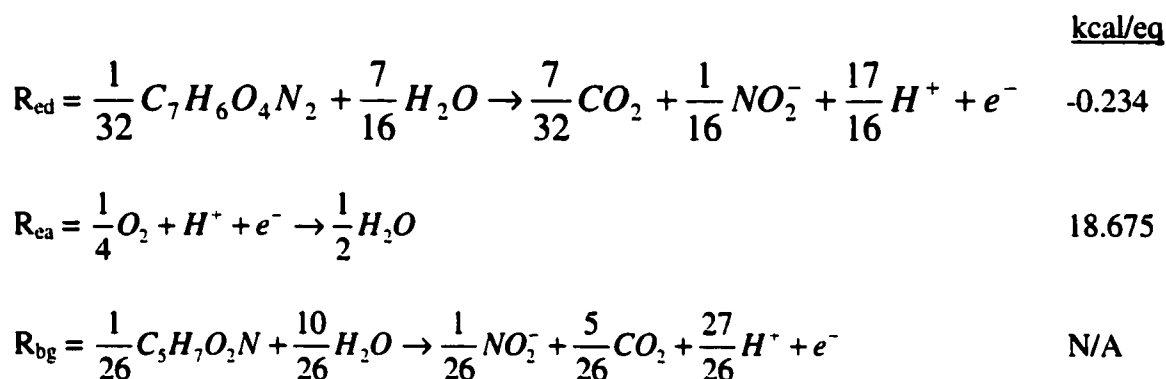
The ΔG value for the DNT reaction shown above is not a published value, but was calculated using the G_f' for each constituent of the reaction. The first step in calculating the ΔG was to determine the free energy of formation G_f' for DNT. This was done using an estimation technique based on the molecular structure of DNT. Estimations of the contributions for several atomic groups have been published. The estimated values for the DNT groups are listed in Table 2.2. These values are used with Equation 2.5 to predict the G_f' for a compound [14]. Once the G_f' was determined for DNT, the ΔG of the reaction was determined using the G_f' for the components of the reaction which are listed in Table 2.3.

$$G_{f 298}' = 53.88 + \sum_{i+1}^{n} N_i \Delta G_i \qquad (2.5)$$

In the thermodynamic approach, the true yield coefficient is the amount of bacteria produced per amount of substrate used. The mathematical description of the true yield

Table 2.2. Atomic Group Contributions to Estimate ΔG_{f298} for DNT. [15] [16]

Atomic Group	ΔG (kcal/mol)
=CH (aromatic)	8.6
=C (aromatic)	1.1
-NO$_2$	6.9
-CH$_3$	8.5

Table 2.3. Free Energies of Formation $G^0{}_f$. [17]

Compound	G_f° (kcal/mol)
CO$_2$	-94.32
H$_2$O	-56.60
H$^+$	-9.5
NO$_2^-$	-8.91
C$_7$H$_6$N$_2$O$_4$	30.90

coefficient is shown in Equation 2.6. In order to determine a_e (equivalent cells/equivalent

electron donor),

$$a_e = \frac{f_s}{f_s + f_e} = \frac{1}{1 + \frac{f_e}{f_s}} = \frac{1}{1 + A} \qquad (2.6)$$

the term A (equivalent electron donor used for energy/equivalent cells synthesized) must

be known. This term can be calculated from an energy balance on the metabolism of the

bacteria. Bacteria metabolism is not 100% efficient because some energy loss occurs in

the transfer reactions, so it is assumed 60% efficient [12], which is described below by ε.

The energy balance on a bacterium can be expressed as

Total energy available for synthesis – Energy lost = Energy consumed

Substituting in the values for these expressions gives Equation 2.7, from which A can be

determined, as shown in Equation 2.8

$$A(\Delta G_r) - (1 - \varepsilon)A(\Delta G_r) = \Delta G_s \qquad (2.7)$$

$$A = \frac{\Delta G_s}{\varepsilon \Delta G_r} \qquad (2.8)$$

where

$$\Delta G_r = \frac{\text{kcal energy avaliable}}{\text{equivalent - e}^- \text{ donor used for energy}}$$

$$\Delta G_s = \frac{\text{kcal energy required}}{\text{equivalent cells synthesized}}.$$

ΔG_r is calculated from the change in Gibbs Free energy for R_{ea} and R_{ed}, which is –

18.909 kcal/equiv. ΔG_s is made up of three components: 1) ΔG_n, 2) ΔG_p, and 3) ΔG_c.

ΔG_n is the energy required to convert the nitrogen source to NH_3. In this case, the

nitrogen source is NO_2^-, so the value of $\Delta G_n = 3.25$ kcal/equiv. ΔG_p is the energy

required to convert the carbon source to pyruvate. The carbon source in this study is an organic electron donor; therefore, $\Delta G_p = 8.31$ kcal/equiv. ΔG_c is the energy required to convert pyruvate and NH_3 to cellular material, which is 7.5 kcal/equiv. Including the metabolic efficiency (ϵ) discussed above, ΔG_s can be defined as shown in Equation 2.9.

$$\Delta G_s = \frac{\Delta G_p}{\epsilon} + 7.5 + \frac{\Delta G_n}{\epsilon} = 26.8 \text{ kcal/equiv} \tag{2.9}$$

Using the calculated values for ΔG_s and ΔG_r and Equation 2.6, a_e is 0.298. This can then be used to predict the true yield coefficient, which is defined by Equation 2.10.

$$Y = \frac{a_e}{1.84} = 0.16 \text{ g X/g COD} = 0.23 \text{ g X/g DNT} \tag{2.10}$$

This yield coefficient matches very well with the one determined by Heinze ([11]).

Another method of relating substrate utilization to biomass production is through biological stoichiometry. Biological stoichiometry is very similar to the stoichiometry used for chemical reactions, except that bacterial growth is added to the equation. This type of stoichiometry provides a simple system for keeping track of reactants and products.

Equation 2.3 can be used to determine the overall balanced stoichiometric equation for the biodegradation of DNT, but the values of f_s and f_e must be known. These values can be calculated from the value of A, as shown in Equation 2.11.

$$f_s = \frac{1}{1+A} \text{ or } f_e = 1 - f_s = \frac{A}{1+A} \tag{2.11}$$

Using this equation, $f_s = 0.298$ and $f_e = 0.702$. Applying these values with the half reactions shown on page 17 to Equation 2.3, the following balanced stoichiometric equation was obtained.

$$C_7H_6N_2O_4 + 5.62\,O_2 \rightarrow$$
$$1.63\,H^+ + 0.90\,H_2O + 1.63\,NO_2^- + 0.37\,C_5H_7O_2N + 5.17\,CO_2 \tag{2.12}$$
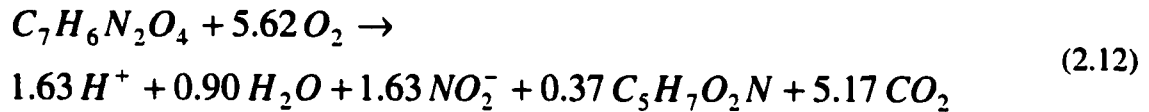
Both the stoichiometric equation and the kinetic equations and parameters developed in this section will be important in modeling DNT in the bioslurry reactors. The kinetic equations and parameters will be used to determine the rate at which DNT is depleted by the bacteria and to predict the rate of bacterial growth. The stoichiometric coefficients can be used to predict the rate and the amount of the other products and reactants in Equation 2-12.

2.1.2 Sorption Properties of 2,4-DNT and 2,6-DNT

The process of a chemical becoming associated with a solid phase is called sorption, which is described by a partition coefficient. This partition coefficient is a ratio of the concentration of the chemical on the solid phase to the concentration of the chemical in the aqueous phase. The concentration of the chemical on the solid phase is a function of the type of sorption the chemical undergoes. Depending on the structure of the compound, on the types and relative abundance of the solids present in the environment, and on solution conditions, a chemical can sorb by many different sorption mechanisms. The partition coefficient and the sorption mechanisms are described below in Equation 2.13 [18].

$$K_d = \frac{C_s}{C_w} = \frac{C_{om}f_{om} + C_{min}A + C_{ie}\sigma_{ie}A + C_{rxn}\sigma_{rxn}A}{C_{w,neutral} + C_{w,ionic}} \tag{2.13}$$

where

C_{om} is the concentration of the chemical associated with the natural organic matter,
f_{om} is the weight fraction of the organic matter,
C_{min} is the concentration of the chemical associated with the mineral surface,
A is the area of the mineral surface per mass of solid,
C_{ie} is the concentration of ionized chemical associated with charged sites on the solid surface,
σ_{ie} is the net concentration of charged sites on the solid surface,
C_{rxn} is the concentration of the chemical bonded by reversible reaction to the solid surface,
σ_{rxn} is the concentration of reactive sites on the solid surface,
$C_{w,neutral}$ is the concentration of the neutral chemical in solution, and
$C_{w,ionic}$ is the concentration of the charged chemical in solution.

For the case of polynitroaromatic chemicals, such as 2,4-DNT and 2,6-DNT, two types of sorption mechanisms are possible. The first is adsorption due to specific interactions with clay mineral surfaces bearing exchangeable NH_4^+ or K^+ cations. The second sorption mechanism is partitioning into the organic matter, since both 2,4-DNT and 2,6-DNT are both neutral hydrophobic compounds.

Adsorption of nitroaromatic compounds to clay mineral surfaces of soils is the major sorption mechanism, if the fraction of organic matter in the soil is less than 10^{-3} kg_{om}/kg_{soild}[19]. Nitroaromatic compounds sorb to these mineral surfaces by forming electron donor-acceptor complexes with the oxygens of the siloxane planes of clays[20]. This type of sorption can occur because the nitro group is a strong π-acceptor and is able to form coplanar complexes with suitable electron donors [21]. Significant sorption of nitroaromatic compounds is observed in the presence of weakly hydrated cations such as K^+ and NH_4^+, but strongly hydrated cations such as H^+, Na^+, and Ca^{2+} can prevent the n-π EDA interaction [19].

Several studies have been performed to determine the extent of the adsorption of nitroaromatic compounds to clay minerals. Haderlein *et. al.* tested three different clay

minerals, and found that the affinity and the adsorption capacity of the clay for

nitroaromatic compounds increase in the order kaolinite < illite < montmorillonite in

aqueous systems [19]. Haderlein *et. al.* also determined the adsorption constants for

homoionic K^+-montmorillonite for 2,4-DNT and 2,6-DNT were 7400 L/kg and 125 L/kg,

respectively.

Weissmahr et. al. determined that electron donor-acceptor complexes can only be

formed with phyllosilicates [20]. It has also been shown that the structure of

nitroaromatic compounds greatly affect their ability to form electron donor-acceptor

complexes [21]. If a nitroaromatic compound is planar with an electron deficient π-

system due to several electron-with-drawing and electron-delocalizing substituents, it will

show the highest adsorption. The adsorption of nitroaromatic compounds decreases if

they contain an alkyl, halogen, or nitro group in the ortho position because the

compounds lose their coplanarity.

If the fraction of organic matter in a soil is greater than 10^{-3} kg_{om}/kg_{soild}, sorption

of the nitroaromatic to the organic matter is the major sorption mechanism. This type of

partitioning can be described by an organic matter-water partition coefficient K_{om}. This

partition coefficient is a ratio of the concentration of the chemical in the organic matter

C_{om} to the concentration of the neutral chemical in the aqueous phase C_w.

$$K_{om} = \frac{C_{om}}{C_w} \qquad (2.14)$$

K_{om} is related to the overall partition coefficient K_d by the fraction organic matter in the

soil (f_{om}), as shown in Equation 2.15.

$$K_d = K_{om} f_{om} \qquad (2.15)$$

Both soils used in this study have a fraction of organic matter greater than 10^{-3}

kg_{om}/kg_{soild}. Therefore, sorption of the DNTs to the organic matter will be the dominant

form of adsorption. There has been no development of a method to predict K_d for

sorption for nitroaromatics, so the K_d used in this study was determined experimentally.

References

1. Hartter, D.R., *The Use and Importance of Nitroaromatic Chemicals in the Chemical Industry*, in *Toxicity of Nitroaromatic Compounds*, D.E. Rickert, Editor. 1985, Hemisphere: Washington D.C. p. 1-13.

2. Nishino, S.F., J.C. Spain, and Z. He, *Strategies for Aerobic Degradation of Nitroaromatic Compounds by Bacteria: Process Discovery to Field Application*, in *Biodegradation of Nitroaromatic Compounds and Explosives*, J.C. Spain, J.B. Hughes, and H.-J. Knackmuss, Editors. 2000, Lewis: Boca Raton. p. 7-61.

3. Spain, J.C., *Introduction*, in *Biodegradation of Nitroaromatic Compounds and Explosives*, J.C. Spain, J.B. Hughes, and H.-J. Knackmuss, Editors. 2000, Lewis Publishers: Boca Raton. p. 3.

4. Nishino, S.F., et al., Mineralization of 2,4- and 2,6-Dinitrotoluene in Soil Slurries. *Environ. Sci. Technol.*, 1999. **33**: p. 1060-1064.

5. Nishino, S.F., G.C. Paoli, and J.C. Spain, Aerobic Degradation of Dinitrotoluenes and Pathway for Bacterial Degradation of 2,6-Dinitrotoluene. *Appl. Environ. Microbiol.*, 2000. **66**(5): p. 2139-2147.

6. Spanggord, R.J., et al., Biodegradation of 2,4-Dinitrotoluene by a Pseudomonas sp. *Appl. Environ. Microbiol.*, 1991. **57**(11): p. 3200-3205.

7. Haigler, B.E., S.F. Nishino, and J.C. Spain, Biodegradation of 4-Methyl-5-Nitrocatechol by Pseudomonas sp. Strain DNT. *J. Bacteriol.*, 1994. **176**(11): p. 3433-3437.

8. Haigler, B.E., et al., Biochemical and Genetic Evidence for *meta*-Ring Cleavage of 2,4,5-Trihydroxytoluene in *Burkholderia* sp. Strain DNT. *J. Bacteriol.*, 1999. **181**(3): p. 965-972.

9. Schuler, M.L. and F. Kargi, *Bioprocess Engineering: Basic Concepts*. 1992, Englewood Cliffs, New Jersey: Prentice-Hall, Inc. 148-172.

10. Smets, B.F., et al., Kinetic Analysis of Simultaneous 2,4-Dinitrotoluene (DNT) and 2,6-DNT Biodegradation in an Aerobic Fluidized-Bed Biofilm Reactor. *Biotechnol. Bioeng.*, 1999. **63**(6): p. 642-653.

11. Heinze, L., M. Brosius, and U. Wiesmann, Biological Degradation of 2,4-Dinitrotoluene in a Continuous Bioreactor and Kinetic Studies. *Acta Hydrochim. Hydrobio.*, 1995. **23**(6): p. 254-263.

12. Rittmann, B.E. and P.L. McCarty, *Environmental Biotechnology: Principles and Applications*. 2001, New York: McGraw-Hill.

13.   Grady, C.P.L. and H.C. Lim, *Biological Wastewater Treatment: Theory and Applications*. Pollution Engineering and Technology, ed. P.N. Cheremisinoff. Vol. 12. 1980, New York: Marcel Dekker, Inc. 290-294.

14.   Perry, R.H. and D.W. Green, eds. *Perry's Chemical Engineers' Handbook*. Seventh ed. . 1997, McGraw-Hill: New York. 2-348 - 2-349.

15.   Mavrovouniotis, M.L., Group Contributions for Estimating Standard Gibbs Free Energies of Formation of Biochemical Compounds in Aqueous Solutions. *Biotechnol. Bioeng.*, 1990. **36**: p. 1070-1082.

16.   Shelly, M.D., *et al.*, Thermodynamic Analysis of Trinitrotoluene Biodegradation and Mineralization Pathways. *Biotechnol. Bioeng.*, 1996. **50**: p. 198-205.

17.   Brock, T.D. and M.T. Madigan, *Biology of Microorganisms*. 6 ed. 1991, Englewood Cliffs: Prentice Hall. 827.

18.   Schwartzenbach, R.P., P.M. Gshwend, and D.M. Imboden, *Environmental Organic Chemistry*. 1993, New York: John Wiley & Sons, Inc. 255-275.

19.   Haderlein, S.B., K.W. Weissmahr, and R.P. Schwartzenbach, Specific Adsorption of Nitroaromatic Explosives and Pesticides to Clay Minerals. *Environ. Sci. Technol.*, 1996. **30**: p. 612-622.

20.   Weissmahr, K.W., S.B. Haderlein, and R.P. Schwartzenbach, Complex Formation of Soil Minerals with Nitroaromatic Explosives and other pi-Acceptors. *Soil Sci. Soc. Am. J.*, 1998. **62**: p. 369-378.

21.   Haderlein, S.B., T.B. Hofstetter, and R.P. Schwartzenbach, *Subsurface Chemistry of Nitroaromatic Compounds*, in *Biodegradation of Nitroaromatic Compounds and Explosives*, J.C. Spain, J.B. Hughes, and H.-J. Knackmuss, Editors. 2000, Lewis: Boca Raton.

CHAPTER THREE

MATERIALS AND METHODS

3.0.0. Chemicals

The following chemicals were obtained in neat liquid form: acetonitrile (ACN)

(HPLC grade, 99.9%, Fisher Scientific) and methylene chloride (GC Resolv, 99.9+%, Fisher

Scientific). 2,4-Dinitrotoluene (DNT) (97%), 2,6-DNT (98%), 2,3-DNT (99%), and 3,4-

DNT (99%) were obtained from Aldrich Chemical Company. Magnesium sulfate certified

anhydrous was obtained from Fisher Scientific.

3.1.0. Soil Samples

Contaminated soils were collected from two former army ammunition plants, the

Volunteer Army Ammunition Plant (VAAP, Chattanooga, TN) and the Badger Army

Ammunition Plant (BAAP, Baraboo, WI). The VAAP soil was collected and stored at

ambient temperature for 6 months before processing. The BAAP soil was collected in 1997

and also stored in drums at ambient temperature. Table 3.1 presents the soil characterization

obtained following homogenization.

Table 3.1. Soil Characteristics

	Moisture (%)	Bulk Density (g/ml)	pH	2,4-DNT (mg/kg)	2,6-DNT (mg/kg)
VAAP	3.07	1.40	4.60	18540[A] 10890[B]	1380[A] 870[B]
BAAP	1.62	1.69	9.35	8940	480

A and B denote two separate batches of VAAP soil.

3.2.0. Analytical methods

Acetonitrile and methylene chloride samples (injection volume 2 μL) were analyzed

on a Hewlett Packard (HP) 6890 gas chromatograph (GC) with a mass selective detector

(MS). This GC was equipped with a HP-5MS 5%Phenyl Methyl Siloxane capillary column

(30 m x 0.25 mm ID x 0.25 μm film). The GC was used in a Splitless mode with an injector

temperature of 250 °C. The oven temperature program was as follows: 80°C to 190°C at

10°C/minute. The MS used 1,200 volts and the quadrupole and source were 150 °C and

230°C, respectively. The carrier gas was helium.

Standards were prepared by adding a known mass of 2,4-DNT and 2,6-DNT to a

known volume of ACN. Serial dilutions were performed on this solution. Also, solutions of

2,3- and 3,4-DNT were prepared to determine retention times of these compounds for

identification purposes only. The retention times are shown in Table 3.2.

Table 3.2. Retention times for dinitrotoluenes.

Analyte	Retention Times (min)
2,4-DNT	9.5
2,6-DNT	8.6
2,3-DNT	9.5
3,4-DNT	10.2

3.2.1. Soil Extraction Procedure

For each soil, five samples (approximately 0.05 g) were collected in a Non-Sterile

UltraFree-MC Millipore 0.22 μm Filter Unit (Fisher Scientific). A micropipette was used to

add (200 μL) ACN to the filter unit. The ACN was allowed to stand (10 minutes). The filter

unit was then placed into a microcentrifuge (Micro14, Fisher Scientific) (5 minutes) at 7000

RPM. After centrifugation, another aliquot of ACN (200 μL) was added to the filter unit and the process was repeated. The ACN in the bottom of the filter unit was collected with a micropipette and placed into a GC vial for analysis. If samples could not be immediately analyzed, they were stored at 4 °C for no longer than 24 hours.

To test extraction efficiency, the above procedure was repeated 3 times on 5 soil samples. For both soils, one extraction removed over 90% of the DNT. The average extraction efficiencies are VAAP soil 92% and BAAP soil 95%.

3.2.2. Procedure for Kd determination

This experiment was set up to mimic the conditions that occurred in the slurry reactor. The experiment was run at 30 °C. A nominal solids loading rate of 20% was used. (It was determined by Zhang that a 20% nominal solids loading rate in the slurry reactor was a 16% (w/v) actual solids loading rate for VAAP soil and a 2.6% (w/v) actual solids loading rate for BAAP soil.) The aqueous phase was a phosphorous buffer of 1 mM Na_2HPO_4 and NaH_2PO_4. Sodium azide (1g/L) was also added to the medium to prevent any bacteria growth.

From both soils, 4 samples of each were added to glass bottles (250 ml) with screw caps. The soil from the soil washing procedure was used because this was the soil that was added to the reactors. For the VAAP soil, soil (32 g) and medium (200 ml) were added to each bottle. For the BAAP soil, soil (5.2 g) and medium (200ml) were added to each bottle. The bottles were placed on stir plates for 24 hours.

3.2.2.1. Soil to Volume Ratio

To determine the soil to volume ratio of the reactors, four samples (30ml) were taken with a glass pipette while the reactors were on the stir plate. These samples were placed into

beakers (50 ml) of known mass and placed into a drying oven at 90 °C overnight. After the beakers cooled, they were weighed and the mass of soil was determined. The mass to volume ratio of the VAAP soil was 0.147 g/ml and BAAP was 0.022 g/ml.

3.2.2.2. Soil Analysis

VAAP Soil

While the reactors were on the stir plate, slurry (300μl) was removed with a micropipette. The sample was placed into a Millipore 0.22um filter unit (see soil extraction procedure) and centrifuged (5 minutes) at 7000 RPM in the microcentrifuge. The aqueous sample was removed from the bottom of the filter unit and a small amount of $MgSO_4$ was added to the bottom of the filter unit. The extraction procedure above was performed on the soil sample.

BAAP Soil

While the reactors were stirring, an aliquot of the slurry (30ml) was removed with a glass pipette and placed into a glass I-Chem vial (40 ml) with screw cap and septa (Fisher Scientific). The sample was centrifuged (15 minutes) at 2500 RPM. The supernatant was poured off and the soil was resuspended into medium (3ml). Three samples (300 μl) were taken from each vial. These samples were treated as the VAAP samples above.

3.2.2.3. Aqueous Phase Analysis

Using a glass pipette (10 ml), samples (30 ml) were taken from the reactors while on the stir plate. The samples were placed into a glass I-Chem vial (40 ml) and centrifuged (15 minutes) at 2,500 RPM. The supernatant of the BAAP soil was pipetted off into another I-Chem vial. The supernatant of the VAAP soil was filtered through a 0.2 um polycarbonate

membrane with a glass syringe before being put into an I-Chem vial. This removed any particulates not removed by centrifugation. The aqueous samples were weighed and methylene chloride (MeCl) added (1.3g per 10g H_2O). The samples were shaken and phases allowed to separate. The MeCl was pipetted out of the vial and placed into a GC vial for analysis.

CHAPTER FOUR

PREVIOUS WORK: BIODEGRADATION OF 2,4-DNT AND 2,6-DNT IN AN AEROBIC SLURRY REACTOR SYSTEM

The purpose of this chapter is to provide the reader with an appropriate

background to the previous work that forms the basis for the current study. The work

presented in this chapter was performed by Dr. Chunlong Zhang under the direction of

Dr. Joseph B. Hughes and in collaboration with Dr. Jim C. Spain and Shirley Nishino

from the United States Air Force Research Lab, Tyndall, FL. This chapter presents

information on soils and inocula used in the previous work and in the current work. It

also gives descriptions of the slurry reactor and it operations, as well as the pertinent

results from the previous study. All of the information provided in this chapter was taken

from reference [1] and reference [2].

4.0.0. BACTERIAL CULTURE

This study used a mixed culture containing the 2,4-DNT degrading strain

Burkholderia cepacia JS872 and the 2,6-DNT degrading strains *B. cepacia* JS850 and

Hydrogenophaga palleronii JS863. This culture was grown in 18-L batches in nitrogen-

free minimal medium supplemented with 2,4-DNT and 2,6-DNT as the sole source of

carbon, nitrogen, and energy. The culture was incubated at 30°C, with stirring at 400

RPM and sparged with air at 15 L/min.

4.1.0. TEST SOILS AND SLURRY PREPARATION

The soils used in this study are the same soils as those detailed in Chapter three,

Section 3.1.0.

Figure 4.1 presents the overall process the soil undergoes before it is placed into

the reactors. Soils were air-dried, gravel and large debris were removed, followed by
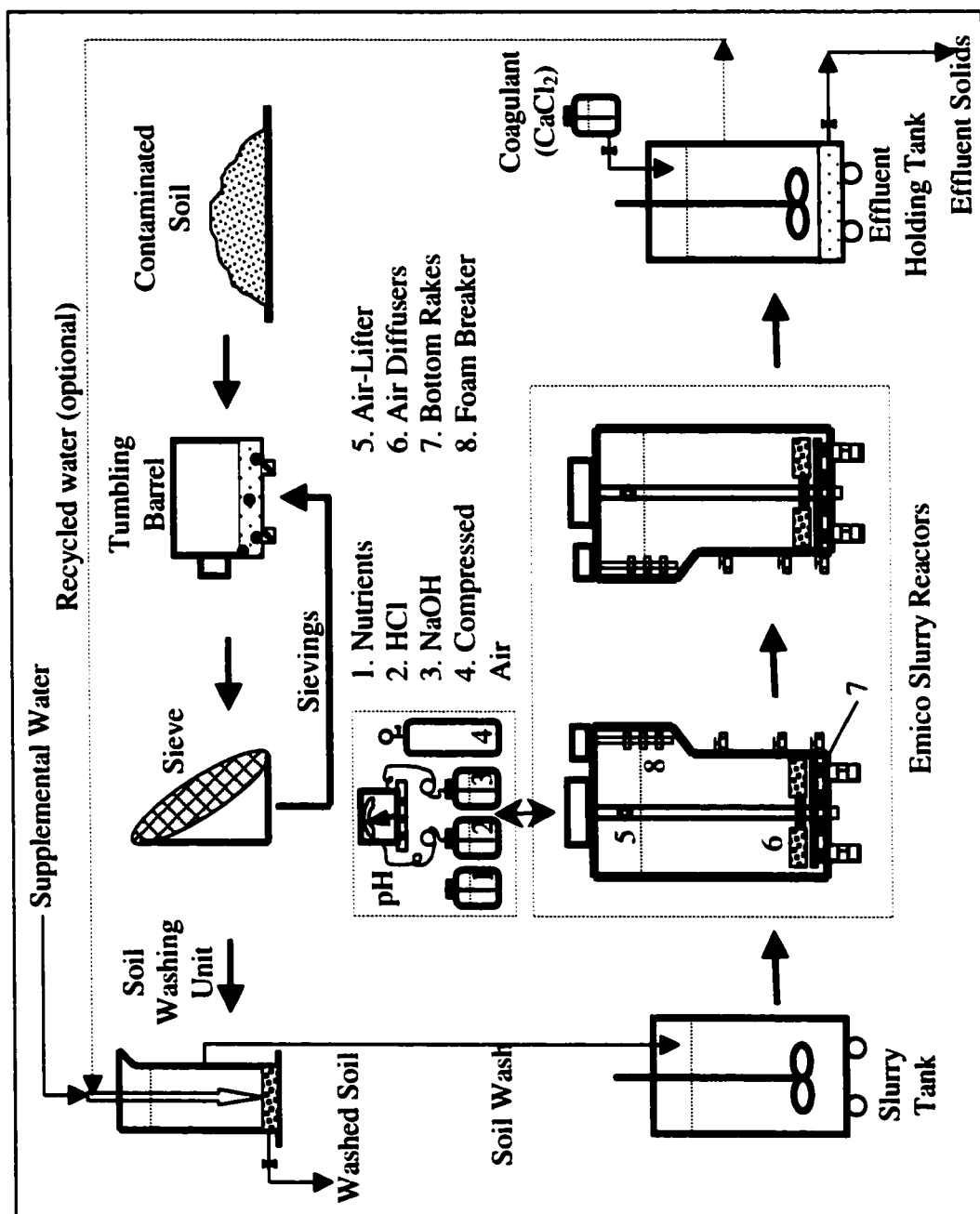
Figure 4.1. Treatment scheme of pilot-scale soil washing and sequential aerobic slurry reactor system

repeated sieving and tumbling processes until all soils were passed through a 20-mesh

sieve. To obtain a homogeneous stock of soils for use in biodegradation studies, soils

were manually mixed and put through a sample splitter.

The soils were treated with soil washing before use because large amounts of sand

interfered with reactor operation. Soil washing was performed with 60°C tap water to

separate the DNT-associated fines from the sands. The resulting soil slurry was used in

the reactor, and the clean sand was discarded. A total of 60 L of water was generally

used to wash one batch of soil, but the ratio of water to soil varied depending on the

desired DNT loading for a cycle. The two soils varied in their DNT concentration and

sand content; therefore, the notation used to describe the amount of material in the slurry

reactor is described as the *nominal solids loading rate*, expressed as percent (w/v). This

term corresponds to the mass of soil introduced into the soil washing apparatus (kg)

divided by the reactor volume (70L). (Note that a nominal 10% solids loading rate is

equivalent to 7 kg of soil used during the soil washing procedure. Table 4.1 shows

difference between the nominal solids loading rate and the actual solids loading rate in

the reactor.

Table 4.1. Nominal solids loading rates vs. actual solids loading concentrations in the reactor.

	Unit	Solids loading rates tested in this study				
VAAP soil						
Nominal solids loading rate	%(w/v)	5	20	30		
Actual solids loading rate	%(w/v)	4	16	25		
SS concentration	g/L	40	160	250		
BAAP soil						
Nominal solids loading rate	%(w/v)	5	10	20	30	40
Actual solids loading rate	%(w/v)	0.7	1.3	2.6	3.9	5.2
SS concentration	g/L	7	13	26	39	52

4.2.0. Slurry Phase Aerobic Reactors

A schematic of the reactor used in the study is shown in Figure 4.2. It is an Eimco Biolift slurry reactor (Model B75LA, Tekno Associates, Salt Lake City, UT). It has a working volume of 75 L and is equipped with agitation, aeration, and temperature control. The temperature was maintained at 30°C and the pH was maintained in the range of 6.75-7.25 with a pH controller and 12.5 N NaOH.

The mixing and aeration in the reactor is performed by the airlifts, bottom rakes, and diffuser tubes. The rake mechanism moves settled material from the bottom of the reactor to a central airlift which lifts the material to the top of the liquid. The diffuser tubes are attached to the rake arms and supply oxygen to the reactor and suspend smaller particles. Three sampling ports were located along the side wall of the reactor at 2, 15, and 40 cm from the bottom of the reactor. Routine samples were taken from the top sampling port.

4.2.1. Reactor operation

Two reactors were operated in sequential mode. The first reactor was charged with soil wash, and the effluent from the first reactor was then fed to the second reactor in series. Initially, the reactor was filled with 60L of soil slurry along with NaH_2PO_4 and Na_2HPO_4 to yield a pH of 7. The final volume in the slurry reactor was brought to 70 L with tap water. After equilibration and pH adjustment, the slurry was inoculated with the mixed bacterial culture. When solid loading rates of 20% and 30% for VAAP soil and 40% for BAAP soil were tested, additional nutrients were added. These nutrients were contained in a nitrogen-free minimal medium containing 1:1000 of 10 g/L $CaCl_2 \bullet 2H_2O$, 2.35 g/L sodium citrate and 2.16 g/L $FeCl_3$ and 20 g/L $MgSO_4 \bullet 7H_2O$.

Diffuser Air Supply

Shaft Motor

Foam Breaker

Airlift Discharge

Rake Shaft/Airlift

Diffuser Air Supply Line

Sample Valves 2,25,40 cm

Aeration Diffusers

Rake with Blades

Airlift Air Supply Line

15" ID
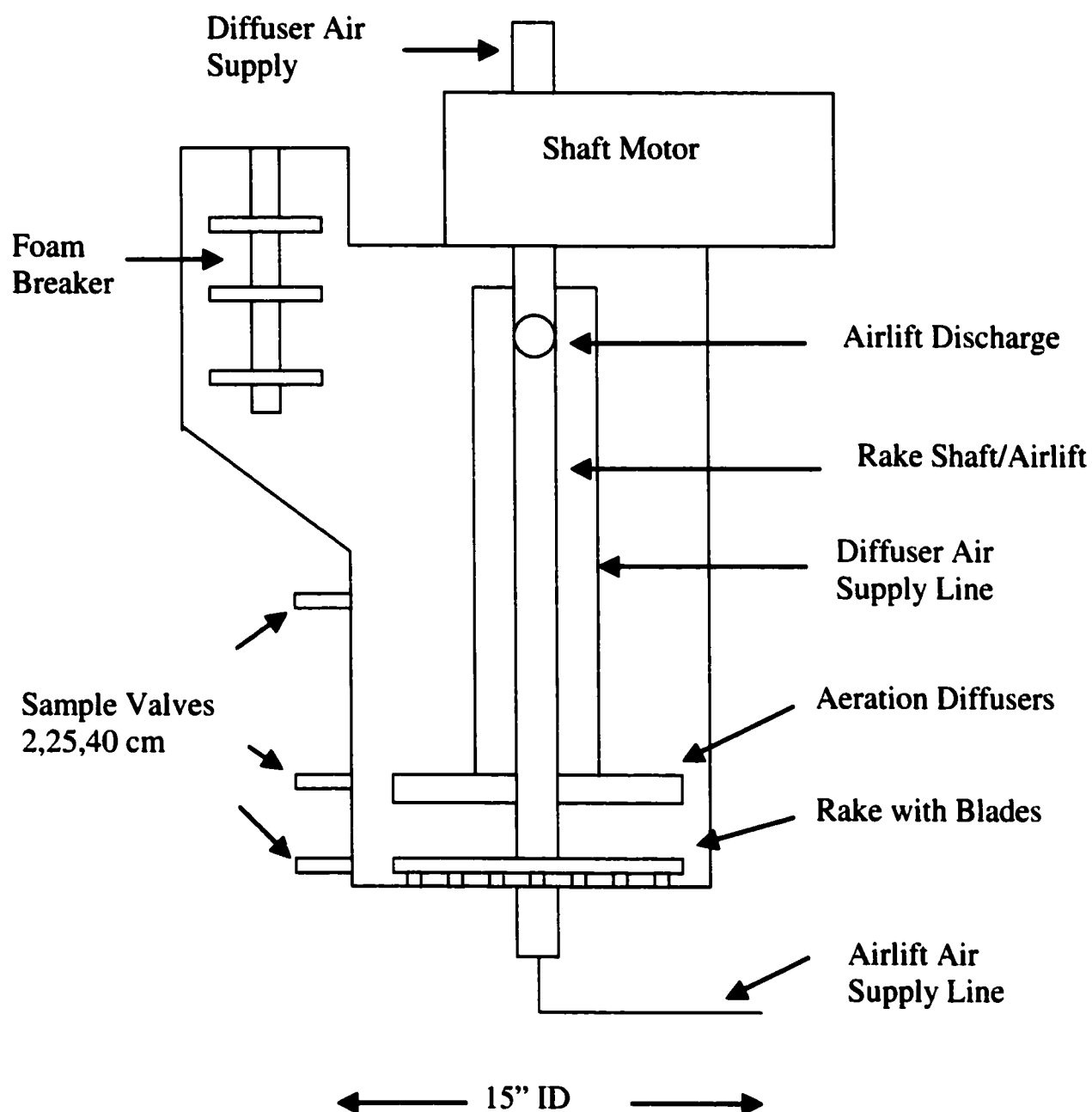
Figure 4.2. Reactor Schematic.

Reactors were operated in a draw-and-fill mode. In routine draw-and-fill

operation, the reactor contents were drained, and 7L of slurry remained for re-

inoculation. Reactors were also operated in sequential draw-and-fill mode where the first

reactor was used for the degradation of 2,4-DNT and the second for the degradation of

2,6-DNT. After reaching the desired level of 2,4-DNT, the reactor contents were

transferred to the second reactor.

4.3.0. RESULTS

During the reactor start-up, the reactors were fed both VAAP and BAAP soil

slurries, at a 10% loading rate, to determine if any indigenous soil microorganisms were

capable of degrading 2,4-DNT and 2,6-DNT. The reactors were allowed to run for 3

days, and no degradation of either DNT isomer was observed.

4.3.1. BAAP Soil

4.3.1.1. 2,4-DNT and 2,6-DNT Degradation

System performance for the BAAP soil was examined in Reactor C at five

nominal solids loading rates, 5%, 10%, 20%, 30%, and 40% (Figure 4.3), corresponding

to actual solids concentrations of 0.7%, 1.3%, 2.6%, 3.9% and 5.2% in the reactor. 2,4-

DNT degradation was very stable over a 7-week period. Several observations can be

made from the data shown in Figure 4.3. First, complete degradation of 2,4-DNT was

demonstrated in the slurry reactor with BAAP soil at a nominal solids loading rate of up

to 40%. This loading rate corresponded to an initial 2,4-DNT concentration of 11,230

μM (2,045 mg/L). The rate of degradation was approximately 71.6 g 2,4-DNT/day for

each reactor, assuming an observed average residence time of ~ 2 days. These results

indicate that the bacteria were capable of degrading 2,4-DNT at high concentrations
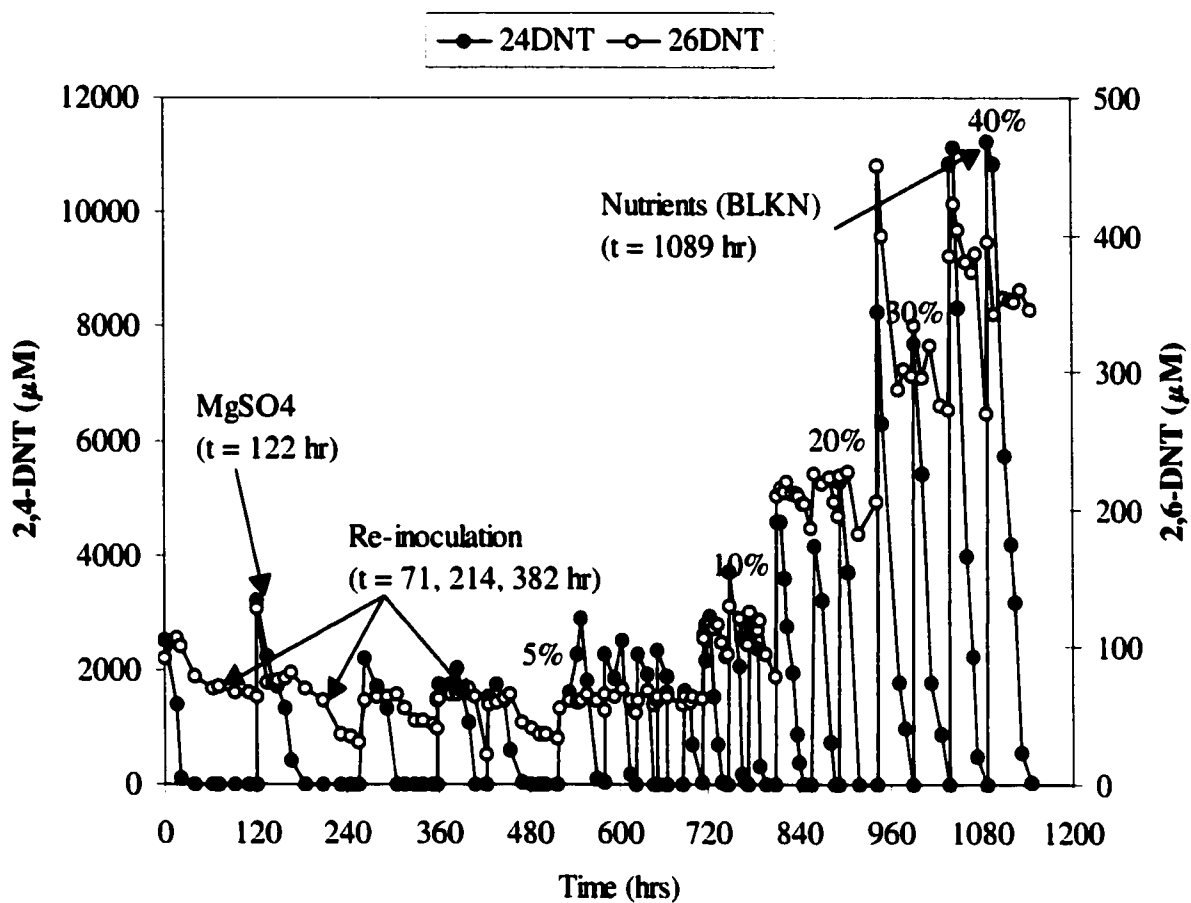
Figure 4.3. Degradation of 2,4-DNT and 2,6-DNT in Reactor C

without noticeable inhibition by 2,4-DNT. Second, the degradation of 2,6-DNT was

negligible, especially at higher solids loading rates of BAAP soil, believed to be a result

of the inhibition of 2,6-DNT degradation by 2,4-DNT. Third, the rate of 2,4-DNT

degradation depended largely on microbial activity regardless of the loading rates. For

instance, a lag and/or a lower degradation rate were observed when the feeding of soil

wash was delayed. This was apparent when comparing the performance between the first

6 cycles and the subsequent 3 cycles, when the reactor was fed at a constant loading rate

of 5%. Finally, the effects of nutrient additions and re-inoculation on Reactor C

performance were minimal. As shown in Figure 4.3, additional nutrients were

supplemented at $t = 122$ hr ($MgSO_4$) and $t = 1089$ hr (BLKN medium). The reactor was

also re-inoculated several times ($t = 71$ hr, 214 hr and 382 hr).

Studies performed in Reactor D emphasized the degradation of 2,6-DNT. The

reactor was first operated in a continuous feeding mode (i.e., continuously pumping soil

wash to the reactor), followed by an intermittent mode with feedings of soil wash instead

of effluent from Reactor C (Figure 4.4). After approximately 600 hours, the reactor was

fed effluent from Reactor C in a fill-and-draw mode with increasing volume of effluent

from 50:50, 35:65, to 10:90 (v/v). The results are given in Figure 4.5. Significant

degradation of 2,6-DNT in Reactor D is shown in Figure 4.4 and 4.5. Although Reactor

D lost activity of 2,6-DNT degradation in certain cycles, the activity recovered after re-

inoculation. Note that the initial concentrations of 2,6-DNT in continuous mode,

intermittent mode, and the first 6 cycles of fill and drawn mode were all below 50 μM in
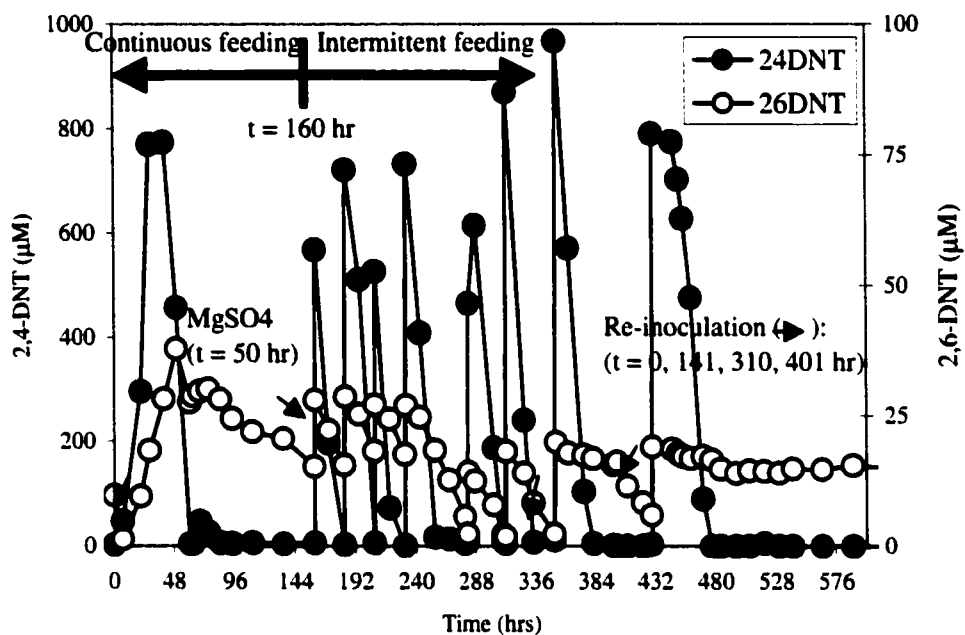
Reactor D.

Figure 4.4. Degradation of 2,4-DNT and 2,6-DNT in Reactor D: Continuous and intermittent feeding modes with BAAP soil wash
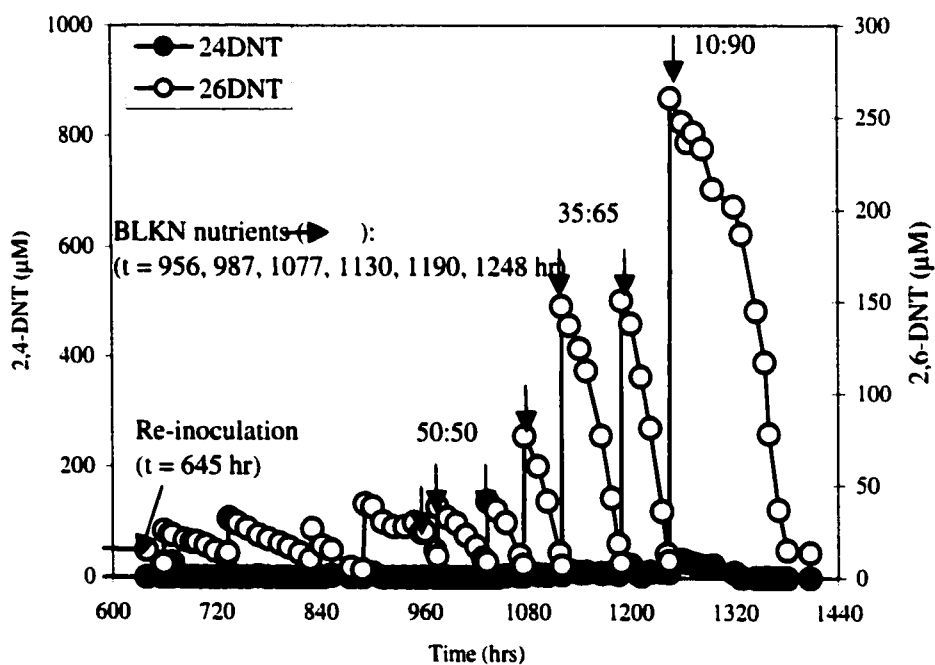
Figure 4.5. Degradation of 2,4-DNT and 2,6-DNT in Reactor D: Fill-and Draw mode with effluent from Reactor C

As mentioned above, several inoculations of 2,6-DNT degrading bacteria were made in Reactor D when a lack of activity was observed. The effects of re-inoculation were significant as compared to the response in Reactor C. Following the re-inoculation at t = 401 hr and 645 hr, 2,6-DNT degradation occurred immediately. Reactor D was also supplemented with additional BLKN nutrients after a prolonged lag phase at t = 956 hr, the activity was recovered again. These results demonstrated the role of DNT-degrading bacteria from the bacterial culture and the significant impact of additional nutrients. However, the physiological reason for the loss of activity in degrading 2,6-DNT is unknown.

4.3.1.2. Nitrite Release

Figure 4.6 shows the production of nitrite in 20 feeding cycles of BAAP soil wash in Reactor C. Similar to the VAAP soil in Reactor A, the pattern of the nitrite production corresponded to the disappearance of dinitrotoluenes shown in Figure 4.3. In addition, the concentrations of nitrite increased proportionally with the increase in solids loading rates. Nitrite release calculated on the basis of dinitrotoluene degraded averaged of 1.7 mole NO_2^-/mole DNT.

The nitrite concentration profile in Reactor D is given in Figure 4.7. During the initial period of continuous feeding, nitrite concentration increased gradually. The concentration remained constant between 5,000 and 10,000 μM during the intermittent feeding. Following the increase in the effluent ratio (therefore the concentration of 2,6-DNT) in the fill-and-draw mode, nitrite concentrations increased significantly from about 5,000 to 35,000 μM. Similar concentrations (~ 40,000 μM) were observed at the
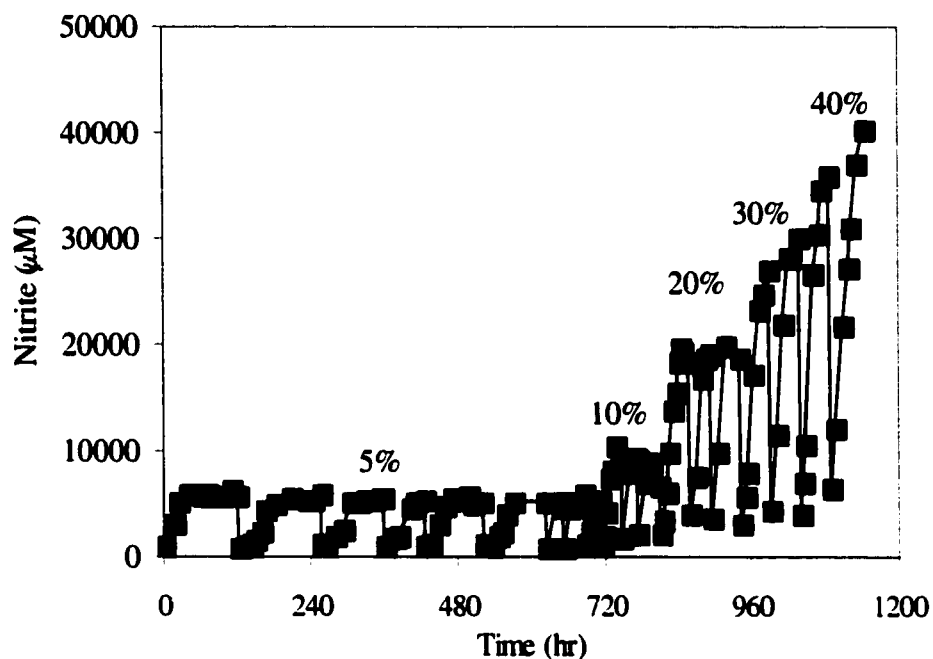
Figure 4.6. Nitrite Concentration in Reactor C
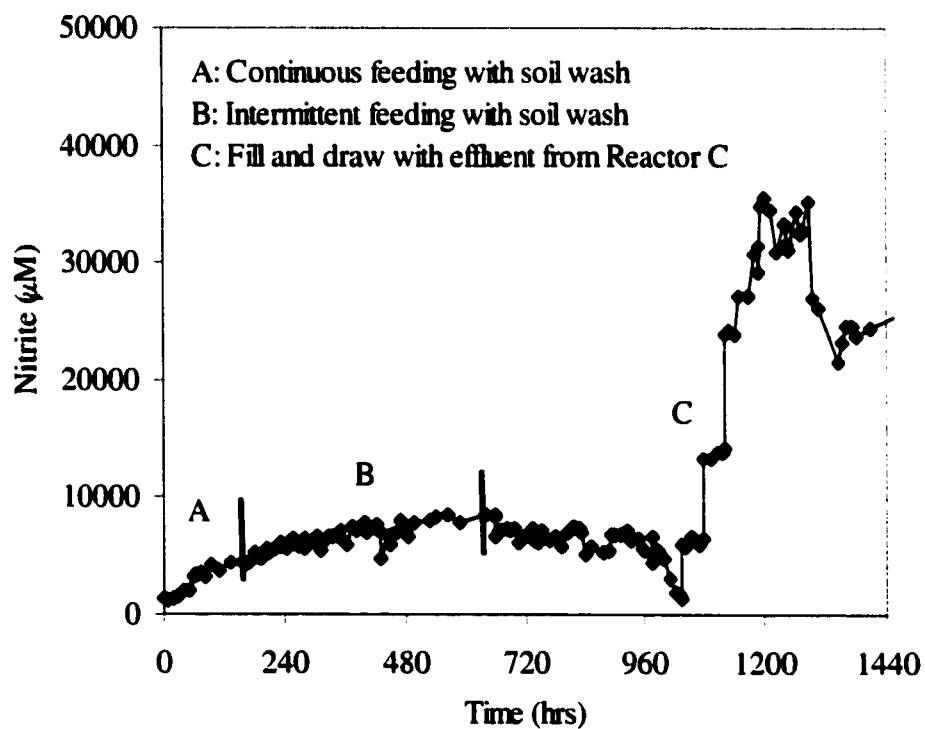
Figure 4.7. Nitrite Concentration in Reactor D

conclusion of Reactor C with a 40% of solids loading rate (Figure 4.6). It is noteworthy that degradation of 2,6-DNT still occurred at these high nitrite concentrations.

4.3.1.3. Oxygen Uptake

In Reactor C, oxygen uptake rates were routinely measured and O_2 uptake rates corresponded to activity in each feeding cycle (data not available for the first cycle) of soil wash was clearly defined (Figure 4.8). It is clear that oxygen uptake rates correlated with the microbial activity of the reactor. The peak oxygen uptake rates increased with increasing solids loading rates, but reached a maximum when the nominal solids loading rate was 20%. The maximum oxygen uptake rate in Reactor C was 2.0 mg/L·min. Oxygen consumption in Reactor D was much lower, especially when the reactor was fed Reactor C effluent containing 2,6-DNT. High oxygen demand was observed only during the continuous and intermittent feeding of soil wash when 2,4-DNT was fed to the reactor (Figure 4.9).

4.3.1.4. NaOH Consumption

The consumption of sodium hydroxide (12.5 N, 50% w/v) is given on a per cycle basis, and the results are shown in Figure 4.10 and 4.11 for Reactor C and D, respectively. The results of NaOH consumption were generally consistent with the degradation pattern of dinitrotoluenes, the nitrite release, and the oxygen uptake rate presented in Figure 4.3-4.9. In Reactor C, more NaOH was consumed as solids loading rates were increased. A linear relationship was found between the two ($R^2 = 0.998$), with a correlation of 4.6 mL of 12.5 N NaOH per 1% (w/v) of BAAP soil. Based on dinitrotoluene degraded, this is equivalent to 1.7 mole of NaOH per mole of DNT. In reactor D, however, NaOH consumption was minimal, except when it was fed soil wash
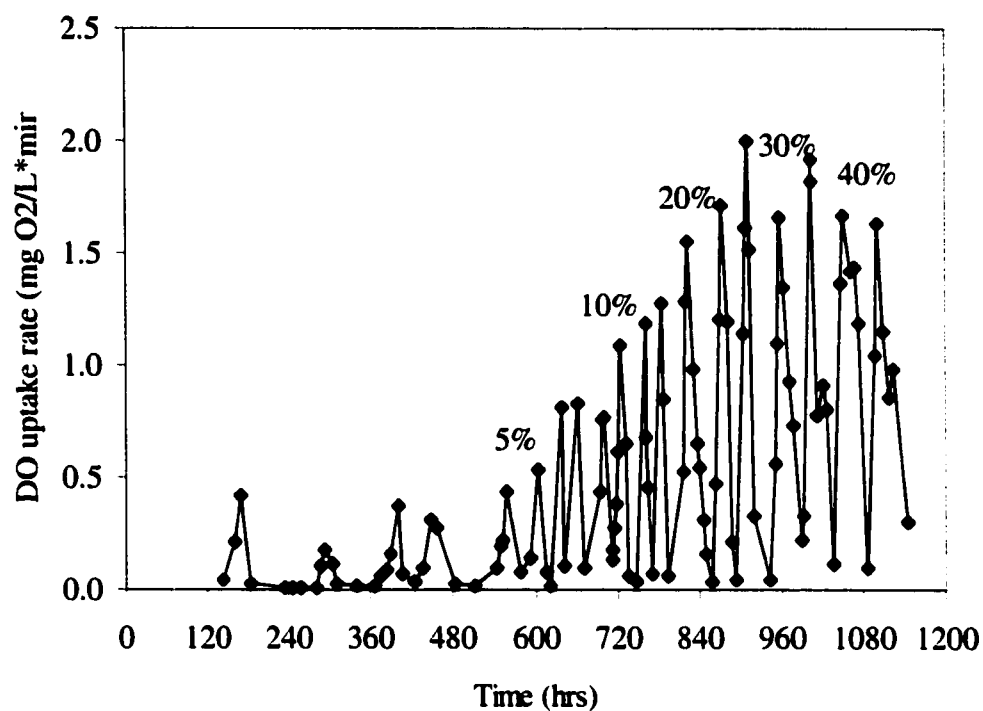
Figure 4.8. Oxygen Uptake Rate in Reactor C
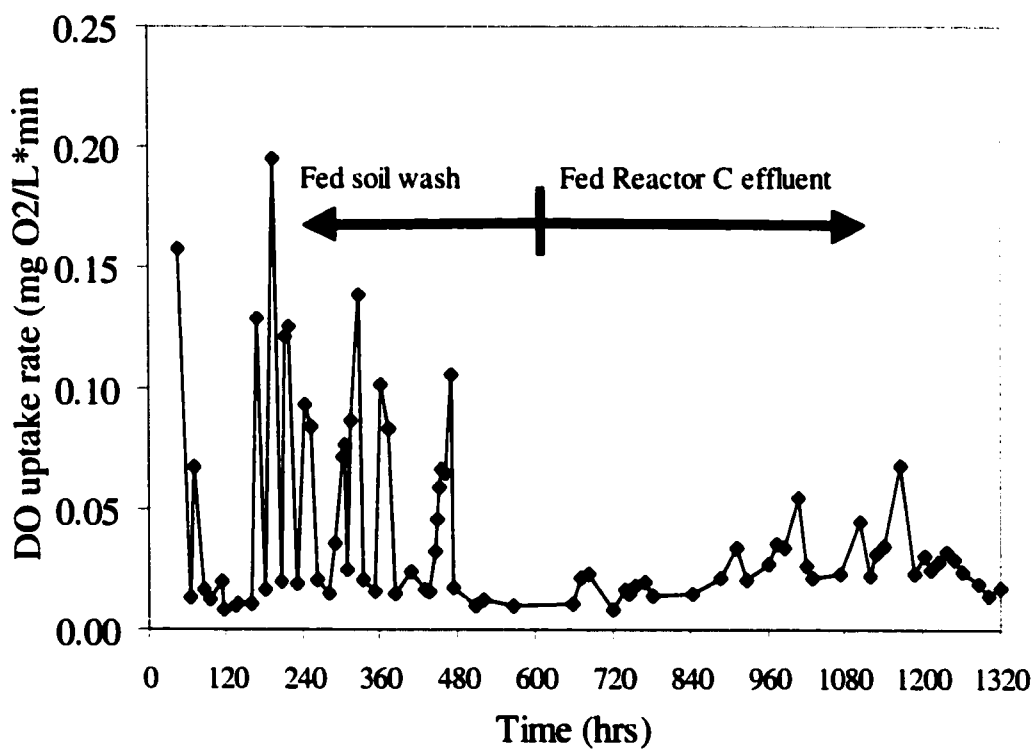
Figure 4.9. Oxygen Uptake Rate in Reactor D
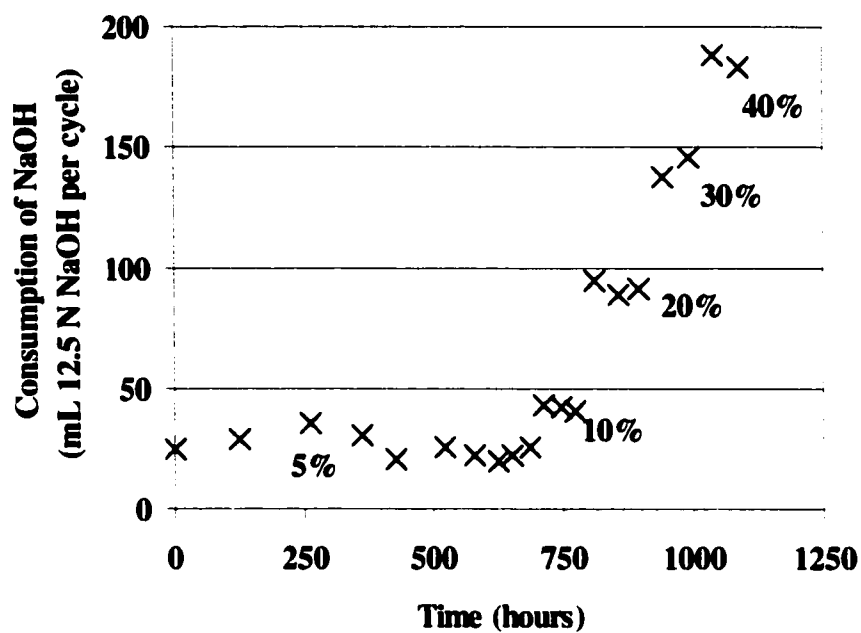
Figure 4.10. NaOH Consumption in Reactor C
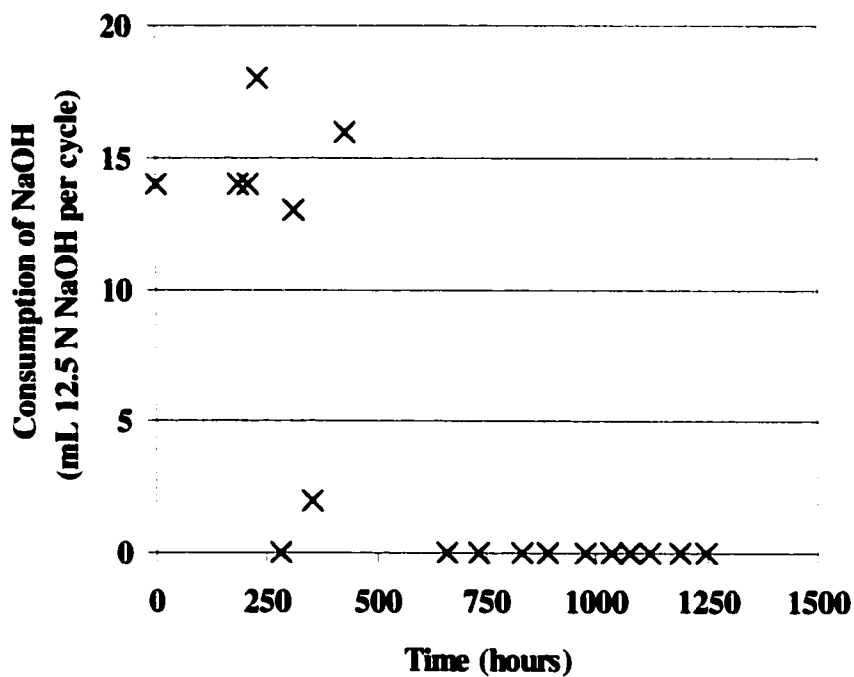
Figure 4.11. NaOH Consumption in Reactor D

containing 2,4-DNT. The theoretical consumption (based on 2 mole NaOH/mole DNT) of 12.5 N NaOH is very small (2.8 mL) for 250 μM of 2,6-DNT. This explains why NaOH consumption was not observed while it was fed Reactor C effluent.

4.3.2.VAAP Soil

4.3.2.1. 2,4-DNT and 2,6-DNT Degradation

For VAAP soil, nearly complete degradation of 2,4-DNT was demonstrated in the slurry reactor at a nominal solids loading rates of 20% (Figure 4.12). When the reactor was fed VAAP soil at a 30% nominal solids loading rate (17,000 μM 2,4-DNT, 1,500 μM 2,6-DNT, and 700 μM TNT), the degradation of 2,4-DNT was not complete, as is shown in Figure 4.12. It was not known whether this was the result of limiting nutrients or the inhibition by nitrite, or both. However, after adding a new batch of soil wash at a reduced loading rate (e.g., 20%), the system performed as previously observed.

During initial studies with VAAP soil slurries, 2,6-DNT degradation was not occurring in the second reactor; therefore, Reactor F was initiated to focus on developing the degradation of 2,6-DNT. This was conducted using Reactor E effluent containing residual 2,6-DNT, and the finished effluent from Reactor D as the active bacterial culture. Reactor F started with an initial 2,6-DNT concentration of approximately 100 μM. The initial 2,6-DNT concentrations were increased continuously over the 8 fill-and-draw cycles to ascertain whether the bacteria were able to degrade 2,6-DNT and to define the maximum tolerable concentration to the bacteria. As shown in Figure 4.13, degradation of 2,6-DNT was successfully demonstrated at a concentration range of 100 – 300 μM. 2,6-DNT at concentrations up to 300 μM showed only a brief lag phase, but the rate of
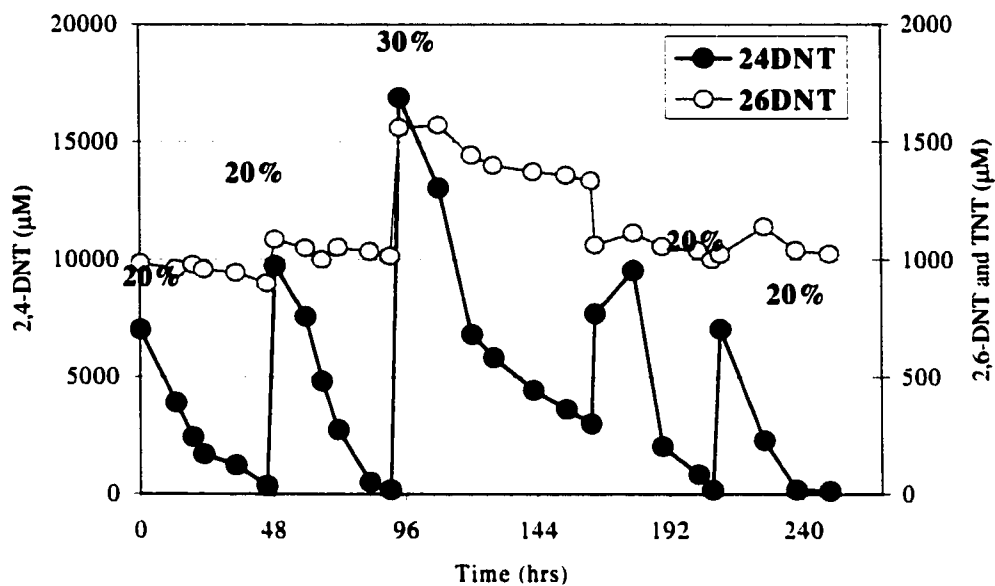
Figure 4.12. Degradation of 2,4-DNT and 2,6-DNT in Reactor E
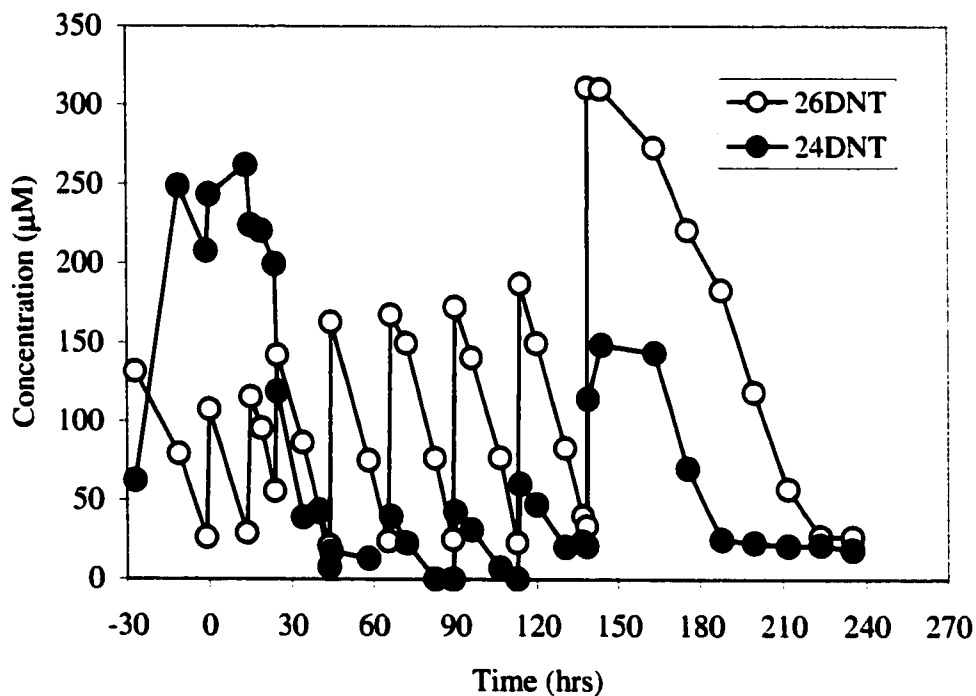
Figure 4.13. Degradation of 2,4-DNT and 2,6-DNT in Reactor F

2,6-DNT degradation appeared to be similar to previous feeding cycles. It was also noted that TNT degradation in Reactor F was minimal. An initial increase in 2,4-DNT concentration in the reactor was observed, this may have been the result of the desorption from residues within the reactor.

4.3.2.2 Nitrite release

The nitrite concentration profiles in Reactor E are given in Figure 4.14. The maximum concentrations were about 35,000 μM at a 20% nominal solids loading rate. Again, the pattern of the nitrite production corresponded to the disappearance of dinitrotoluenes shown in Figure 4.12. Note that the maximum concentration at a 30% loading rate remained about the same as the concentrations at a 20% loading rate. This is because a fill-and-draw was initiated prior to the complete degradation of 2,4-DNT.

Similar to the concentration profile in the other reactors in series (Reactor D), the nitrite concentrations in Reactor F fluctuated and did not correspond to the fill-and-draw patterns of 2,6-DNT degradation in the reactor (Figure 4.15). Again, this is presumably due to the high background concentrations carried over from the first reactor, and the small amount of nitrite released from the relatively low concentrations of 2,6-DNT.

4.3.2.3. Oxygen uptake

Oxygen uptake rates in Reactor E were routinely measured, no oxygen uptake data are available in Reactor F. The shape of the curve corresponding to each feeding cycle of soil wash in Reactor E was evident (Figure 4.16). It is clear that oxygen uptake rates responded to the microbial activities in the reactor. The peak oxygen uptake rates remained high between 1.3 and 2.6 mg/L·min, as compared to the observed maximum oxygen uptake rate in Reactor C of 2.0 mg/L·min.
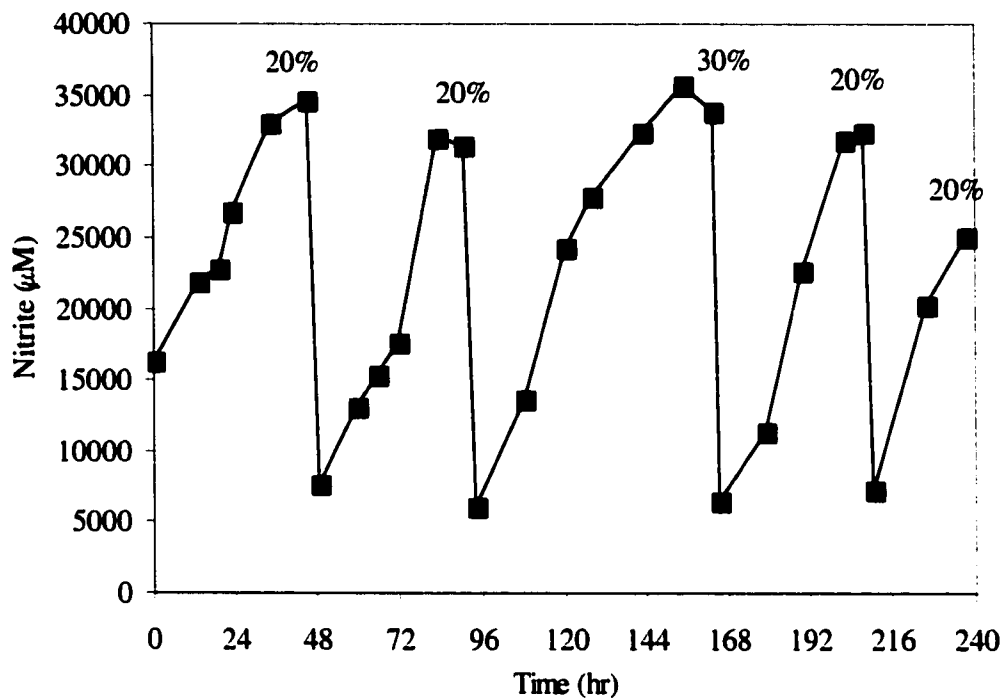
Figure 4.14. Nitrite Concentration in Reactor E
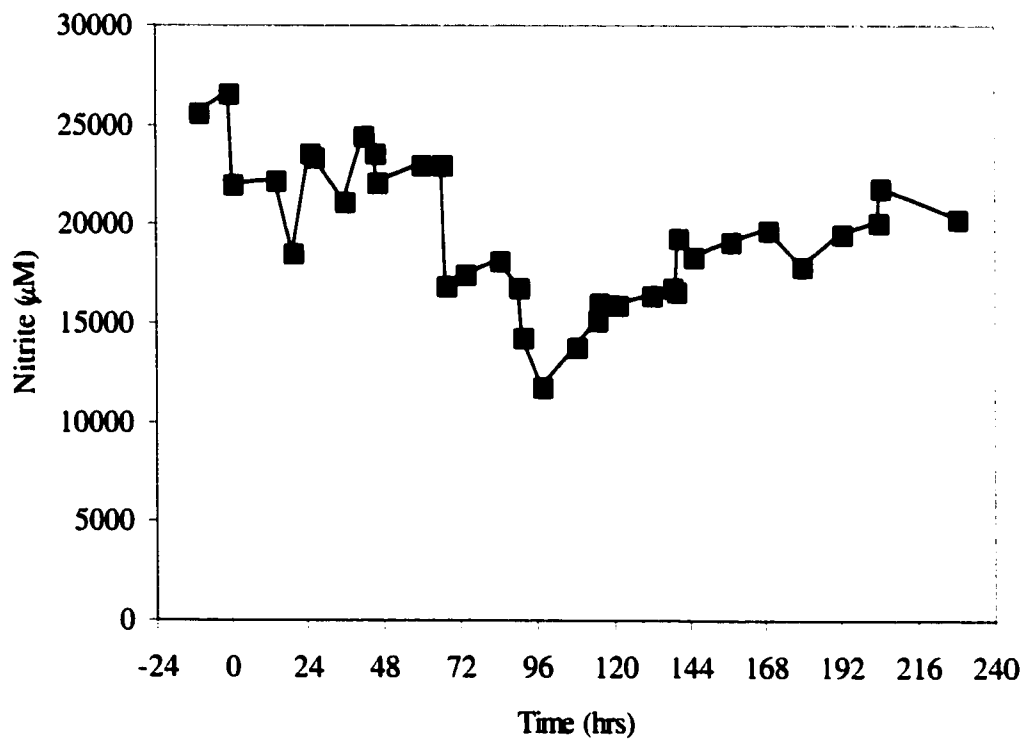
Figure 4.15. Nitrite Concentration in Reactor F
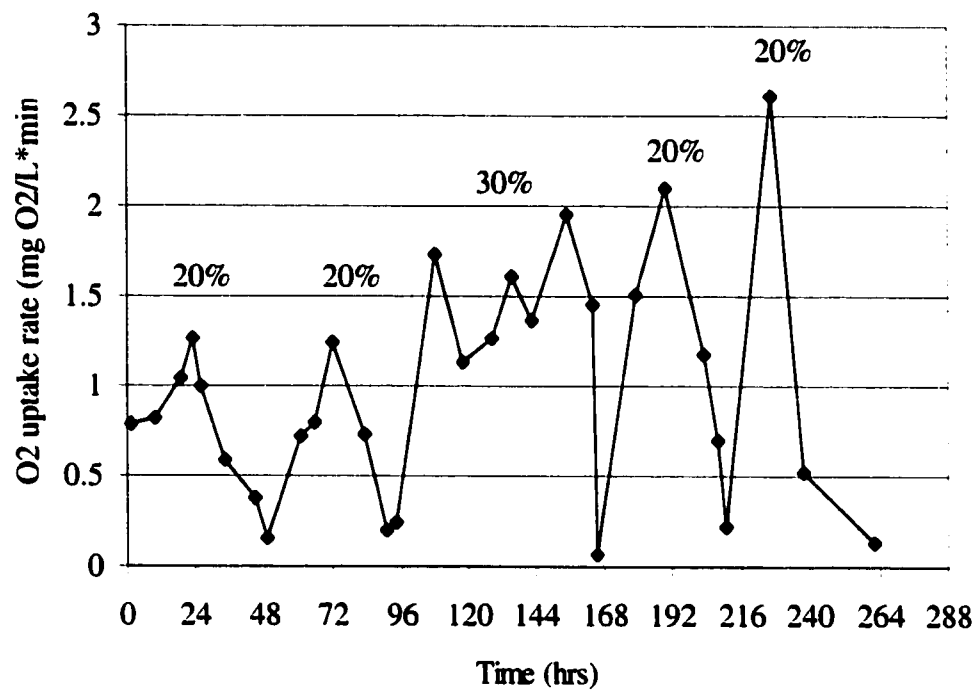
Figure 4.16. Oxygen Uptake Rate in Reactor E

4.3.2.4. NaOH Consumption

The consumption of sodium hydroxide (12.5 N, 50% w/v) in Reactor E is given on a per cycle basis, and the results are shown in Figure 4.17. In Reactor F, pH remained neutral, no consumption of NaOH was observed.

4.4.0. Inhibition of 2,4-DNT on 2,6-DNT degradation

A series of shake-flask experiments were conducted to assess possible impacts of 2,6-DNT or 2,4-DNT concentration on 2,6-DNT degradation. The effects of 2,6-DNT concentration on its own biodegradation are shown in Figure 4.18. Complete 2,6-DNT degradation occurred in all cases, including concentrations as high as 650 μM. The 2,4-DNT concentrations in the suspension were low (~ 6 μM) throughout.

The effects of 2,4-DNT on 2,6-DNT degradation were determined in an experiment with a series of flasks containing the same concentration of 2,6-DNT and various concentrations of 2,4-DNT (Figure 4.19). At a concentration of 50 μM, 2,4-DNT did not affect the degradation of 2,6-DNT. 2,4-DNT concentrations of 500 and 1000 μM inhibited 2,6-DNT degradation, but after 2,4-DNT was degraded, 2,6-DNT degradation began. At a 2,4-DNT concentration of 2,500 μM, inhibition appeared to be irreversible, as 2,6-DNT was not degraded even after 2,4-DNT was completely degraded. The two highest 2,4-DNT concentrations tested exceeded the solubility limit of 2,4-DNT, thus similarly high aqueous phase concentrations were reached in both systems (Figure 4.19B).
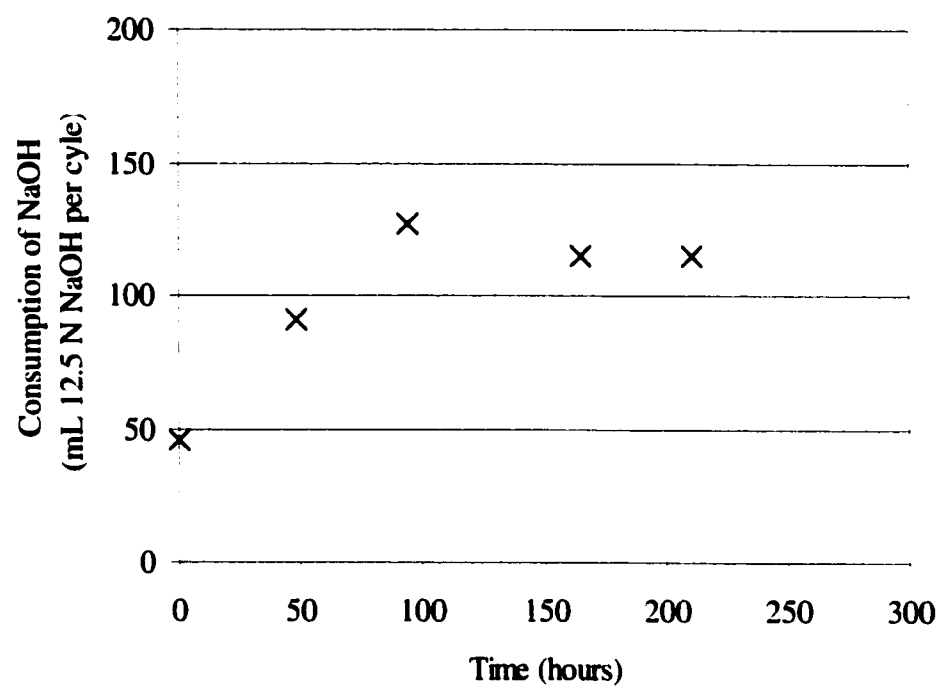
Figure 4.17. NaOH Uptake Rate in Reactor E
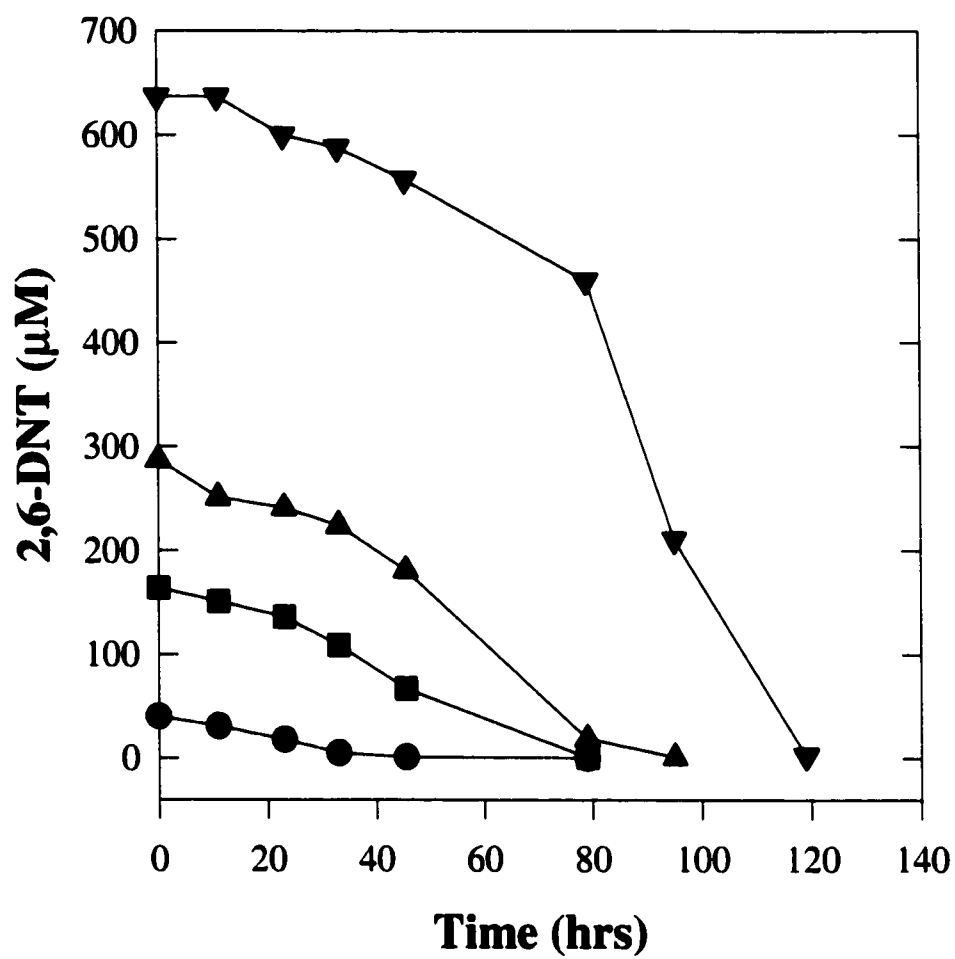
Figure 4.18. Degradation of 2,6-DNT at various initial conditions
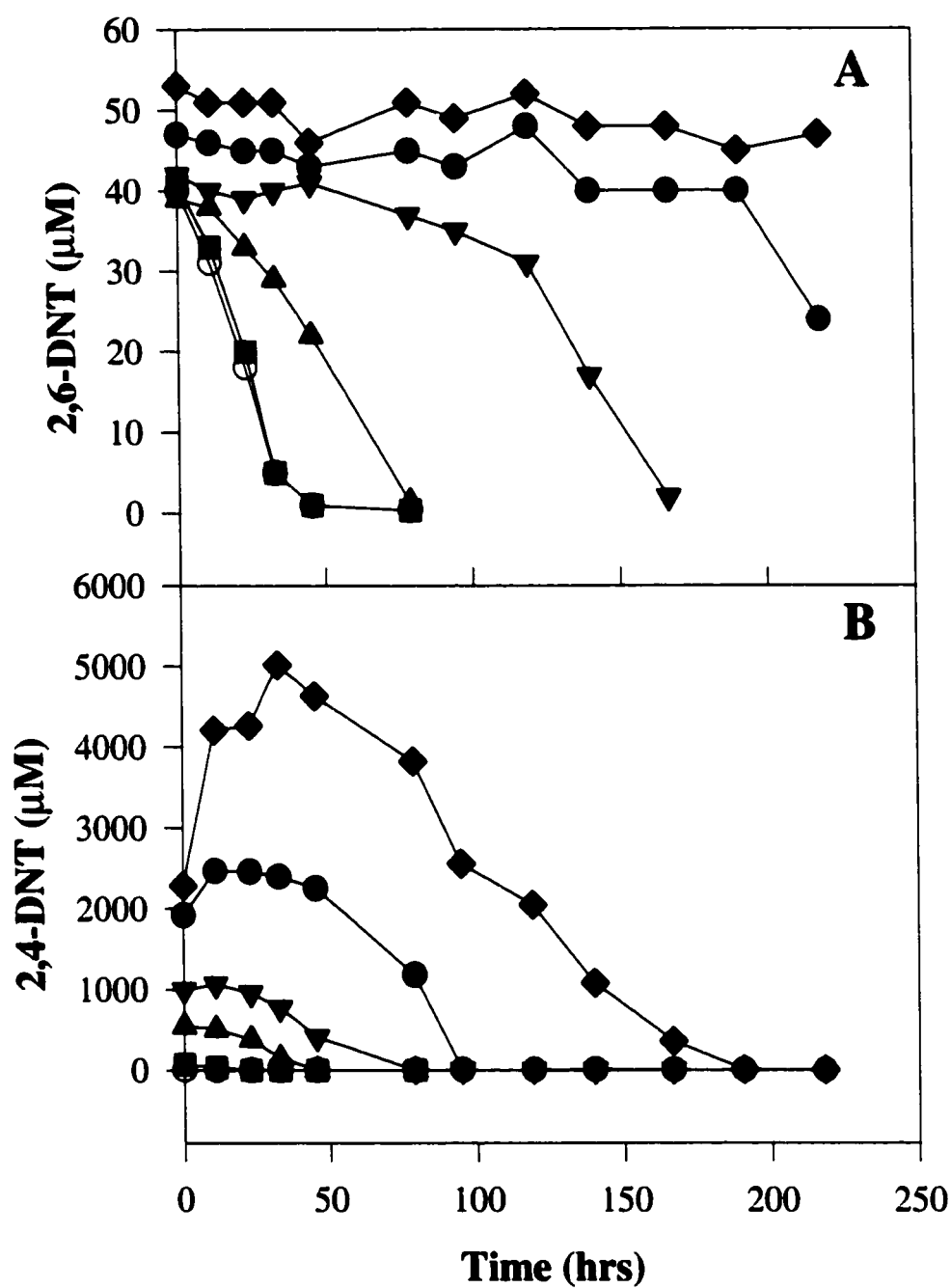
Figure 4.19. Effects of 2,4-DNT concentration on 2,6-DNT biodegradation in shake flasks. Slurry phase concentrations of 2,6-DNT (A) and 2,4-DNT (B).

4.5.0. Conclusions

The following major conclusions can be drawn from this study:

- Soil washing was an effective pretreatment for slurry reactors by removing large particulates and recovering 2,4-DNT, 2,6-DNT and TNT from contaminated soils.

- Augmentation of slurry reactor with dinitrotoluene-mineralizing bacteria resulted in the oxidative biodegradation of 2,4-DNT and 2,6-DNT with both VAAP and BAAP soils.

- A sequential mode of operation optimized the rate and extent of 2,4-DNT and 2,6-DNT degradation because high concentrations of 2,4-DNT inhibited 2,6-DNT degradation.

- Stoichiometry of nitrite release and sodium hydroxide consumption during the course of dinitrotoluene biodegradation has been established in pilot-scale study.

References

1.   Zhang, C. and J.B. Hughes, Biodegradation of 2,4-Dinitrotoluene and 2,6-Dinitrotoluene in a Pilot-Scale Aerobic Slurry Reactor System, . 1999, Department of Environmental Science and Engineering, Rice University: Houston, TX.

2.   Zhang, C., *et al.*, Slurry-Phase Biological Treatment of 2,4-Dinitrotoluene and 2,6-Dinitrotoluene: Role of Bioaugmentation and Effects of High Dinitrotoluene Concentrations. *Environ. Sci. Technol.*, 2000. 34(13): p. 2810-2816.

CHAPTER FIVE

MODEL DEVELOPMENT

This chapter presents the development of the model used to predict the

partitioning and biodegradation of DNT in the bioslurry reactor discussed in the Chapter

4. This chapter begins with a discussion of the program used to develop the model and

then it gives a general discussion of the processes occurring in the reactor. The chapter

also details all assumptions and equations used to develop the model. Finally, an

example of the data the model generates is presented.

5.0.0. MATLAB

The model was developed using MATLAB 5.3 (Version 5.3.0.620a, The Math

Works, Inc.) The MATLAB scripts are provided in Appendix I. There are separate

programs for both the VAAP and the BAAP soil to accommodate differences in the

solids loading rates and the partition coefficients (K_d) of the two soils.

5.1.0. Model Description

In order to mathematically describe the partitioning and biodegradation of DNT in

the reactor, it is important to understand what processes occur in the reactor. In the

reactor, DNT is in three forms: crystalline, sorbed, and aqueous. The bacteria consume

only the dissolved DNT, which causes the dissolution of the crystals and desorption of

the sorbed DNT. For development of the model, it was assumed that dissolution of the

crystalline DNT occurred first. Thus the aqueous concentration was saturated and no

desorption of soil-bound DNT occurred while crystals were present. After the crystalline

DNT was gone, the aqueous concentration could drop below saturation and desorption of DNT from the soil could occur. It was also assumed that degradation rates could be predicted by Monod kinetics.

The model requires the user to input the total mass of DNT (μmol) added into the reactor. This number was calculated by multiplying the concentration of DNT in the soil by the mass of soil used in the soil washing procedure. The mass of soil used in the soil washing was calculated using the definition of nominal solids loading rate given in Chapter 4, section 4.2.0. and is shown in Table 5.1. This mass was used with the concentrations listed in Table 3.1 to determine the total DNT added to the reactor, shown in Table 5.1. These values for the total DNT were used for all subsequent tests with the model.

Table 5.1. Calculated values for mass of DNT into reactor for each solids loading rate.

Soil	Solids Loading	Mass Soil used in Soil Washing (kg)	Total DNT into Reactor (μmol)
BAAP	5%	3.5	171,923
	10%	7	343,846
	20%	14	687,692
	30%	21	1,031,538
	40%	28	1,375,385
VAAP*	5%	3.5	209,423
	20%	14	837,692
	30%	21	1,256,538

*Total DNT into reactor was calculated based on 10.89 g DNT/kg soil for VAAP soil

After this information is inputted to the model, the mass of DNT crystals present in the reactor is calculated. To calculate the mass of DNT crystals present, a mass balance must be performed on the DNT in the reactor. This is shown in Equation 5.1.

$$M_T = M_a + M_s + M_C \qquad (5.1)$$

In this equation, M_T is the total mass of DNT (μmol) present in the reactor, M_a is the mass of DNT in the aqueous phase (μmol), M_s is the mass of DNT associated with the soil (μmol), and M_C is the mass of DNT crystals in the reactor (μmol). Equation 5.1 can be modified to be in terms of the aqueous phase concentration as shown in Equation 5.2.

$$M_T = C_W V + C_W K_d masssoil + M_C \qquad (5.2)$$

In this equation, C_W is the concentration of DNT (μmol/L) in the aqueous phase, V is the volume of the reactor (L), K_d is the partition coefficient for DNT from the soil to the aqueous phase (L/kg), and masssoil is the mass of soil added to the reactor (kg). This equation is rearranged to solve for M_C to obtain the mass of crystals in the reactor. This equation can only be solved if it is assumed that when DNT crystals are present, the aqueous concentration is the solubility of DNT (1500 μmol/L). When this is assumed Equation 5.3 is obtained, which is used to solve for the mass of DNT crystals in the reactor.

$$M_C = M_T - (1500*V + 1500*K_d*masssoil) \qquad (5.3)$$

After the mass of crystals in the reactor is calculated, the first script, *crystals*, is called by the program. This script is only called if DNT crystals are present because it calculates the biomass produced, nitrite produced and total DNT consumed when crystals are the source of DNT for the aqueous phase. This script was written using the same assumption above that when DNT crystals are present in the reactor, the aqueous concentration of DNT is a constant. If this is applied to the Monod equation (Equation 5.1) for the change in biomass with time,

$$\frac{d[X]}{dt} = Y\left(\frac{k[S][X]}{K_s + [S]}\right) - k_d[X] \tag{5.4}$$

the equation becomes the first order differential equation shown in Equation 5.5

where $A = Y\left(\dfrac{k[S]}{K_s + [S]}\right) - k_d$.

$$\frac{d[X]}{dt} = A[X] \tag{5.5}$$

This equation can be easily solved to obtain Equation 5.6.

$$[X] = [X_0]\exp(A * t) \tag{5.6}$$

Equation 5.6 can be solved for the amount of time necessary to degrade the crystals

present in the reactor, which is shown by Equation 5.7, where "masscry" is the mass of

crystals (μmol) in the reactor and V is the volume (L) of the reactor.

$$t = \frac{\ln\left[\dfrac{\left[\dfrac{masscry * Y}{V} + [X_0]\right]}{[X_0]}\right]}{\dfrac{Y * k * S}{K_S + S} - b} \tag{5.7}$$

This time is designated as "tstop". This time is used to tell the script when crystals are no

longer present in the reactor. This script calculates the biomass concentration and nitrite

concentration in the reactor at different time steps until this "tstop" is reached. The

biomass concentration is calculated using Equation 5.5 and the nitrite concentration is

calculated based on stoichiometry. The final values of biomass concentration, total DNT,

nitrite concentration, aqueous concentration, and time are then sent to the second script

nocrystals.

Nocrystals was written assuming that the dissolution of the DNT crystals is complete, so desorption of DNT from the soil is now the source for dissolved DNT. For this script, the MATLAB function ode15s, a stiff differential equation solver was used. The solver requires the user to input an initial time, final time and an initial condition for each equation being solved. Four differential equations based on Monod kinetics were developed for *nocrystals*, which are shown in Equations 5.8, 5.9, and 5.10. Equation 5.8 is the differential equation for the change in total mass of DNT with time. Equation 5.9 is differential equation for the change in nitrite concentration with time. In this equation, Y_n represents the yield of nitrite, which is the stoichiometric coefficient for nitrite in the overall DNT biodegradation equation. Equation 5.10 is the differential equation for the change in aqueous concentration with time. The fourth differential equation used in this script is Equation 5.4, which calculates the biomass concentration with time. The time and initial conditions were given to this script from the previous script *crystals*.

$$\frac{d[M]}{dt} = -\left(\frac{\dfrac{k[X][M]}{K_d * masssoil + V}}{\dfrac{K_s + [M]}{K_d * masssoil + V}} \right) * V \qquad (5.8)$$

$$\frac{d[N]}{dt} = Y_n \left(\frac{k[S][X]}{K_s + [S]} \right) \qquad (5.9)$$

$$\frac{d[S]}{dt} = -\left(\frac{k[S][X]}{K_s + [S]} \right) \qquad (5.10)$$

The data from *crystals* and *nocrystals* is combined into one data set for all cycles. This data can then be saved and used in Excel for any other calculations.

The model also requires the user to denote the microbial kinetic parameters k, K_s, Y, and b. The data from the previous work did not allow for the calculation of the bacterial kinetic parameters. The spreadsheet method developed by Smith et. al. [1] was used in an attempt to determine the kinetic parameters for DNT degrading bacteria in the reactor, but spreadsheet method did not converge. This method is a non-linear regression that minimizes the sum of the least squares to determine the best fit of the kinetic parameters to the substrate concentration with time. This type of method requires that there is data for the substrate concentration on both sides of the saturation constant. In the experimental data shown in Chapter 4, the concentration of DNT is vastly above the saturation constant; therefore, this method could not converge. Since the kinetic coefficients could not be determined by a statistical analysis of the experimental data, the model was tested with the values determined by Heinze et. al. [2] The model was also tested by varying k and K_s to see their effect on the model's prediction.

The values published by Heinze were changed to match the units used by the model (k = 4.92 μmol DNT/μmol X d, K_s = 10 μmol DNT/L, Y = 0.48 μmol X/μmol DNT, and b equals 0.1 d^{-1}). Several tests were performed to determine to effect of K_s and k on the biodegradation of DNT in the reactor. For all soils and solids loading rates, K_s was tested using 5, 10, and 20 μmol DNT/d with k equal to 4.92 μmol DNT/μmol X d. For all solids loading rates, except 5% VAAP and BAAP, k was tested using 2.5, 4.92, and 10 μmol DNT/μmol X d with K_s equal to 10 μmol DNT/L. For the VAAP soil with a solids loading rate of 5%, k was tested with 1.5, 2.5, and 4.92 μmol DNT/μmol X d, and for BAAP soil with a solids loading rate of 5%, k was tested with 1, 2.5, 4.92, and 10 μmol DNT/μmol X d, both with K_s equal to 10 μmol DNT/d.

The final parameter that the user must input into the model is the initial biomass concentration. The biomass could not be measured directly in the experiments outlined in Chapter 4, so the model was used as a predictive tool to obtain the biomass concentrations in the reactor. To predict the biomass concentrations for each soil and solids loading rate, the order in which the soils and loading rates were tested is important because the effluent from the first experiment was used to inoculate the reactor for the next experiment. This procedure was followed for all solids loading rates. The order in which the soils and solid loading rates were tested in the previous work is as follows: 5% VAAP soil, 5% BAAP soil, 10% BAAP soil, 20% BAAP soil, 30% BAAP soil, 40% BAAP soil, 20% VAAP soil, and 30% BAAP soil. Therefore, the effluent from the 5% VAAP soil experiment was used to inoculate the reactor used to test the 5% BAAP soil.

The model was used to predict the initial biomass concentrations by varying the initial biomass concentration for 5% VAAP soil for several cycles (using the kinetic parameters determined by Heinze). The results for this test are shown in Figure 5.1. In this figure, an initial biomass concentration of 10 μmol/L is represented by the blue line, an initial biomass concentration of 154 μmol/L is represented by the green line and an initial biomass concentration of 1000 μmol/L is represented by the red line. The dotted line that runs along the bottom of the plot shows where the biomass concentration is equal to 154 μmol/L. This test proves that the biomass concentration at the beginning of each cycle is independent of the initial biomass concentration given to the model because
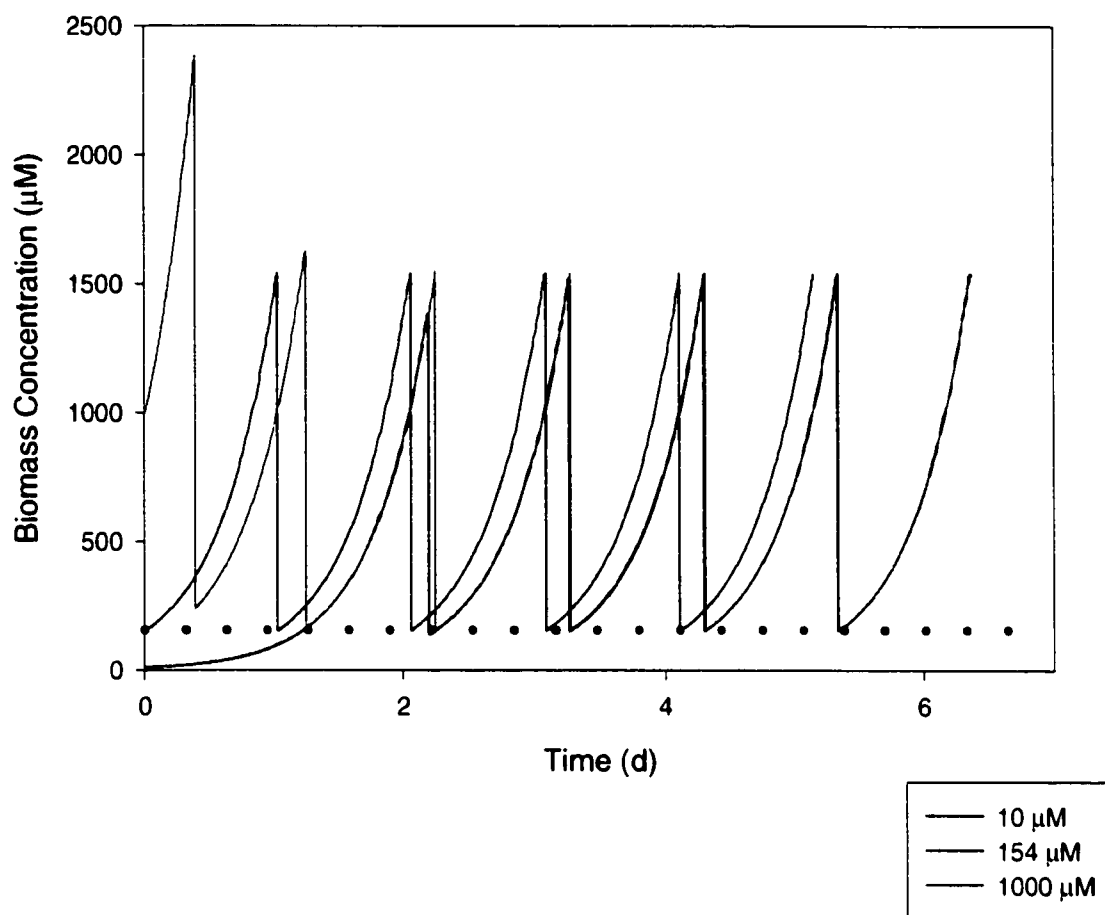
Figure 5.1. Effect of varying initial biomass concentration on biomass at end of cycle. (k = 4.92 μmol DNT/μmol X d, K_s = 10 μmol DNT/L, Y = 0.48 μmol X/μmol DNT, and b equals 0.1 d^{-1}).

all three initial biomass concentrations gave the same biomass concentration at the beginning of each cycle (154 μM).

This initial biomass concentration was then applied to the model to predict the initial biomass concentrations for the remaining soil and all solids loading rates. The results from this test are shown in Table 5.2. This table presents the initial biomass concentration that was used in the model, the average biomass produced from each cycle, the initial biomass predicted by the model after each cycle, and the standard deviation of the initial biomass concentration predicted by the model for both soils and all solids loading rates. The initial biomass concentrations shown in this table in column five are the values used for the initial biomass input into the model for all subsequent modeling tests.

Table 5.2. Model predicted initial biomass concentrations.

Soil	% Loading	Initial Biomass into Model[a] (μM/L)	Average Biomass Produced[b] (μM/L)	Average Initial Biomass[c] (μM/L)	Standard Deviation[d]
VAAP	5%	154.14	1541.93	154.14	0.15
BAAP	5%	154.14	1259.53	126.26	0.93
	10%	126.26	2565.33	255.08	4.30
	20%	255.08	5179.76	515.05	8.73
	30%	515.05	7794.78	776.52	8.79
	40%	776.52	10409.72	1038.06	8.66
VAAP	20%	1038.06	6316.66	636.18	13.40
	30%	636.18	9487.03	943.98	14.02

a – Initial condition for biomass into model
b – Average biomass predicted at end of cycle by model
c – Average initial biomass predicted by model at beginning of each cycle
d – Standard deviation of the average initial biomass predicted by model

An example of the data that the model created can generate is presented in Figure

5.2, for 5 cycles using BAAP soil with a nominal solids loading rate of 10% using the

kinetic parameters published by Heinze and an initial biomass concentration of 126 μM.

In this figure, the blue line is the aqueous DNT concentration, the black line is the nitrite

concentration, and the red line is the biomass concentration, all of which use the left y-

axis. The green line is the total DNT consumed in the reactor, which uses the right y-

axis.
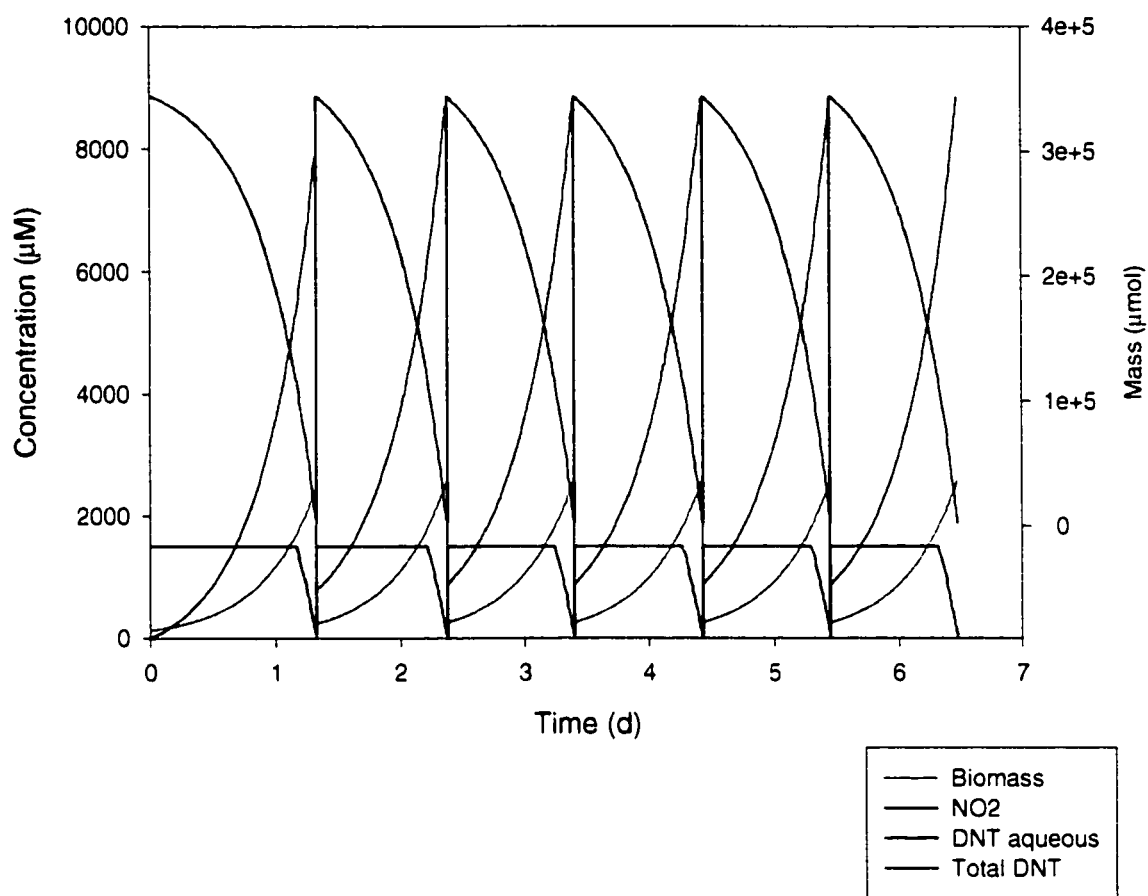
Figure 5.2. Data generated by model using BAAP soil with a 10% nominal solids loading rate (k = 4.92 μmol DNT/μmol X d, K_s = 10 μmol DNT/L, Y = 0.48 μmol X/μmol DNT, and b equals 0.1 d⁻¹).

Figure 5.2. Data generated by model using BAAP soil with a 10% nominal solids loading rate (k = 4.92 μmol DNT/μmol X d, K_s = 10 μmol DNT/L, Y = 0.48 μmol X/μmol DNT, and b equals 0.1 d^{-1}).

References

1. Smith, L.H., P.L. McCarty, and P.K. Kitanidis, Spreadsheet method for evaluation of biochemical reaction rate coefficients and their uncertainties by weighted non-linear least-squares analysis of the integrated monod equation. *Appl. Environ. Microbiol.*, 1998. **64**: p. 2044-2050.

2. Heinze, L., M. Brosius, and U. Wiesmann, Biological Degradation of 2,4-Dinitrotoluene in a Continuous Bioreactor and Kinetic Studies. *Acta Hydrochim. Hydrobio.*, 1995. **23**(6): p. 254-263.

CHAPTER SIX

RESULTS: REMEDIATION OF DINITROTOLUENE CONTAMINATED SOILS FROM FORMER AMMUNITION PLANTS: SOIL WASHING EFFICIENCY AND MINERALIZATION STOICHIOMETRY IN BIOSLURRY REACTORS

The contents of this chapter are the result of a collaborative effort with Dr.

Chunlong Zhang. This work has been submitted to the Journal of Hazardous Materials

(received January 2001). It is reproduced here with the permission of Dr. Zhang and as

submitted with the only alteration being re-numbering of tables and figures to adhere to

the formatting of the thesis.

6.0.0. Abstract

A pilot-scale bioslurry system was used to test the treatment of soils highly contaminated with 2,4-dinitrotoluene (2,4-DNT) and 2,6-dinitrotoluene (2,6-DNT). The treatment scheme involved a soil-washing process followed by two sequential aerobic slurry reactors augmented with 2,4-DNT- and 2,6-DNT-mineralizing bacteria. Test soils were obtained from two former army ammunition plants, the Volunteer Army Ammunition Plant (VAAP, Chattanooga, TN) and the Badger Army Ammunition Plant (BAAP, Baraboo, WI). Soil washing was used to minimize operational problems in slurry reactors associated with large particulates. The Eimco slurry reactors were operated in a draw-and-fill mode for 3 months and were monitored for the biodegradation of 2,4-DNT and 2,6-DNT, nitrite production, NaOH consumption, and oxygen uptake rate. Results show that soil washing was very effective for the removal of sands and the recovery of soil fines containing 2,4-DNT and 2,6-DNT. Bioslurry reactors offered rapid and nearly complete degradation of both DNT isomers, but require real time monitoring to avoid long lag periods upon refeeding. Results found a significant discrepancy between the measured DNT concentrations and calculated DNT concentrations in the slurry reactors because of solids profiles in the slurry reactors and the presence of floating crystal of DNTs. Based on the actual amount of dinitrotoluene degradation, nitrite release, NaOH consumption, and oxygen uptake were close to the theoretical stoichiometric coefficients of complete DNT mineralization. Such stoichiometric relationships were not achieved if the calculation was based on the measured DNT concentrations due to the heterogeneity of DNT in the reactor. Results indicate that nitrite release, NaOH consumption, and oxygen uptake rates provide a fast assessment of

2,4-DNT degradation and microbial activity in a slurry reactor, but could not be extended to a second reactor in series where the degradation of a much lower concentration of 2,6-DNT degradation was achieved.

6.1.0. Introduction

Dinitrotoluene (DNT) isomers are common soil contaminants at Department of Defense (DoD) and commercial polyurethane foam facilities. The two primary isomers of dinitrotoluene found at these facilities are 2,4-DNT and 2,6-DNT, and the U.S. EPA lists both as priority pollutants. Soils contaminated with DNTs can be treated by traditional means such as incineration, but the cost is high. Over the past decades, aerobic bioremediation of DNT contaminated media has been an area of extensive research [1,2,3,4,5] in an attempt to develop a low-cost alternative.

In a previous report [6], we demonstrated the use of pilot-scale aerobic slurry-phase bioreactors to treat highly contaminated soils containing both 2,4-DNT and 2,6-DNT following augmentation of DNT-mineralizing bacteria. Two factors that complicated the operation of these systems were identified. First, sands or other large particulates clogged the reactors and eliminated mixing. Second, the sustainability of rapid degradation rates required that systems be adequately monitored throughout feeding cycles (carried out by HPLC analysis). If DNT was allowed to be completely depleted from a reactor for as short as several hours without refeeding, a long lag period followed and reduced levels of activity were observed. In extreme cases, activity was lost and reinoculation was required. This need for nearly continuous monitoring – relying on HPLC analysis – for biodegradation activity translated into a significant component of the overall cost estimates for treating contaminated soils with this approach [7].

The clogging of the bioreactors was addressed by the use of a soil washing process to remove sands from the contaminated soils before addition to the reactors. Despite the fact that only fine grain material was then fed to the reactor, a heterogeneous solids concentration existed in tested pilot-scale systems. For example, fine DNT crystals were observed floating as a mat in the slurry reactor initially after feeding. Also, mixing was not ideal and accumulation of solids at the base of the system occurred. This heterogeneous solids concentration complicated the ability to directly assay contaminant levels, and to monitor the rates of degradation actually occurring. Furthermore, the inability to analyze the actual levels of contaminants in the system created uncertainty in the levels of amendments required.

The results of soil washing process efficiency and various low-cost monitoring strategies are presented herein as surrogates to direct measures of DNT degradation in these slurry reactor studies. The surrogate measures tested include release of nitrite, consumption of NaOH, and oxygen uptake rates. The comparison of results from HPLC analysis and these surrogate parameters suggest that effective routine monitoring of 2,4-DNT degradation (the primary contaminant in soils tested) can be obtained without HPLC if the effectiveness of the soil wash process is known. The extension of these surrogate analytes as guides of 2,6-DNT degradation was problematic.

6.2.0. Experimental Section

6.2.1. Description of contaminated sites

Two soils obtained for study came from the Volunteer Army Ammunition Plant (VAAP, Chattanooga, TN) and the Badger Army Ammunition Plant (BAAP, Baraboo, WI). At the VAAP site, soil was collected from 4 points along the drainage ditch outflow

from the Acid Recovery House of TNT production Line 4. Soil containing up to 200

g/kg of 2,4-DNT was found within 5 m of the Acid Recovery House, and soil with lower

concentrations of 2,4-DNT (2-3 g/kg) but higher concentrations of 2,6-DNT (0.5-1 g/kg)

were collected approximately 50 to 150 m down gradient. The soil was stored in 55-

gallon drums at ambient temperature for 6 months before processing. At the BAAP site,

soil core samples were collected in 1997 from Propellant Burning Ground Waste Pit-1, -

2, and -3. Several drums of contaminated soils were shipped to Air Force Research Lab

in February 1999.

6.2.2. Treatment scheme

A schematic of the unit process and unit operation developed in this study is

shown in Figure 6.1. The treatment scheme involved a soil pretreatment unit, a soil

washing unit, two identical bioslurry reactors operated in series, and a coagulation /

sedimentation tank. Soils from contaminated sites were air-dried followed by the removal

of gravel and large debris. The dried soils were repeatedly passed through a sieving and

tumbling machine until uniform soils were obtained. Because large amounts of sand

interfered with reactor operation, soils were treated by soil washing before use. Soil

washing was performed in a 14-L cylinder with an upward jet flow of warm (60 °C) tap

water to separate DNT-associated fines from the clean sand. The resulting soil slurry was

used in bioreactors and the sand was discarded.

Slurries generated from soil washing were pumped into a 75-L Eimco Biolift

slurry reactor (Model B75LA, Tekno Associates, Salt Lake City, UT). Two reactors

were operated in series for the treatment of both isomers in a sequential mode as

described previously [6]. Both reactors were equipped with agitation, aeration, and
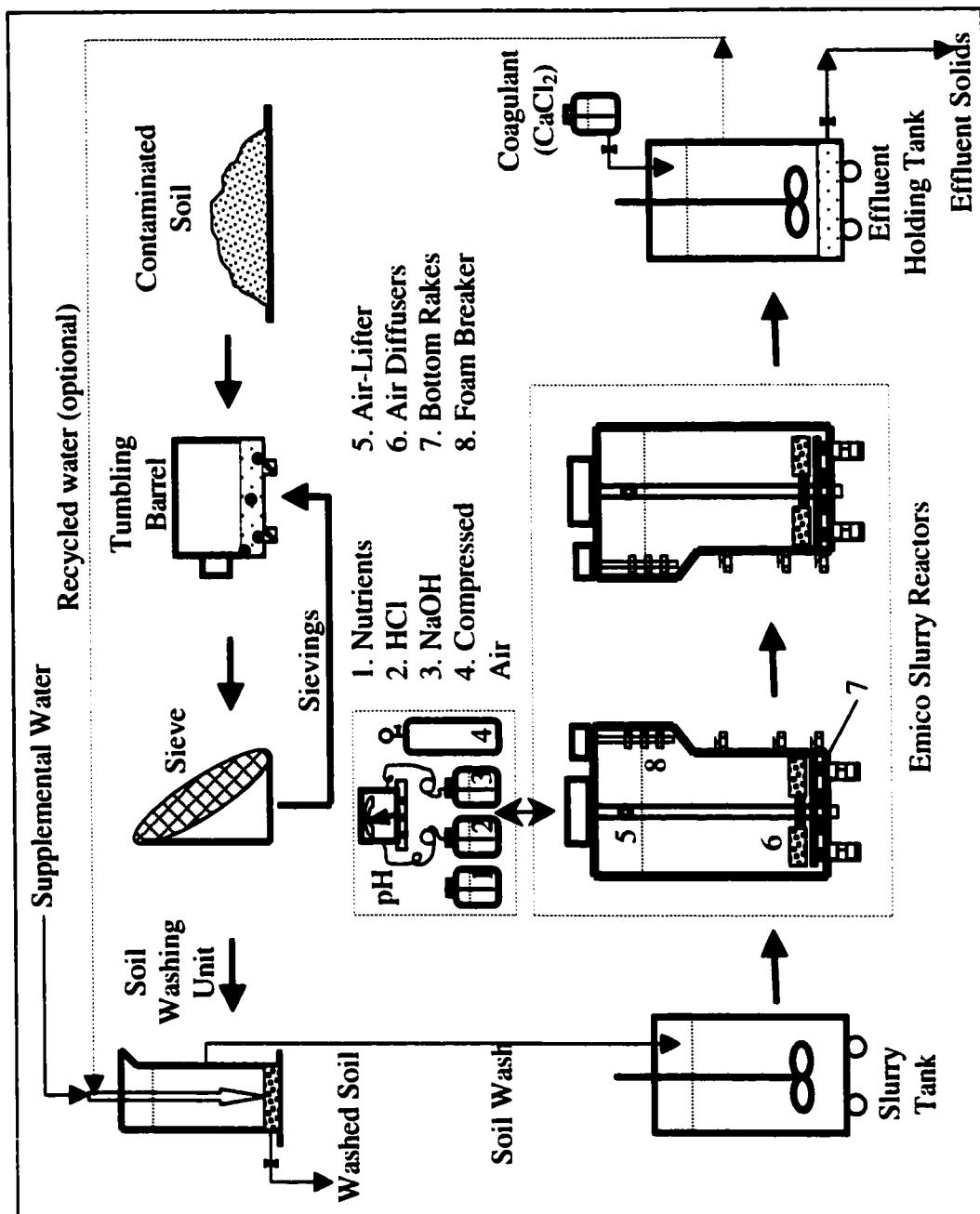
Figure 6.1. Treatment scheme of pilot-scale soil washing and sequential aerobic slurry reactor system

temperature control. The temperature was maintained at 30 °C, and pH was maintained

in the range of 6.75 ~ 7.25 using a pH controller and NaOH (12.5 N).

Effluent from the second slurry reactor was further treated in a holding tank. This

was accomplished by addition of a coagulant ($CaCl_2$), followed by the gravity separation

of solids and supernatant liquid.

6.2.3. Slurry reactor operation

Two identical reactors were operated simultaneously and continuously for a period

of 3 months. Solids loading rate (i.e., mass of soil added per unit volume of reactor

(w/v)) is typically used to describe the levels of soils added to slurry reactors. However,

contaminated soils were not added directly to the reactors in this study, so the actual

solids concentration in a reactor depended on the amount of soil added to the soil wash

unit, and the percentage (weight basis) of large soil particulates removed by the soil

washing process. For this reason, the term "nominal solids loading rate" is used

throughout this paper to reflect levels of soil treated by the overall process. For example,

a nominal 10% solids loading is equivalent to 7 kg of soil added to the soil washing

process, which became feed for fill-and-draw operation, since the operating volume of

the reactor was 70 L. VAAP soil was tested at nominal solids loading rates of 5, 20, and

30%, whereas BAAP soil was tested at nominal solids loading rates of 5, 10, 20, 30, and

40% (Table I). A comparison of the nominal solids loading rates and actual solid

concentrations in reactors along with DNT concentrations in reactors is presented in

Table 6.1.

As shown in Table 6.1, the actual solids concentration in the reactor was lower

than the nominal solids loading rate. The difference was more evident for sandy soils

Table 6.1. Solids loading, suspended solids, and initial DNT concentrations in the slurry reactor[1]

	Unit	Solids loading rates tested in this study				
VAAP soil:						
Nominal solids loading rate	% (w/v)	5	20	30		
Actual solids loading rate	% (w/v)	4	16	25		
Suspended solid (SS)	×10³ mg/L	40	160	250		
2,4-DNT	μM	2990	11960	17940		
2,6-DNT	μM	240	960	1440		
BAAP soil:						
Nominal solids loading rate	% (w/v)	5	10	20	30	40
Actual solids loading rate	% (w/v)	0.7	1.3	2.6	3.9	5.2
Suspended solid (SS)	×10³ mg/L	7	13	26	39	52
2,4-DNT	μM	2450	4900	9800	14700	19600
2,6-DNT	μM	130	260	520	780	1040

[1]The removal of large soil particulates was assumed to be 18% for VAAP soil and 87% for BAAP soil, based on the averaged data from experiment. Reactor volume = 70 L.

(e.g., BAAP soil) than clay soils (VAAP soil) since a higher percentage of large soil particulates were associated with sandy soil. Note also that the suspended solids concentration is a calculated concentration based on the actual mass of soil entered into the reactor, assuming a homogeneous distribution.

6.2.4. System monitoring and sample analysis

Three sampling ports (bottom, middle, and top) were located along the side-wall of the reactor at 2, 15, and 40 cm from the bottom of the reactors. Routine samples were taken from the top sampling port of the reactor side-wall. Slurry samples taken from the reactor were transferred to a beaker and mixed vigorously with a magnetic stir plate. Sub-samples were withdrawn through a large-bore pipette tip.

To determine DNT concentrations, samples were extracted and analyzed by a Hewlett Packard series 1050 HPLC equipped with a UV detector according to previously described methods [8]. The extraction procedure allowed for the determination of the aqueous phase concentration, the solid phase concentration (centrifugation of slurry samples, followed by the extraction of solids with acetonitrile), or the overall slurry concentration. The mass of 2,4-DNT in the reactors often exceeded its aqueous solubility, and crystalline DNT was often present at the beginning of the cycles. Therefore, the results of HPLC analysis are presented as the slurry phase concentration, which corresponds to the total amount of DNT per liter of slurry [6].

Subsamples for nitrite analysis were centrifuged and the supernatant was immediately withdrawn and subjected to analysis using a modified colorimetric method [9]. Absorbance readings were made at 560 nm on an EL340 Automated Microplate Reader (Bio-Tek Instruments, Inc., Winooski, VT). Slurry samples taken for oxygen

uptake rate analysis were placed directly in a 300-mL BOD bottle. After re-aeration at 30 °C, dissolved oxygen concentrations were measured using a YSI Model 58 dissolved oxygen meter with a YSI 5905 BOD probe (Yellow Springs Instrument Co., Inc., Yellow Spring, OH). A typical oxygen consumption curve demonstrated zero-order kinetics, and the oxygen uptake rate was determined directly by linear regression.

The reactors were also routinely monitored by the measurement of temperature, pH, SS, and NaOH consumption. Treated soil wash (sludge) samples were also taken for the analyses of residual 2,4-DNT and 2,6-DNT [10]. These samples were taken after the settling of the reactor effluent from representative runs and subsequent decanting of the supernatant. The wet sludge samples were oven-dried overnight at temperature below 55°C and subjected to homogenization prior to analysis.

6.3.0. Results and Discussion

6.3.1. Soil washing unit performance

In an attempt to improve reactor mixing and overcome clogging problems when soils were fed directly, soil washing studies were conducted to evaluate the potential to remove contaminants from the sand with a repeated resuspension in water – simulating a soil washing procedure. Preliminary results from bench studies (data not shown) indicated that soil washing could effectively remove sandy materials while leaving most of the DNT in the slurry phase. Further studies were conducted to determine the ability to reduce the volume of water required, so that the procedure could be implemented for use as a pretreatment for both soils.

Figure 6.2A shows the mass of particulates removed in soil wash. In general, soil washing was very successful in separating large particles from both soils. On a weight
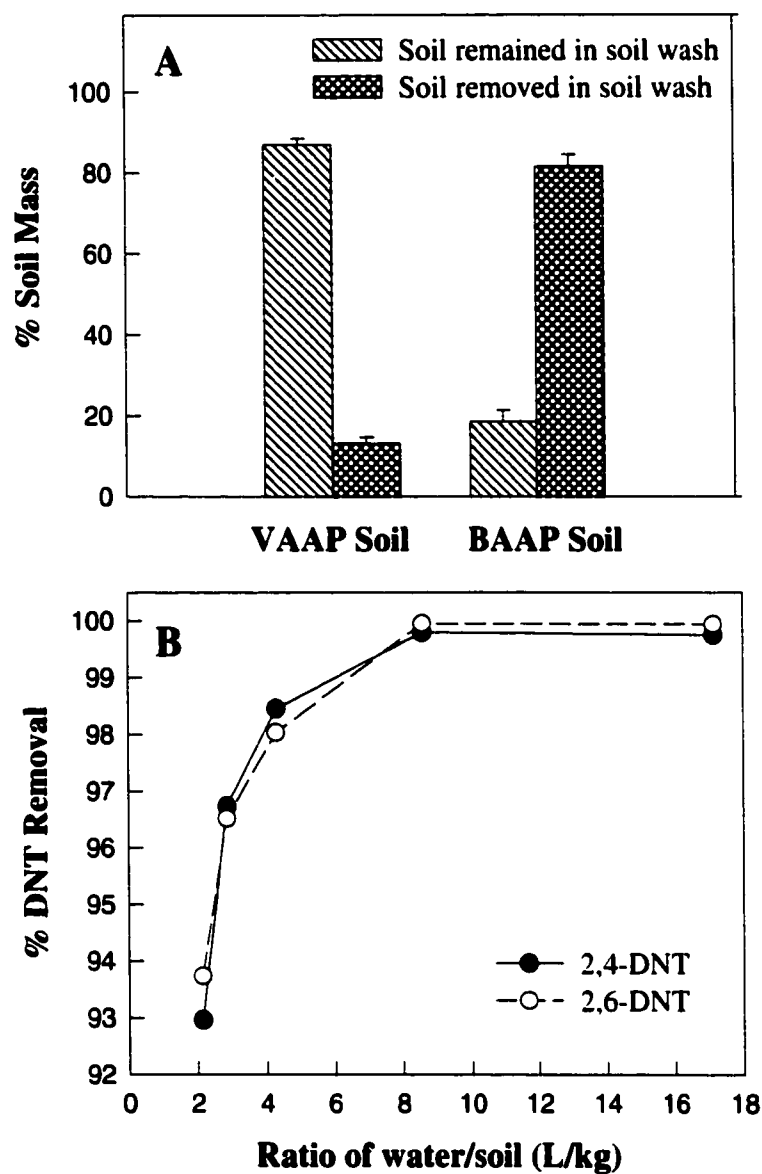
Figure 6.2. (A) Soil mass distribution after soil washing process: VAAP soil vs. BAAP soil; (B) Effects of water / soil ratio on soil washing efficiency (BAAP soil)

basis, 87% of large particles in BAAP soil were removed after soil washing. The remaining 13% were finer particles suspended in the soil slurry. For VAAP soil, the distribution after soil washing was nearly reversed, as VAAP soil was comprised primarily of fine particles. Approximately 18% of VAAP soil (weight basis) was removed after soil washing, and 82% of the soil was fine particles suspended in the slurry phase.

Figure 6.2B shows the mass of DNT retained in the slurry phase for BAAP soil. The efficiency was examined at different ratios of water/soil to determine the appropriate water volume required for preparation of reactor feed. The results suggest that a water/soil ratio of 10 L/kg or greater resulted in nearly complete retention of contaminants after removal of the sands. However, a ratio of 5 L/kg or less resulted in reduced efficiency and significant DNT levels remained associated with residuals. For VAAP soil, a similar pattern was noticed (data not shown). Increasing water/soil ratio apparently improved soil washing efficiency. However, VAAP soil appeared to have higher residual concentrations when compared to BAAP soil at identical operational conditions. A water/soil ratio of 17 L/kg was necessary to maintain a 98% or higher reduction in concentration. Under the operational conditions tested in this study, an efficiency of 99.3% or greater was achieved in all soil washing steps.

Without the use of soil washing pretreatment, clogging of the airlift in the slurry reactor occurred even at a 5% solids loading rate. The ability to effectively remove DNT in a soil wash process to improve the reliability of slurry phase bioremediation is an important concern in application. Residual levels of DNT in coarse materials may

require some additional level of treatment before disposal; however, the biodegradation potential of trace levels of residual DNT was not evaluated.

6.3.2. Slurry reactor performance and monitoring for 2,4-DNT degradation

Samples taken from the slurry reactor immediately after feeding were analyzed by HPLC and compared to the DNT concentration that should have resulted based upon the known mass of DNT in the feed slurry (analyzed by HPLC). Results are presented in Figure 6.3A at different solids loadings of BAAP soil (5%, 10%, 20%, 30% and 40%). These results show a significant discrepancy between the measured DNT concentrations and the calculated DNT concentrations in the slurry reactors (the known mass of DNT added to the reactor divided by the reactor volume). A similar discrepancy was observed in VAAP soil (Figure 6.3B). For both soils, the discrepancies increased as the solids loading rates increased, suggesting that sampling procedures did not take into account the heterogeneous nature of the reactor. This hypothesis is supported by the observation of DNT crystals floating as a mat in the reactors shortly after feeding, which disappeared as degradation proceeded.

The implications of this finding are of consequence to the ability of the operation and monitoring of the reactor. In terms of reactor operation, the inability to measure true levels on DNT in the system can lead to an underestimation of the nutrient or electron acceptor requirements. In terms of monitoring, the inability to measure actual levels of contamination reduces the ability to assess the extent to which biodegradation is, or is not, occurring. Therefore, parameters other than slurry-phase DNT were tested for monitoring reactor performance.
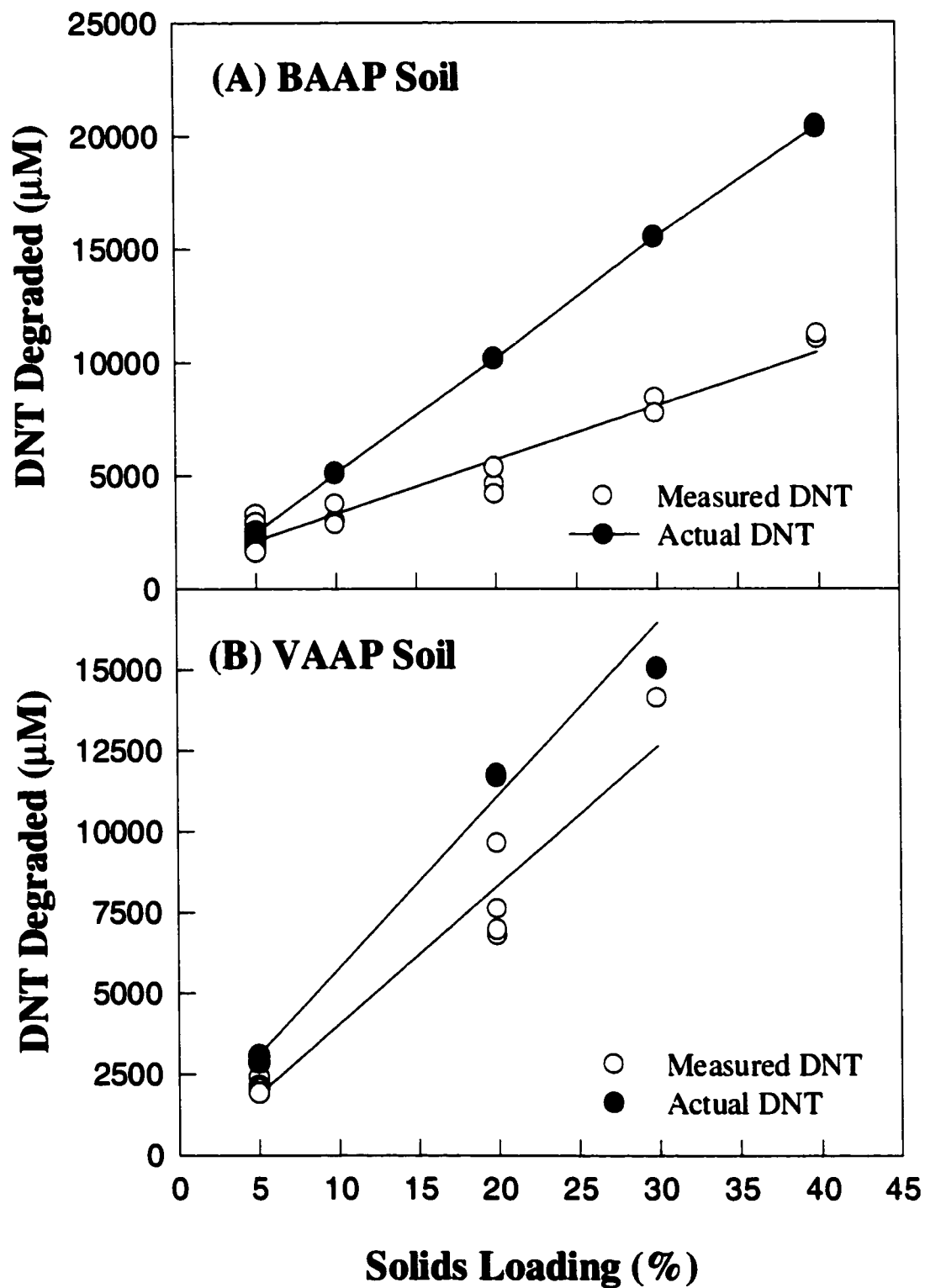
Figure 6.3. Measured DNT degradation vs. actual 2,4-DNT degradation at different solids loading rates: (A) BAAP soil; (B) VAAP soil

Figure 6.4A presents the production of nitrite in 20 feeding cycles of BAAP soil

wash during the course of 2,4-DNT degradation. As expected, the pattern of the nitrite

production corresponded to the disappearance of dinitrotoluene, and concentrations of

nitrite produced increased proportionally with increases in solids loading rates. Figure

6.4B presents the oxygen uptake rate obtained in each feeding cycle (data not available for

the first cycle). Oxygen uptake rates appear to correlate with the overall 2,4-DNT

degradation activity in the reactor, with peak oxygen uptake rates increasing with

increasing solids loading rates. A maximum oxygen uptake rate was observed when the

nominal solids loading rate reached 20% ($\approx$2.0 mg/L*min).

Figure 6.5A presents 2,4-DNT and nitrite concentration profiles in VAAP soil

slurry reactors. The maximum nitrite concentrations were approximately 35,000 μM at a

20% nominal solids loading rate. As with BAAP soil, the pattern of nitrite production

corresponded to the disappearance of dinitrotoluene (Note that the maximum

concentrations at a 30% loading rate remained about the same as the concentrations at a

20% loading rate because a fill-and-draw was initiated prior to the complete degradation of

2,4-DNT). Figure 6.5B presents the oxygen uptake rate in the same soil, and again oxygen

uptake rates appear to correspond with microbial DNT degradation activity in the reactor.

The peak oxygen uptake rates ranged between 1.3 and 2.6 mg/L*min, as compared to the

observed maximum oxygen uptake rate of 2.0 mg/L*min for BAAP soil.

NaOH data was collected as volume (ml) consumed per feed cycle (data not

shown). For the BAAP soil, the NaOH consumption was consistent with the degradation

pattern of DNT. At 5, 10, 20, 30 and 40% nominal solids loading, average NaOH
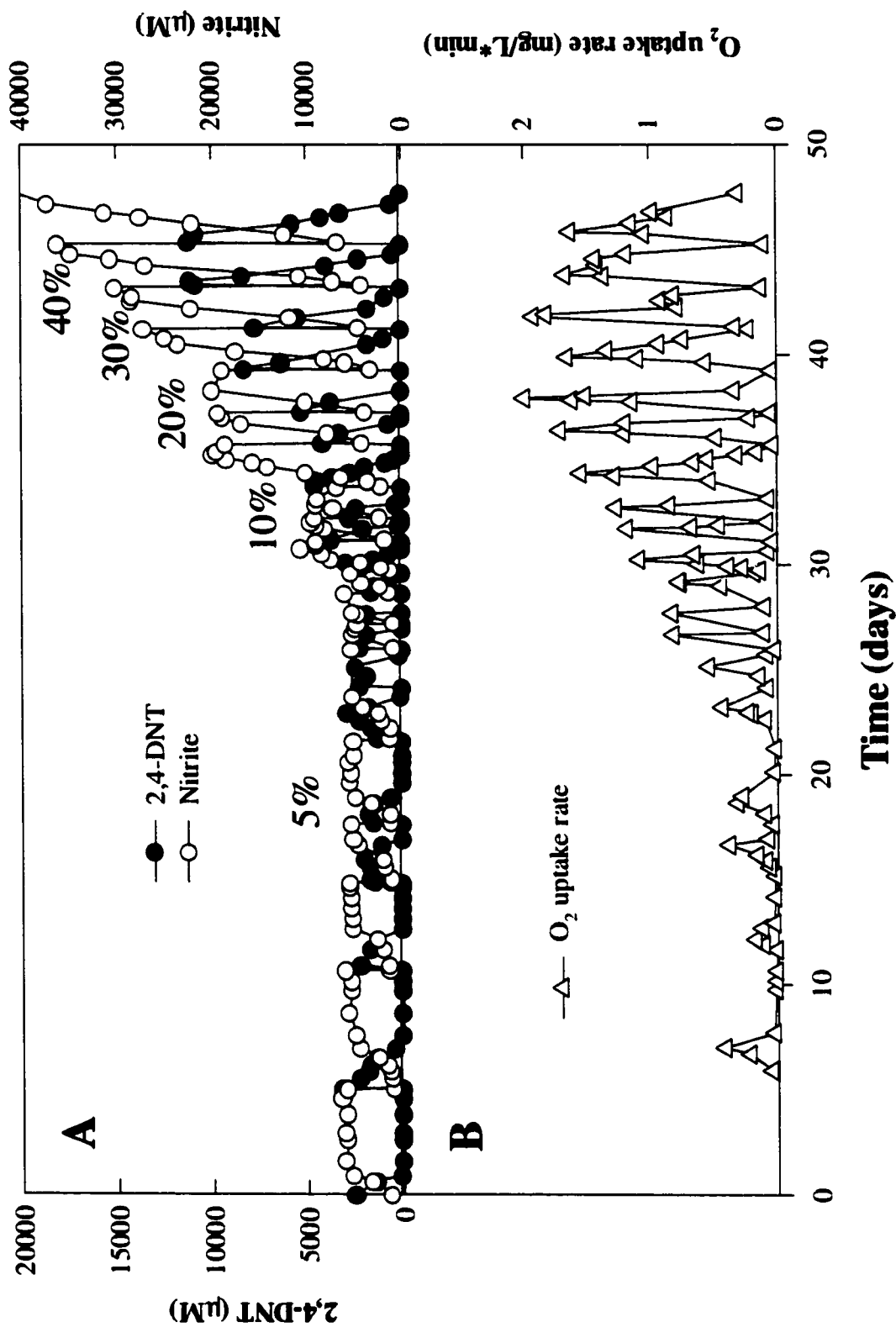
Figure 6.4. Temporal concentration profiles of (A) 2,4-DNT and nitrite (data for 2,4-DNT concentration previously reported in [8]); (B) oxygen uptake rate with BAAP soil (% are nominal solids loading rates)
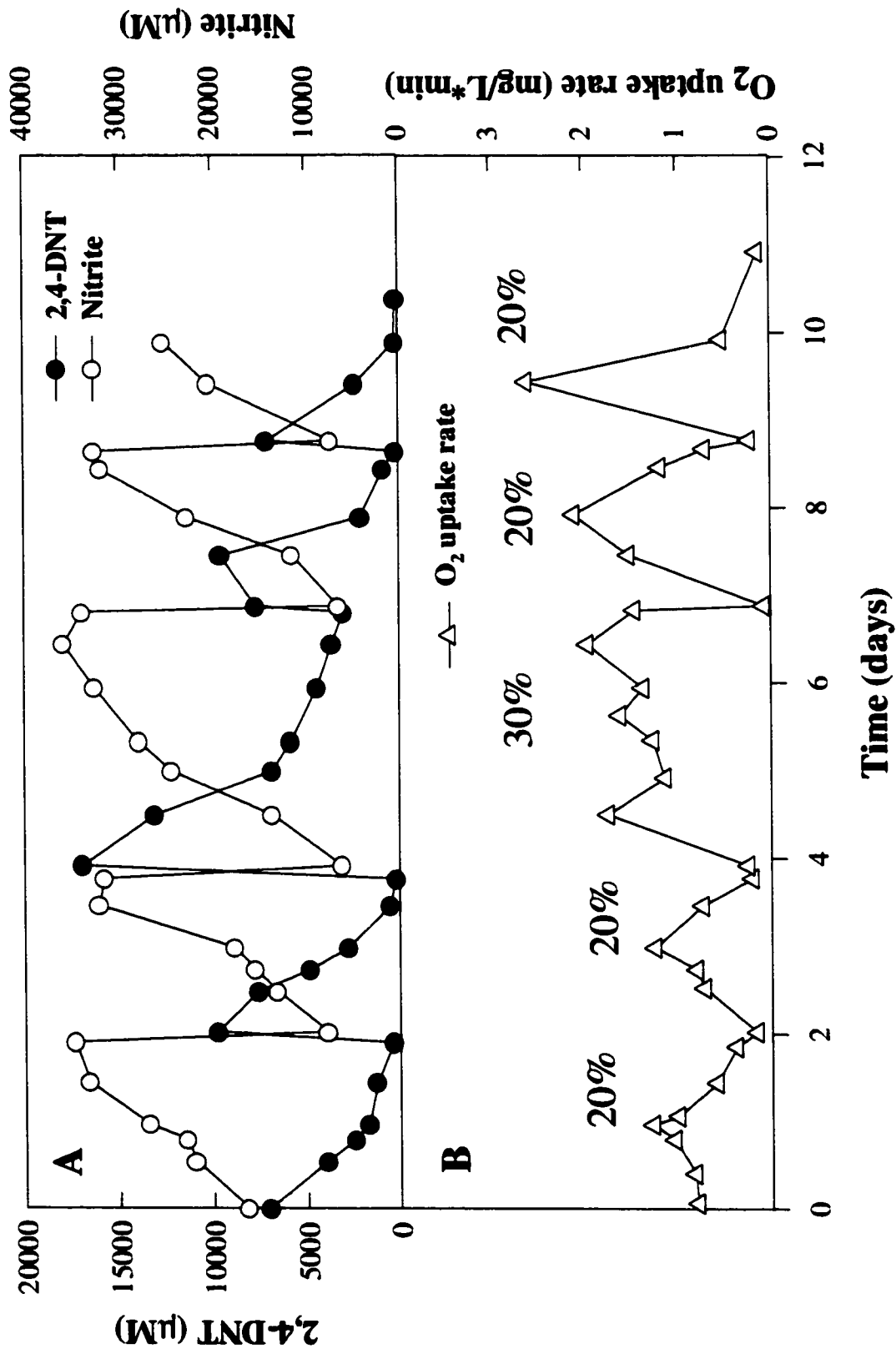
Figure 6.5. Temporal concentration profiles of (A) 2,4-DNT and nitrite (data for 2,4-DNT concentration previously reported in [8]); (B) oxygen uptake rate with VAAP soil (% are nominal solids loading rates)

consumption was 26, 42, 92, 142 and 186 ml, respectively. The NaOH consumption for VAAP soil was also consistent with the DNT degradation pattern. The average NaOH consumption at a 20% nominal solids loading rate was 94 ml.

The nitrite production, oxygen uptake rate, and NaOH consumption data can be used to calculate the molar ratio of each compound produced or consumed to DNT degraded. These molar ratios can then be compared to the molar ratio predicted from the stoichiometry of the biodegradation of DNT. The oxidation of DNT to CO_2 and nitrite results in the consumption of oxygen and the production on H^+. A balanced reaction for complete DNT oxidation is shown in Equation 1.

$$C_7H_6N_2O_4 + 8O_2 \rightarrow 7CO_2 + 2H_2O + 2NO_2^- + 2H^+ \tag{6.1}$$
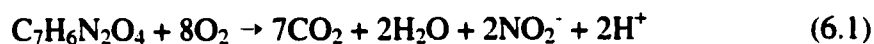
However, this reaction does not consider biomass synthesis. To obtain the stoichiometry of the reaction with biomass synthesis considered, bioenergetic calculations for the biodegradation of DNT were performed. These calculations were completed using the procedure developed by McCarty [11,12]. First, the half reaction of DNT was developed:

$$1/32 \; C_7H_6N_2O_4 + 7/16 \; H_2O \rightarrow 7/32 \; CO_2 + 1/16 \; NO_2^-$$
$$+ \; 17/16 \; H^+ + e^- \quad \Delta G_f^0 = -0.234 \; kcal/eq \tag{6.2}$$
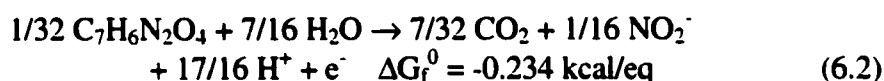
The free energy of formation values published by Mavrovouniotis [13] and Brock and Madigan [14] were used to calculate the standard free energy of formation of the DNT half reaction. The free energy of formation for DNT is not a published value; it was calculated using the group contribution method developed by Mavrovouniotis [13] with the NO_2 contribution determined by Shelly et. al. [15]. The efficiency of energy transfer by dinitrotoluene degraders was assumed 60% [16] because a value has not been determined

experimentally. The bioenergetic calculations resulted in the following stoichiometry that

includes biomass synthesis:

$$C_7H_6N_2O_4 + 5.62 \ O_2 \rightarrow 5.17 \ CO_2 + 1.63 \ NO_2^- + 1.63 \ H^+$$
$$+ 0.90 \ H_2O + 0.37 \ C_5H_7O_2N \qquad (6.3)$$
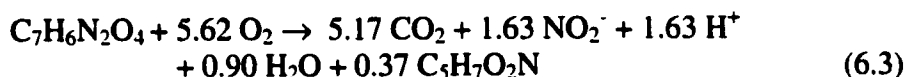
The stiochiometry appears to be different from a previous study reported by Lendenmann

et al [17]. In this fluidized-bed reactor study, 9 moles of oxygen were required for one

mole of DNT. However, this value was derived solely on chemical oxidation (i.e., no

biomass synthesis) and included the impact of nitrite-oxidizing bacteria that were present

in the fluidized-bed reactor. In the slurry reactors, nitrate production was not detected at

any significant levels.

Assuming that the stoichiometry in Equation 6.3 is predictive of the biological

activity in the reactor (i.e., degradation of other organic material is an insignificant

contribution to the consumption/production of constituents in the aforementioned reaction)

it is possible to use oxygen consumption, nitrite release, and acid neutralization as control

parameters. Of these three, only the analysis of oxygen demand is complicated by

heterogeneous solids profiles, as our method for oxygen demand required the monitoring

of oxygen uptake by a slurry sample taken from the reactor.

The overall stoichiometric relationship obtained between nitrite production and

total dinitrotoluene degraded (based on soil washing efficiency) in BAAP soil at five

different loading rates is presented in Figure 6.6A. The mole ratio of [NO$_2^-$]/[DNT] was

1.61 based on DNT degraded. Figure 6.6B shows a similar stoichiometric relationship for

VAAP soil at three different solids loadings. Although data were slightly more scattered

for VAAP soil, a similar mole ratio of 1.85 [NO$_2^-$]/[DNT] was obtained.
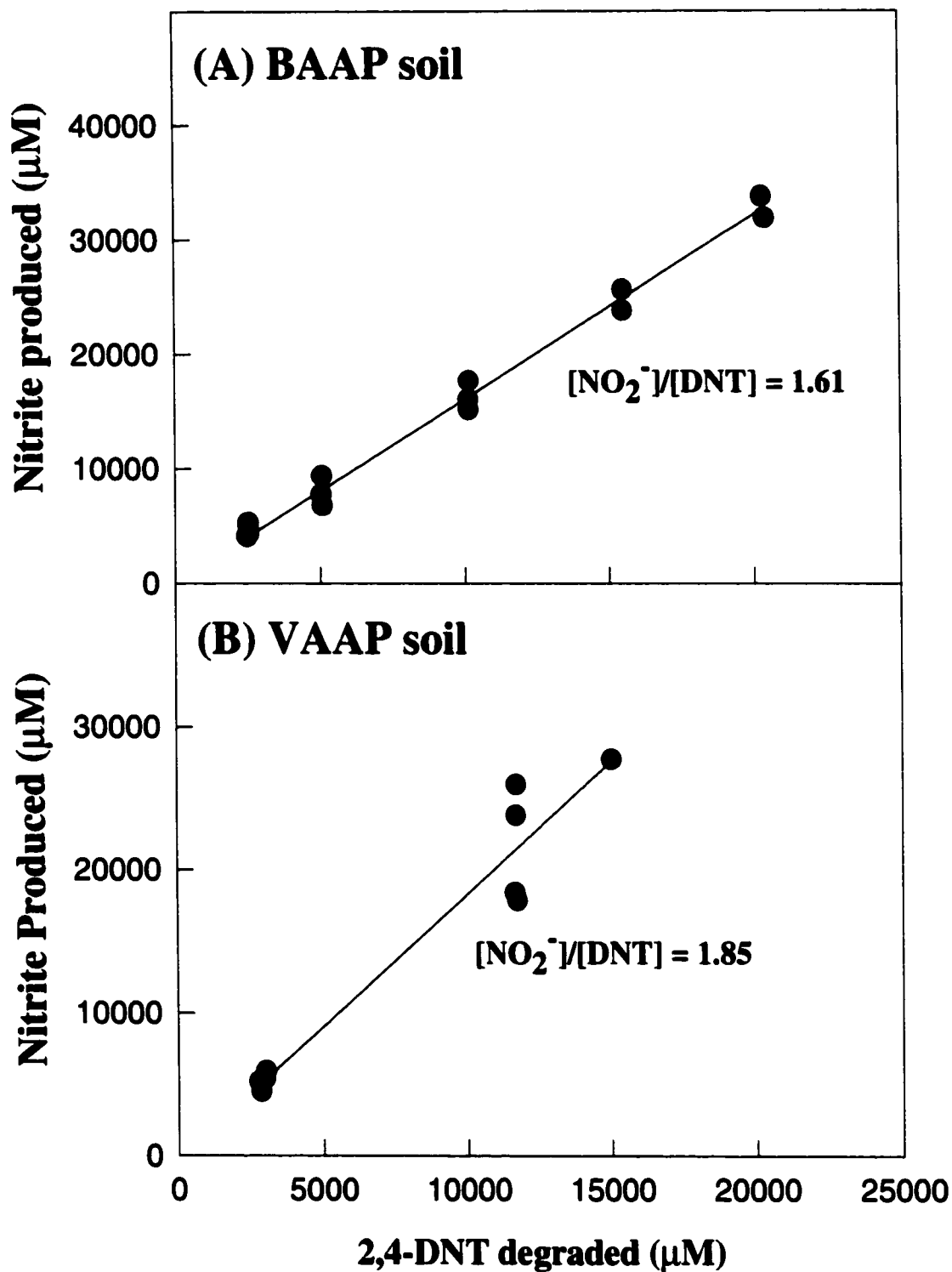
Figure 6.6. Stoichiometric relationships between 2,4-DNT degradation and nitrite production at various test loading rates: (A) BAAP soil, (B) VAAP soil

Figure 6.7A is the stoichiometric relationship between NaOH consumption and the

amount of total dinitrotoluene degraded in BAAP soil at five different loading rates. The

mole ratio of [NaOH]/[DNT] was 1.63 based on actual DNT degraded. Figure 6.8B is the

same stoichiometric relationship for VAAP soil at three different solids loadings. The

mole ratio of [NaOH]/[DNT] obtained was 1.66.

Oxygen consumption was calculated using the sum of the average rate of oxygen

uptake over discrete time intervals, and the DNT degradation that occurred during that time

interval. Figure 6.8A presents observed oxygen consumption during the degradation of

dinitrotoluene in BAAP soil, and Figure 6.8B presents observed oxygen consumption for

VAAP soil. (Note data in Figure 6.8A and 6.8B were from a single feeding cycle). The

molar ratio of oxygen consumption to DNT degradation was 6.82 for BAAP soil and 5.64

for VAAP soil.

The values of nitrite production, NaOH addition, and oxygen consumption compare

favorably with what is predicted by stoichiometry. NaOH addition was the most accurate

and least variable of all parameters assessed. Cumulative oxygen consumption was the

most difficult parameter to evaluate because it is extrapolated from instantaneous oxygen

uptake rate data. Also, cumulative oxygen uptake has the potential interference of

metabolism of organics other than DNT in the reactor. For example, BAAP soils had a

noticeable fuel odor prior to soil washing. Presumably, some of these fuel-related organics

were degraded (a parameter not measured directly) in the reactor, which would explain the

higher molar O_2/DNT ratio observed.
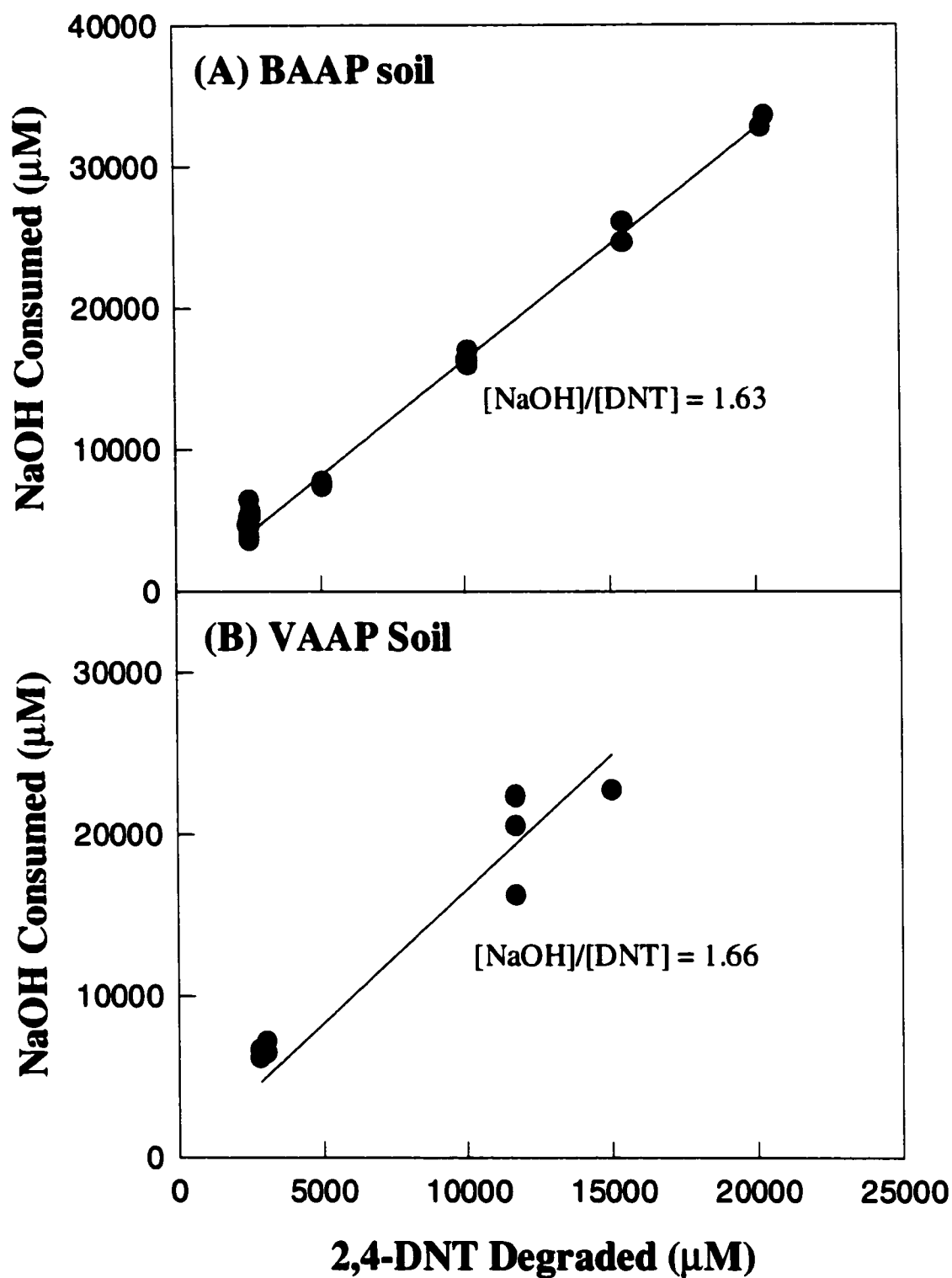
Figure 6.7. Stoichiometric relationships between 2,4-DNT degradation and NaOH consumption at various test loading rates: (A) BAAP soil, (B) VAAP soil same stoichiometric relationship for VAAP soil at three different solids loadings.
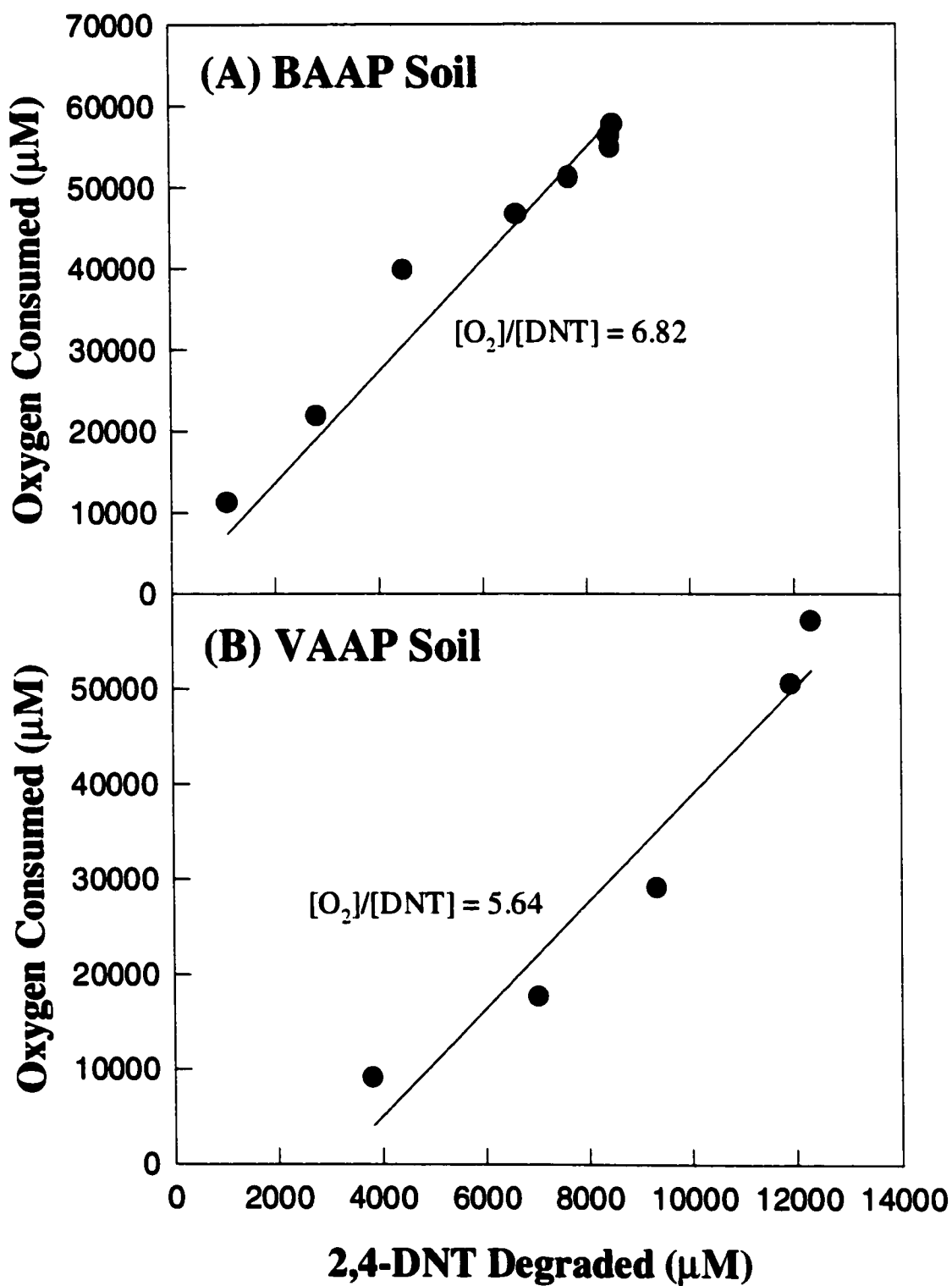
Figure 6.8. Stoichiometric relationships between 2,4-DNT degradation and oxygen consumption

Beyond the overall reaction stoichiometry observed, the use of surrogate

parameters to determine reactor performance overcame the difficulties in assessing activity

through the measurement of 2,4-DNT concentrations in the slurry reactor. Figure 6.9

presents the relationship between 2,4-DNT degradation and two related monitoring

parameters: nitrite production and oxygen uptake rate. Data shown is from a single

feeding cycle of BAAP at 5% (A), 10% (B), 20% (C) and of VAAP at 20% (D),

respectively. In all feeding cycles, the initially measured levels of DNT in the reactor do

not indicate rapid biodegradation activity; however, nitrite production and oxygen uptake

rates clearly demonstrate the microbes are active and that DNT degradation is taking place.

As time progresses, the onset of complete 2,4-DNT degradation corresponds with a

decrease in oxygen uptake and constant nitrite concentrations. Thus, the use of surrogate

parameters was important in the understanding of 2,4-DNT degradation – both at the

beginning, and at the end of a feeding cycle.

6.3.3. Slurry reactor performance and monitoring for 2,6-DNT degradation

Stoichiometric relationships could not be established in the second reactor treating

residual 2,6-DNT from either soil. This is due to several factors including, the high nitrite

carried over from the first reactor and the low levels of DNT degradation occurring in the

second reactor. For instance, the second reactor treating BAAP soils had initial nitrite

concentrations ranging between 5,000 and 10,000 μM as nitrite was carried over from the

first reactor. Any additional nitrite production from the degradation of low 2,6-DNT

concentration was difficult to detect. Similarly, NaOH consumption was minimal in the

second reactor. The theoretical consumption (based on 1.65 mole NaOH/mole DNT) of
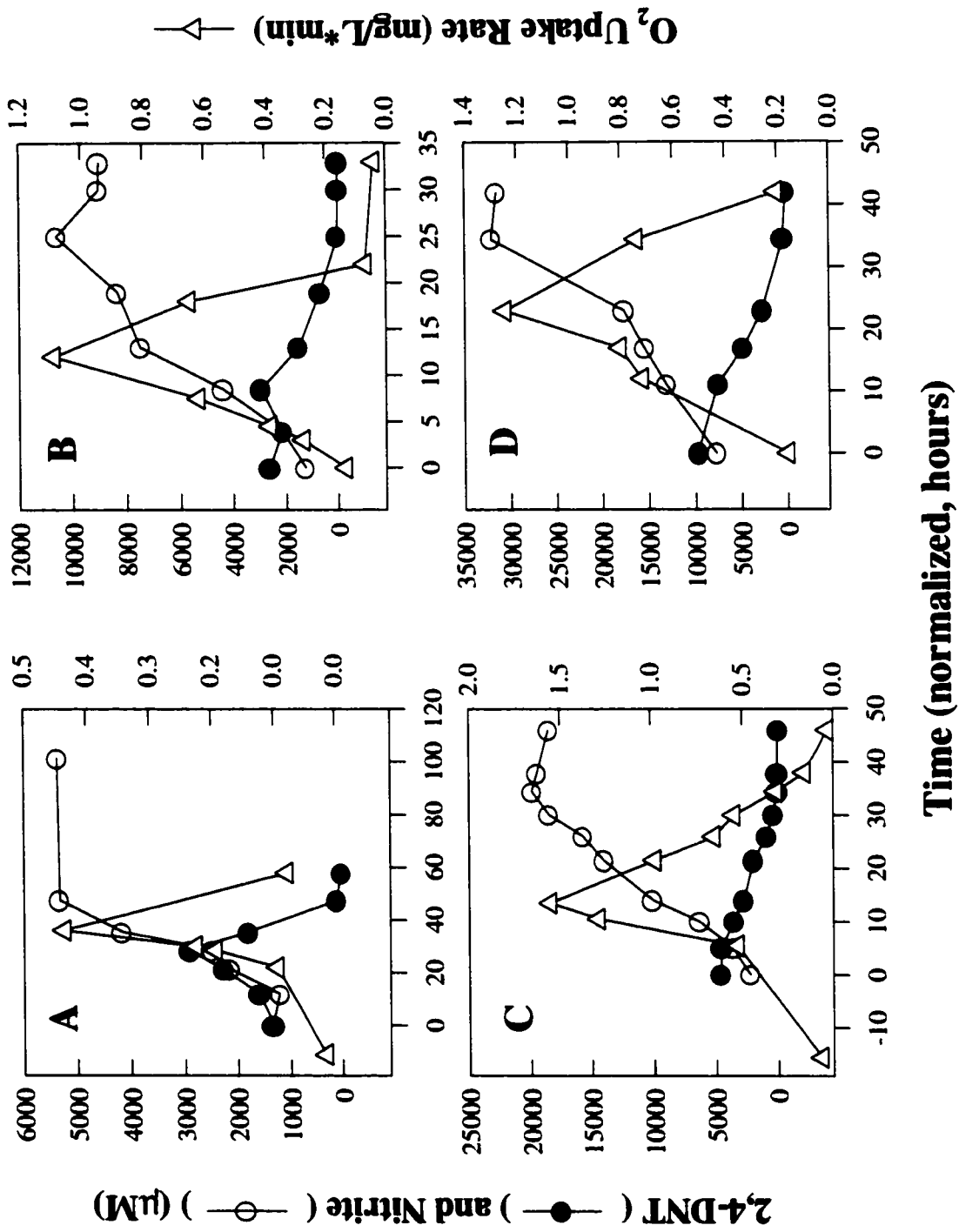
Figure 6.9. Temporal concentration profiles of 2,4-DNT, nitrite and oxygen uptake rate of BAAP soil at 5% (A), 10% (B), 20% (C) and of VAAP soil at 20% solids loading rates

12.5 N NaOH is very small (3.0 ml) for 250 μM of 2,6-DNT, and NaOH addition was

often not needed to keep pH above 6.75. Oxygen uptake in the second reactor was also

minimal, and correlation with DNT degradation could not be established. The maximum

oxygen uptake rates observed in the second reactors were 0.7 – 0.75 mg O_2/L*min, which

were approximately 20 times lower than that in the first reactor. Interestingly, this ratio

was comparable to the relative concentrations of 2,4-DNT to 2,6-DNT degraded in the

separate reactors.

6.4.0. Conclusions and Implications

The main problem that was encountered in process monitoring for these slurry

reactors was the heterogeneous nature of the DNT-distribution in the systems, which in

turn led to a non-representative analysis of contaminant levels. Without the ability to

directly determine contaminant levels, the ability to determine nutrient or electron acceptor

requirements can become complicated. Also, this difficulty in analysis decreases the

ability to accurately assess the rates at which degradation is occurring, particularly in the

early stages of the feed cycles.

Since monitoring 2,4-DNT concentrations was not always indicative of degradation

activity, oxygen consumption, nitrite production and NaOH consumption were tested as

surrogate monitoring parameters. It was determined that oxygen consumption is a less

reliable indicator of reactor performance because of the difficulty in obtaining samples and

the possibility of other organics being present in the soil that could contribute to the

oxygen consumption. Nitrite production and NaOH consumption were determined to be

the best surrogate monitoring parameters. Nitrite production can be used to accurately

assess the microbial activity and NaOH consumption can be used to correctly predict the amount of DNT degraded. Therefore, nitrite production and NaOH consumption are both inexpensive monitoring parameters that can be used for accurate routine process control.

The use of surrogate monitoring parameters did not extend to the second reactor in series. Low levels of 2,6-DNT were the main reason for the lack of correlation between 2,6-DNT degradation and surrogate monitoring parameters in the second reactor. In addition, carry over from the first reactor caused difficulty in detecting some parameters. For example, nitrite production from the degradation of 2,6-DNT was masked by the high levels of nitrite that carried over from the first reactor. Therefore, monitoring reactors with low concentrations of 2,6-DNT could only be conducted by direct measurement of 2,6-DNT concentrations by HPLC. If the 2,6-DNT concentrations were higher, the use of surrogate monitoring parameters may have become an accurate test in predicting reactor performance.

6.5.0. Acknowledgements

References

1. R.J. Spanggord, J.C. Spain, S.F. Nishino, and K.E. Mortelmans, Biodegradation of 2,4-dinitrotoluene by a *Pseudomonas* sp., Appl. Environ. Microbiol., 57 (1991) 3200-3205.

2. P.M. Bradley, F.H. Chapelle, J.E. Landmeyer, and J.G. Schumacher, Potential for intrinsic bioremediation of a DNT-contaminated aquifer, Ground Water, 35 (1997) 12-17.

3. S.F. Nishino, G. Paoli, and J.C. Spain, Aerobic degradation of dinitrotoluenes and pathway for bacterial degradation of 2,6-dinitrotoluene. Appl. Environ. Microbiol., 66 (2000) 2139-2147.

4. B.E. Haigler, S.F. Nishino, and J.C. Spain, Biodegradation of 4-methyl-5-nitrocatechol by Pseudomonas sp. strain DNT, J. Bacteriol., 181 (1994) 3433-3437.

5. D.R. Noguera and D.L. Freedman, Reduction and acetylation of 2,4-dinitrotoluene by *Pseudomonas aerginosa* strain, Appl. Environ. Microbiol., 62 (1996) 2257-2263.

6. C. Zhang, J.B. Hughes, S.F. Nishino and J.C. Spain, Slurry-phase biological treatment of 2,4-dinitrotoluene and 2,6-dinitrotoluene: Role of bioaugmentation and effects of high dinitrotoluene concentrations, Environ. Sci. Technol., 34(13) (2000) 2810-2816.

7. D.E. Jerger and P. Woodhull, Applications and costs for biological treatment of explosives-contaminated soils in the U.S., In: J.C. Spain, J.B. Hughes and H-J. Knackmuss (Eds), *Biodegradation of nitroaromatic compounds and explosives*, Lewis Publishers, New York, 2000, Chapter 14.

8. S.F. Nishino, J.C. Spain, and H-J. Knackmuss, Mineralization of 2,4- and 2,6-dinitrotoluene in soil slurries, Environ. Sci. Technol., 33(7) (1999) 1060-1064.

9. APHA, AWWA, and WEF (1998), *Standard Methods for the Examination of Water and Wastewater*, 20th edition, American Public Health Association, Washington, D.C.

10. C. Zhang, J.B. Hughes, S.F. Nishino and J.C. Spain, Biodegradation of 2,4-dinitrotoluene and 2,6-dinitrotoluene in a pilot-scale aerobic slurry reactor system; Final Report to the U.S. Air Force Research Laboratory on Grant F08637-9B-C-6002; Tyndall AFB, FL, 1999.

11. P.L. McCarty, Thermodynamics of biological synthesis and growth, Int. J. Air Wat. Poll., 9 (1965) 621-639.

12. P.L. McCarty, Energetics of organic matter degradation, in: R. Mitchell (Ed) *Water pollution microbiology*, Wiley-Interscience, New York, 1972, Chapter 5.

13. M.L. Mavrovouniotis, Group contributions for estimating standard Gibbs free energies of formation of biochemical compounds in aqueous solution, Biotechnol. Bioeng., 36 (1990) 1070-1082.

14. T.D. Brock and M.T. Madigan, *Biology of Microorganisms*, 6th Edition, Prentice-Hall, Inc, Englewood Cliffs, New Jersey, 1991.

15. M.D. Shelly, R.L. Autenreith, J.R. Wild and B.E. Dale, Thermodynamic analysis of trinitrotoluene biodegradation pathways and mineralization pathways, Biotechnol. Bioeng., 50 (1996) 198-205.

16. B.R. Rittman and P.L. McCarty, *Environmental Biotechnology: Principles and Applications*, McGraw Hill, New York, 2001.

17. U. Lendenmann, J.C. Spain, B.F. Smets, Simultaneous biodegradation of 2,4-dinitrotoluene and 2,6-dinitrotoluene in an aerobic fluidized-bed biofilm reactor, Environ. Sci. Technol., 32(1) (1998) 82-87

CHAPTER SEVEN

MODEL RESULTS AND DISCUSSION

7.0.0. Effect of K_s and k on DNT degradation

The model developed employs Monod kinetics, which is dependent on four

kinetic parameters Y, b, K_s, and k. As discussed in Chapter 2, Y is the yield coefficient,

b is the decay coefficient, K_s is the half-saturation constant, and k is the maximum

substrate utilization rate. As discussed in Chapter 5, the values of these parameters could

not be determined directly from the data obtained from DNT depletion in the reactor(s),

so the values published by Heinze[1] were used as initial input values for the model. The

values published by Heinze were chosen because his work used the same DNT-degrading

culture used in the reactor study, and because his was performed in a batch reactor, which

resembles the system used in this study. The value for Y determined by Heinze was 0.48

μmol X/ μmol DNT, which is similar to the value determined by thermodynamic

calculations (Chapter 2, 0.37 μmol X/ μmol DNT) and was deemed reasonable. The

values for K_s and k could not be determined by regression, so the model was used to

determine the effects of K_s and k on the degradation rates of DNT in the reactors and

compared to results obtained in the slurry reactor under a range of solids loading rates.

The first test performed with the model was the variation of K_s to determine its

effect on the degradation rate of DNT. The values of K_s used in the comparison were 5,

10, and 20 μmol DNT/L and k was 4.92 μmol DNT/μmol X-d (value published by

Heinze), for both soils and all solids loading rates. To determine if the value of K_s had

any effect on the observed degradation of DNT, the time required for complete DNT

degradation was compared between model predictions at various values of K_s. The

results are shown in Table 7.1. Notice, the time required for complete degradation of

DNT was approximately the same regardless of the soil or the solids loading rate;

therefore, the published value of K_s (10 µmol DNT/d) was used in all further testing.

Further testing was performed with the model to determine what values of K_s would have

a strong effect on the rate of DNT degradation in the reactor. This testing showed that a

K_s value of 800 µmol DNT/d would be required to double the time required for DNT and

that values as low as 0.00005 µmol DNT/d had no effect on the time to complete DNT

degradation.

Next, the model was used to determine the effect of varying k on the degradation

of DNT. The values of k used for this comparison were 2.5, 4.92, and 10 µmol

DNT/µmol X-d (these values were chosen as half and double the published value) with

K_s equal to 10 µmol DNT/L, for all soils and solids loading rates. As with K_s, the

predicted time required for complete degradation of DNT was compared for all values of

k. The results are shown in Table 7.2. This table shows that k has a strong effect on the

rate of DNT degradation in the reactor. When k is half the published value by Heinze

(2.5 µmol DNT/µmol X-d), the time for complete DNT degradation doubles, and when k

is double the published value by Heinze (10 µmol DNT/µmol X-d), the time for complete

DNT degradation is cut in half. Therefore, k strongly influences the results of modeling

these systems – unlike K_s.

7.1.0. Comparison of model to experimental data

Chapter 4 outlined the data obtained in the previous work. This included aqueous

DNT concentrations, nitrite concentrations, oxygen uptake rates, and sodium hydroxide

Table 7.1. Effect of varying K_s on DNT degradation rates.

Soil	Solids Loading Rate	K_s (μmol DNT/L)	Mass DNT Degraded (mmol)	Time (d)	Average Time (d)	Standard Deviation
BAAP	5%	20	170	1.03	1.04	0.01
		10	170	1.02		
		5	170	1.01		
	10%	20	341	1.05		
		10	341	1.05		
		5	341	1.04		
	20%	20	686	1.06		
		10	686	1.05		
		5	686	1.04		
	30%	20	1,030	1.05		
		10	1,030	1.04		
		5	1,030	1.04		
	40%	20	1,373	1.04		
		10	1,373	1.04		
		5	1,373	1.03		
VAAP	5%	20	208	1.04	1.03	0.02
		10	208	1.03		
		5	208	1.02		
	20%	20	836	1.01		
		10	836	1.00		
		5	836	1.00		
	30%	20	1,255	1.05		
		10	1,255	1.05		
		5	1,255	1.04		

Table 7.2. Effect of varying k on DNT degradation rates.

Soil	Solids Loading Rate	k (μmol DNT/μmol X-d)	Mass DNT Degraded (mmol)	Time (d)
BAAP	5%	2.5	170	2.12
		4.92	170	1.03
		10	170	0.50
	10%	2.5	341	2.13
		4.92	341	1.03
		10	341	0.50
	20%	2.5	686	2.13
		4.92	686	1.04
		10	686	0.50
	30%	2.5	1,030	2.13
		4.92	1,030	1.04
		10	1,030	0.50
	40%	2.5	1,373	2.13
		4.92	1,373	1.04
		10	1,373	0.50
VAAP	5%	2.5	208	2.12
		4.92	208	1.03
		10	208	0.49
	20%	2.5	836	2.13
		4.92	836	1.04
		10	836	0.50
	30%	2.5	1,255	2.13
		4.92	1,255	1.04
		10	1,255	0.50

consumption in the reactor. In Chapter 6, the heterogeneity in the reactor and how this

caused large discrepancies between the actual DNT concentrations in the reactors and the

measured DNT concentrations was discussed. Because of these heterogeneities, the

aqueous DNT concentration was not used for comparison to model generated data.

Instead, the nitrite concentration data was used because, as shown in Chapter 6, the nitrite

concentrations are homogeneous throughout the reactor. These nitrite concentrations

were converted to total DNT degraded (using stoichiometry and the volume of the

reactor) and compared with the predicted DNT degradation from the model.

The data generated by the model in the previous section where k is the state

variable are presented in the following figures (7.1-7.8) and compared to the

experimental data from Chapter 4. All figures in this series have been plotted with mass

of DNT degraded vs. normalized time. The normalized time is calculated from the data

by subtracting the time at the beginning of a cycle from the time at the end of a cycle.

The lines on the plot are the predictions of the model at various values of k. Most tests

were performed with k values of 2.5, 4.92, and 10 μmol DNT/μmol X-d, but if the data

from the pervious work did not lay within this range, other values were tested. This data

is presented in the order in which the soils were tested in the reactor.

Figure 7.1 shows the results from varying k for the VAAP soil with a 5% solids

loading rate. The data in red on the plot represents a phosphate concentration of 20 mM

in the reactor, and the data in blue represents a 1 mM phosphate concentration. This plot

demonstrates the large effect k has on the model prediction of the rate of DNT

degradation. If k was 1.5 μmol DNT/μmol X-d it would take the bacteria almost four

Figure 7.1. Comparison of amount of DNT degraded between experimental data and model predictions for VAAP soil at a solids loading rate of 5% (K_s = 10 μmol/L, b = 0.1 d^{-1}, Y= 0.48 μmol X/ μmol DNT). Legend shows what time span (days) the samples were taken.

days to degrade the DNT in the reactor compared to when k was 10 μmol DNT/μmol X-d

it would take only one day to degrade the DNT in the reactor. In addition, most of the

experimental data from the previous work lies between when k is 4.92 μmol DNT/μmol

X-d and 10 μmol DNT/μmol X-d. This analysis of results is also shown in all subsequent

plots.

Figure 7.2 presents the results from varying k for the BAAP soil with a 5% solids

loading rate. The top plot shows experimental data from the previous work, which was

collected from day zero to day 24.1 of reactor operation. This data is best represented by

a k value of 2.5 μmol DNT/μmol X-d. The bottom plot shows data collected from day

26.6 to day 29.6. During this time period in the reactor, the data is best represented by a

k value between 4.92 μmol DNT/μmol X-d and 10 μmol DNT/μmol X-d.

The next figures (7.3 and 7.4) show the results from varying k for BAAP soil at a

solids loading rate of 10% and 20%. The experimental data for 10% loading rate is best

described by a k value between 4.92 μmol DNT/μmol X-d and 10 μmol DNT/μmol X-d.

The experimental data for the 20% loading rate seems to follow the same trend until

approximately half of the DNT is degraded, then the data shifts upward and is

representative of a k between 2.5 μmol DNT/μmol X-d and 4.92 μmol DNT/μmol X-d.

Figures 7.5 and 7.6 show the results for varying k for BAAP soil with a 30%

solids loading rate and a 40% solids loading rate, respectively. The same trend that was

shown in the 20% solids loading rate is shown for both the 30% and 40% solids loading

rates; the data taken before half of the DNT is degraded is representative of a k value

between 4.92 μmol DNT/μmol X-d and 10 μmol DNT/μmol X-d, but the subsequent data

is representative of a k between 2.5 μmol DNT/μmol X-d and 4.92 μmol DNT/μmol X-d.
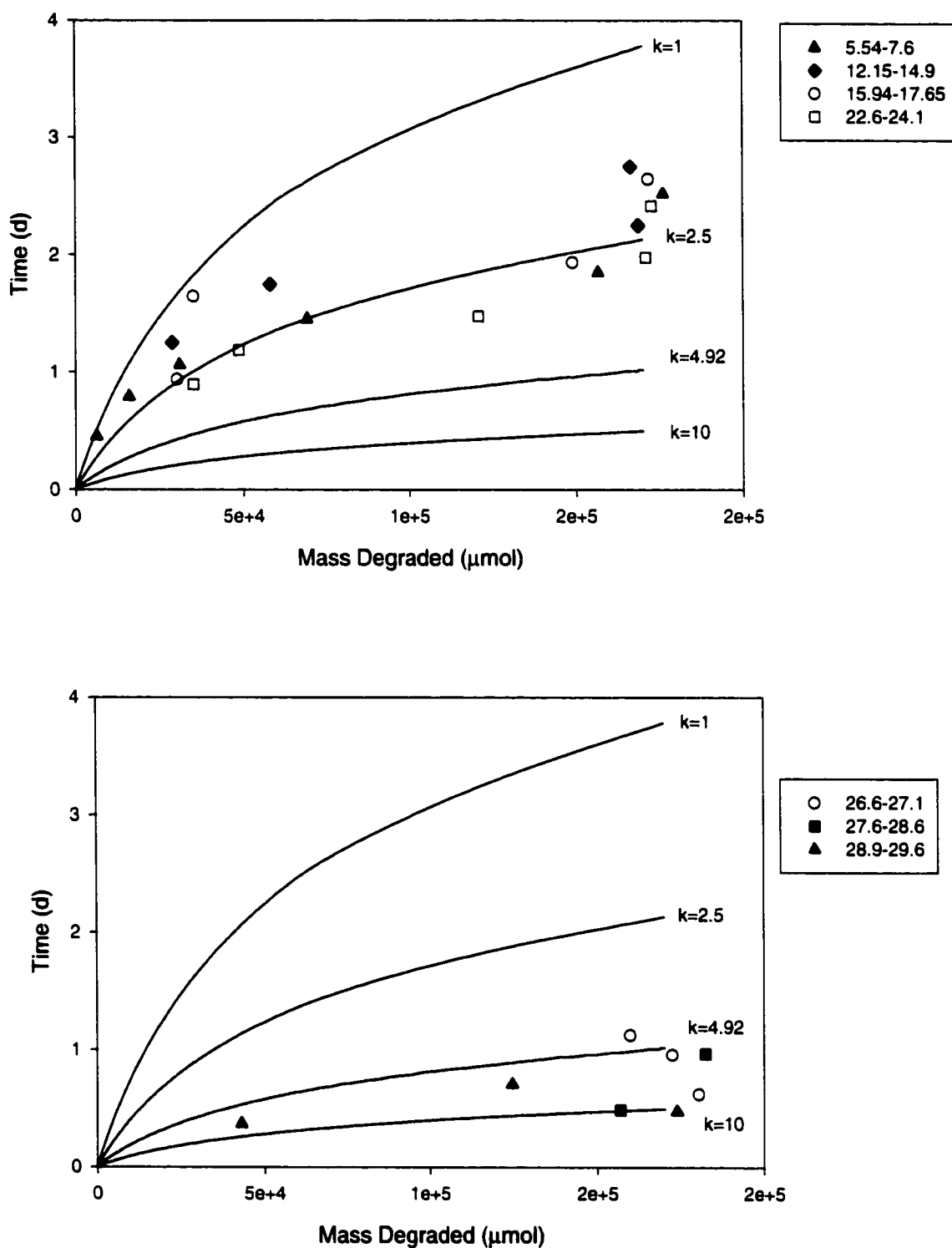
Figure 7.2. Comparison of amount of DNT degraded between experimental data and model predictions for BAAP soil at a solids loading rate of 5% (K_s = 10 μmol/L, b = 0.1 d^{-1}, Y= 0.48 μmol X/ μmol DNT). Legend shows what time span (days) the samples were taken.
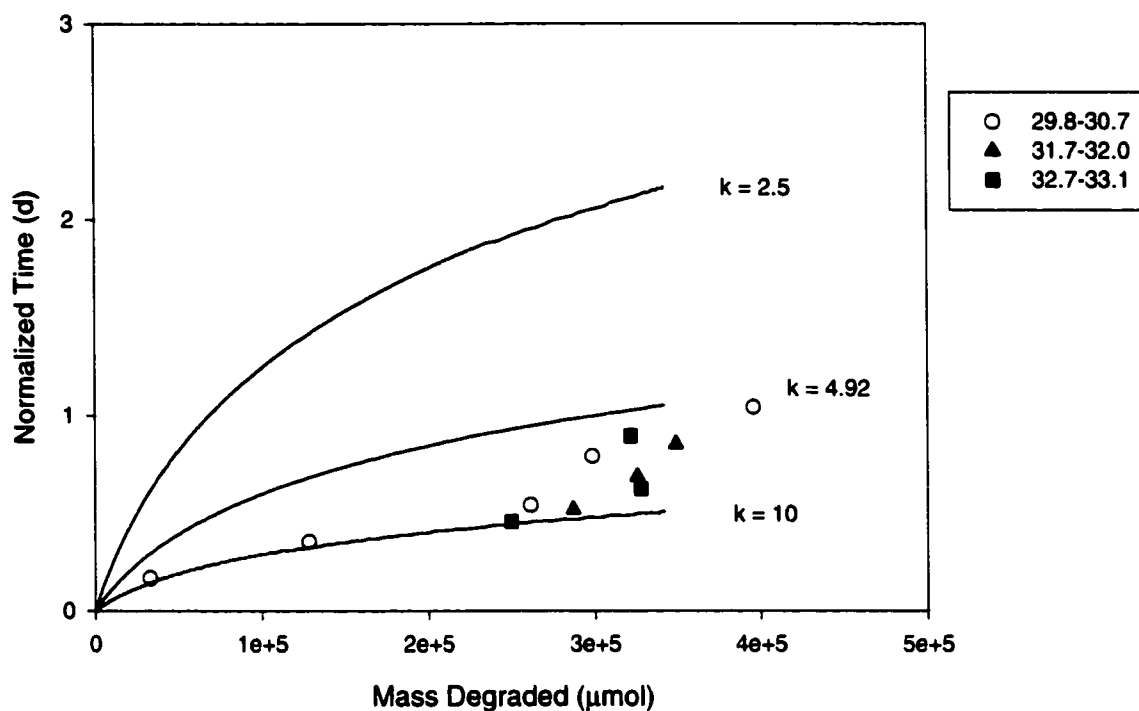
Figure 7.3. Comparison of amount of DNT degraded between experimental data and model predictions for BAAP soil at a solids loading rate of 10% (K_s = 10 μmol/L, b = 0.1 d^{-1}, Y= 0.48 μmol X/ μmol DNT). Legend shows what time span (days) the samples were taken.
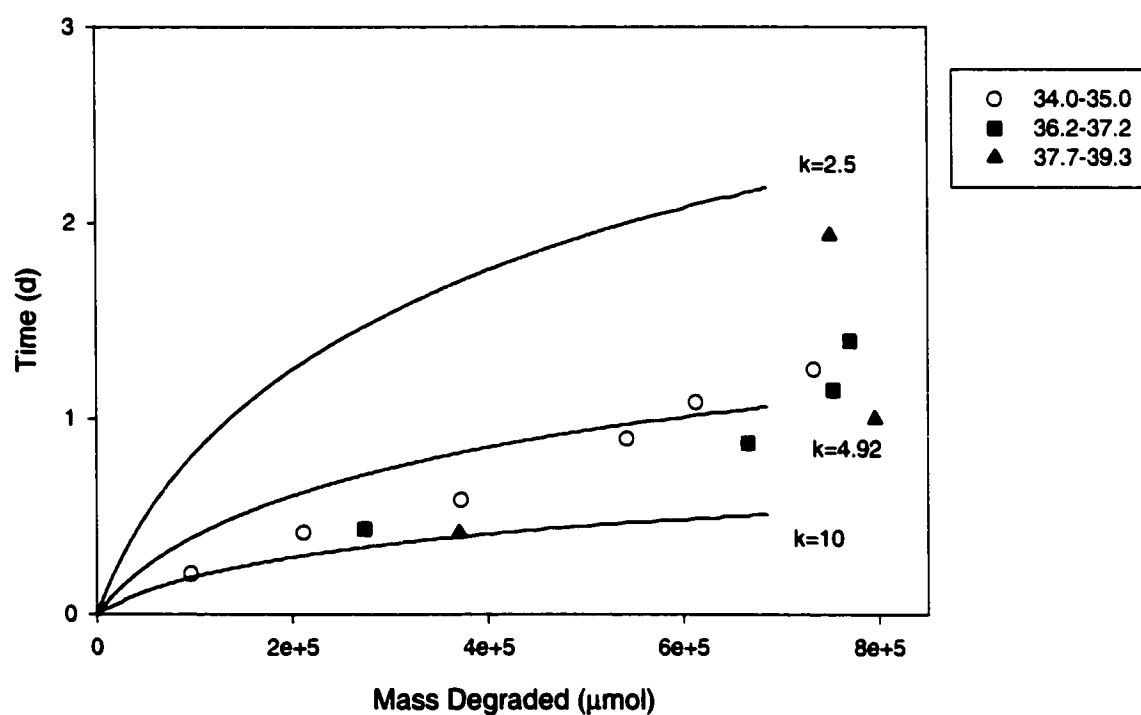
Figure 7.4. Comparison of amount of DNT degraded between experimental data and model predictions for BAAP soil at a solids loading rate of 20% (K_s = 10 μmol/L, b = 0.1 d^{-1}, Y= 0.48 μmol X/ μmol DNT). Legend shows what time span (days) the samples were taken.
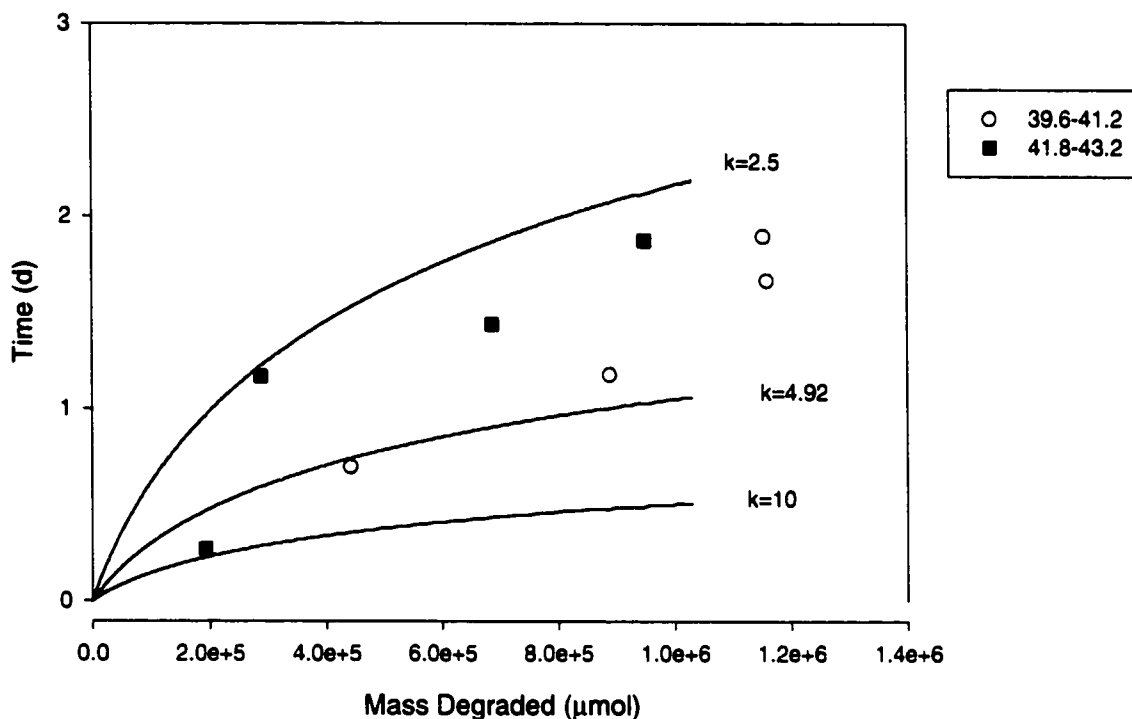
Figure 7.5. Comparison of amount of DNT degraded between experimental data and model predictions for BAAP soil at a solids loading rate of 30% (K_s = 10 μmol/L, b = 0.1 d^{-1}, Y= 0.48 μmol X/ μmol DNT). Legend shows what time span (days) the samples were taken.
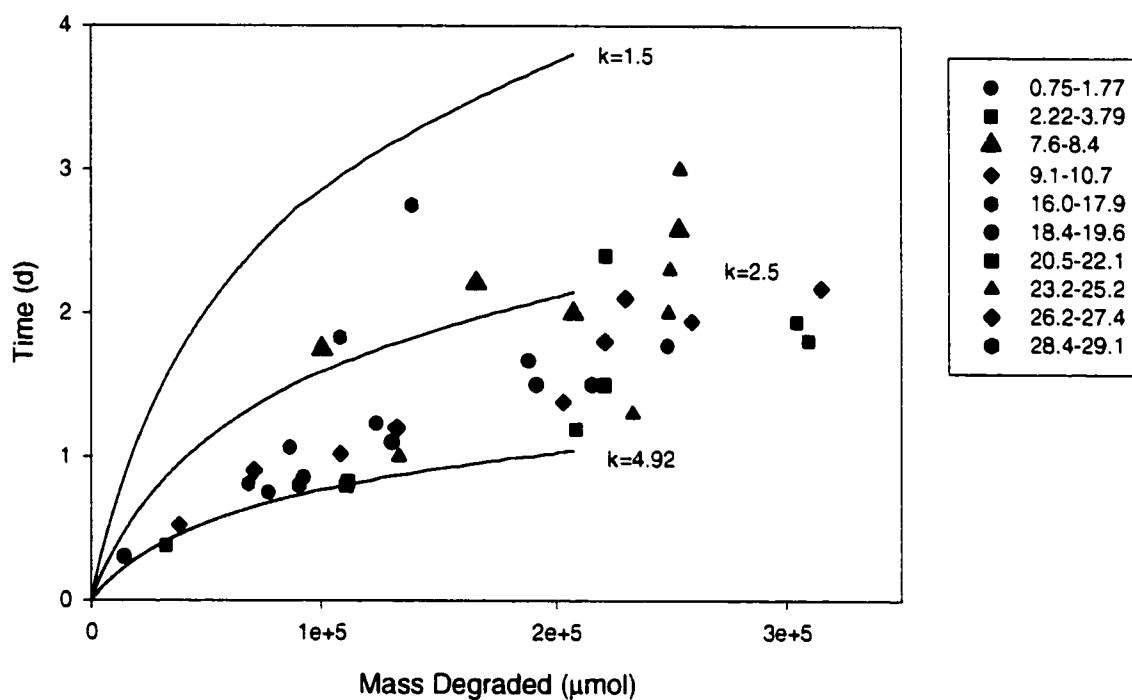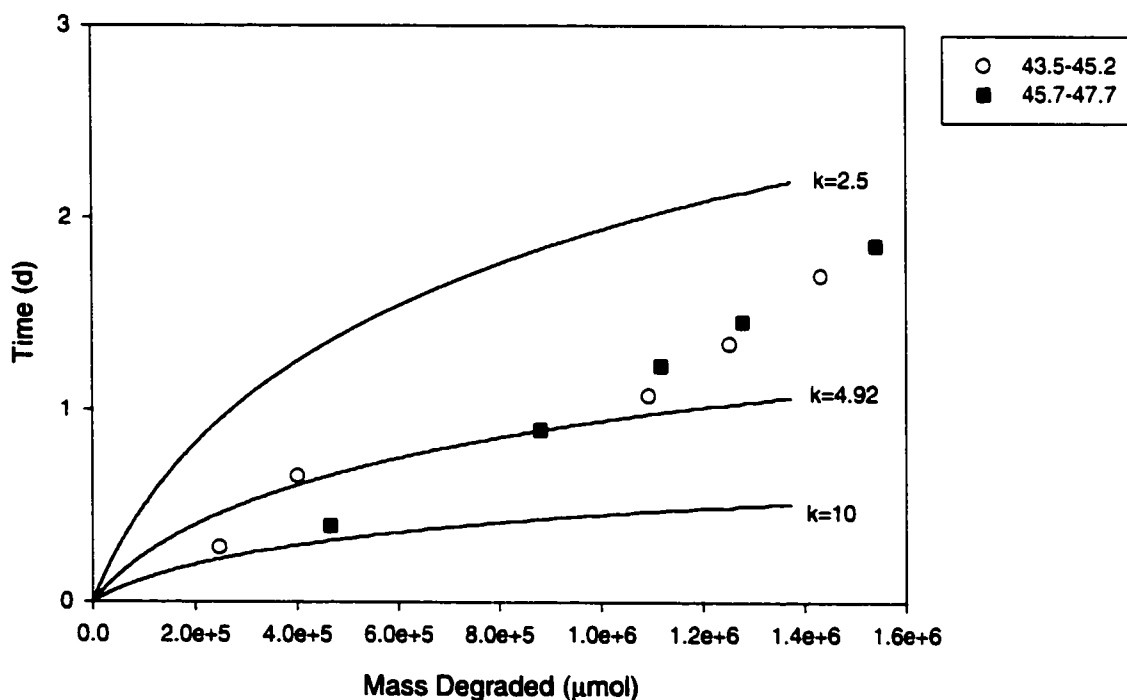

Figure 7.6. Comparison of amount of DNT degraded between experimental data and model predictions for BAAP soil at a solids loading rate of 40% (K_s = 10 μmol/L, b = 0.1 d^{-1}, Y= 0.48 μmol X/ μmol DNT). Legend shows what time span (days) the samples were taken.

The last figures in this series are Figure 7.7 and 7.8. These figure shows the effect of varying k for VAAP soil with solids loading rate of 20% and 30%. For both the 20% and 30% experimental data, the same trend as the previous figure is shown, the data taken after half of the DNT is degraded is best represented by a lower k than the data taken before half of the DNT is degraded.

7.2.0. Throughput of Soil

In first section of this chapter, it was shown that the kinetic parameter k was the determining factor in the rate of degradation of DNT and K_s had little influence on results observed. Assuming that k is the parameter that determines the rate of DNT degradation, it will also determine the throughput of soil in a remediation system. Table 7.3 presents the experimental throughput of soil (kg soil/d) and Table 7.4 presents the model predicted throughput of soil (kg soil/d) for both soils at all solids loading rates.

In Table 7.3, the first column of data shows the number of cycles that were used to determine the average length of a cycle in the reactor (Some solids loading rates had very few cycles available for this calculation. For example, VAAP soil at a solids loading rate of 30% had only one cycle). The second column in the table shows the average lengths of the cycles for each solids loading rate. The time for a cycle ranges from 0.84 days (BAAP, 10%) to 2.52 days (VAAP 30%). The third column shows the standard deviation for the average length of a cycle and the last column shows the possible throughput of soil for the reactor under the given conditions.

The model predicted data is shown Table 7.4. The columns are arranged so the predicted length of a cycle for a given value of k is shown first and then the subsequent column presents the throughput of soil expected for the time predicted from that value of
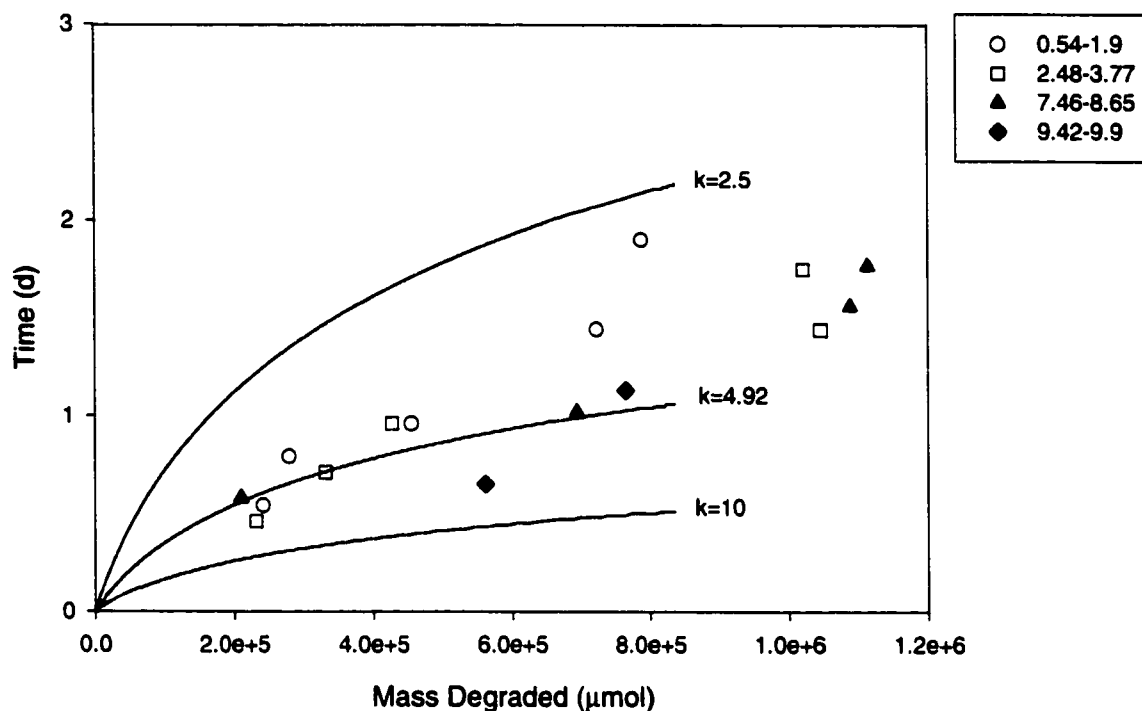
Figure 7.7. Comparison of amount of DNT degraded between experimental data and model predictions for VAAP soil at a solids loading rate of 20% (K_s = 10 μmol/L, b = 0.1 d^{-1}, Y= 0.48 μmol X/ μmol DNT). Legend shows what time span (days) the samples were taken.
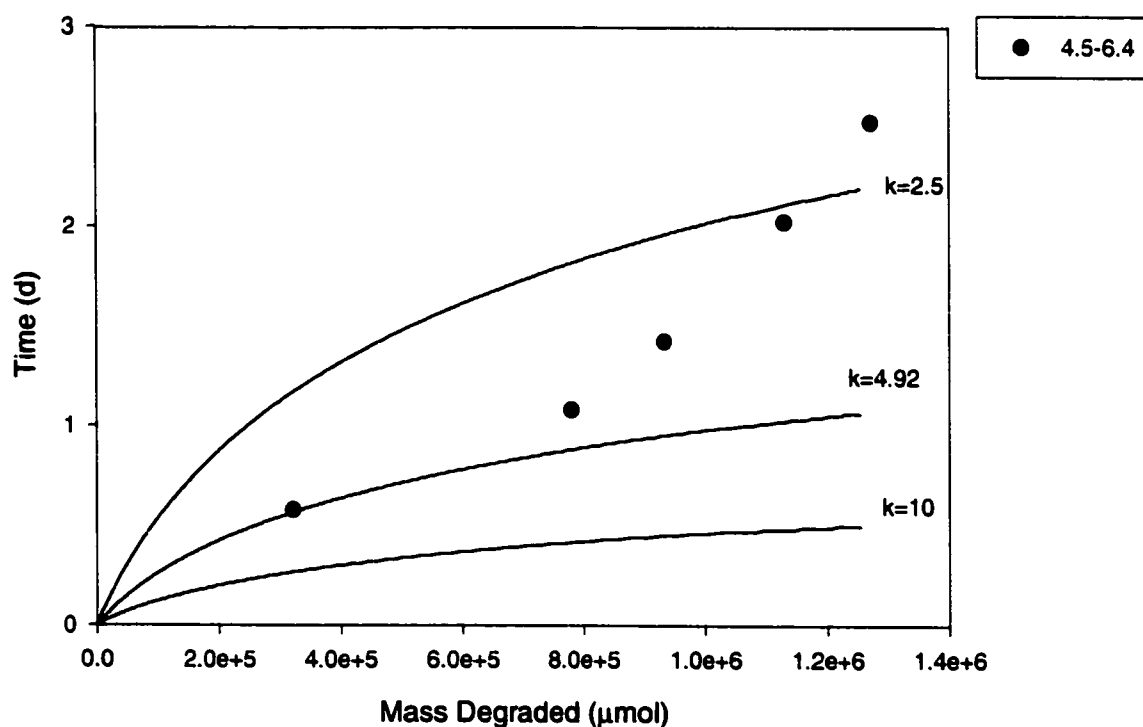
Figure 7.8. Comparison of amount of DNT degraded between experimental data and model predictions for VAAP soil at a solids loading rate of 30% (K_s = 10 μmol/L, b = 0.1 d^{-1}, Y= 0.48 μmol X/ μmol DNT). Legend shows what time span (days) the samples were taken.

Table 7.3. Throughput of soil from experimental data.

Soil	Solids Loading	Number of Cycles	Experimental Length of Cycle (d)	Standard Deviation	Throughput (kg soil/d)
BAAP	5%	7	2.04	0.87	1.71
	10%	3	0.84	0.21	8.33
	20%	3	1.59	0.30	8.80
	30%	2	1.66	0.31	12.68
	40%	2	2.14	0.28	13.11
VAAP	5%	14	1.96	0.46	1.78
	20%	4	1.76	0.11	7.95
	30%	1	2.52	n/a	8.33

Table 7.4. Model predicted throughput of soil using various values of k.

Soil	Solids Loading	Model Predicted Length of Cycle (d) (k=2.5 μmol DNT/μmol X-d)	Throughput (kg soil/d)	Model Predicted Length of Cycle (d) (k=4.92 μmol DNT/μmol X-d)	Throughput (kg soil/d)	Model Predicted Length of Cycle (d) (k=10 μmol DNT/μmol X-d)	Throughput (kg soil/d)
BAAP	5%	2.119	1.65	1.026	3.41	0.496	7.06
	10%	2.128	3.29	1.035	6.77	0.498	14.06
	20%	2.131	6.57	1.036	13.51	0.498	28.09
	30%	2.132	9.85	1.037	20.26	0.499	42.11
	40%	2.132	13.13	1.037	27.01	0.499	56.14
VAAP	5%	2.124	1.65	1.033	3.39	0.495	7.07
	20%	2.133	6.56	1.037	13.50	0.499	28.07
	30%	2.133	9.84	1.037	20.24	0.497	42.29

k. For example, for BAAP soil with a solids loading rate of 20%, if k has a value of 4.92

μmol DNT/μmol X-d then the expected length of time for a cycle is 1.04 days and the

throughput of soil is 13.5 kg soil/d for a 70 L reactor.

7.3.0 Nutrient, Oxygen, and Sodium Hydroxide Requirements

To assure the bacteria are capable of degrading all of the DNT in the reactor, the

proper amount nutrients, oxygen, and sodium hydroxide must be present in the reactor.

Oxygen is needed because the bacteria are aerobic, and sodium hydroxide is necessary to

neutralize the hydrogen ions produced during the biodegradation of DNT. There are

several nutrients needed by bacteria to survive, but in this system phosphorous is most

likely to be the limiting nutrient.

The rate at which oxygen is added to the reactors must be greater that the rate at

which the bacteria consume the oxygen to assure the environment remains aerobic. Table

7.5 presents the calculated average oxygen consumption rates for the bacteria for both

soils and all solids loading rates. First, the total amount of oxygen required (μmol) is

calculated from the total DNT added into the reactor using stoichiometry. These values

are used with the predicted times for the length of a cycle (d) for k values of 2.5, 4.92,

and 10 μmol DNT/μmol X-d (from section 7.1) to calculate an average oxygen

consumption rate in mg O_2 / L*min.

These oxygen consumption rates can be compared to the experimental average

oxygen consumption rates. The experimental oxygen consumption rates were presented

in Figure 4.8 for BAAP soil and Figure 4.16 for VAAP soil. The data for these figures

was averaged for each solids loading rate and is presented in Table 7.5. The

experimental average oxygen consumption rates are between the model predicted oxygen

Table 7.5. Experimental and model predicted oxygen consumption rates (units of k are µmol DNT/µmol X-d)

Soil	Solids Loading	Total DNT (mmol)	Oxygen Required (mmol)	Oxygen Consumption Rate (mg O_2/L*min)			Average Oxygen Consumption Rate (mg O_2/L*min)
				k=2.5	k=4.92	k=10	
BAAP	5%	172	963	0.07	0.15	0.31	0.24
	10%	344	1,926	0.14	0.30	0.61	0.65
	20%	688	3,851	0.29	0.59	1.23	0.84
	30%	1,032	5,777	0.43	0.88	1.84	1.01
	40%	1,375	7,702	0.57	1.18	2.45	1.02
VAAP	5%	209	1,173	0.09	0.18	0.38	0.41
	20%	838	4,691	0.35	0.72	1.49	0.88
	30%	1,257	7,037	0.52	1.08	2.25	1.33

consumption rates for a k of 4.92 and 10 μmol DNT/μmol X-d for both soils and all

solids loading rates.

Table 7.7 presents the volume (mL) of sodium hydroxide necessary to neutralize

the hydrogen ions produced during the DNT degradation. This number is calculated

using the total DNT fed into the reactor, the stoichiometry presented in Chapter 2,

Equation 2.12, and the fact that the sodium hydroxide used is 12 N. If this amount of

sodium hydroxide is not added, the pH of the system will drop and would inhibit DNT

degradation by the bacteria.

The volume of sodium hydroxide consumed (presented in Figure 4.10 for BAAP

soil and Figure 4.17 for VAAP soil) for both soils and all solids loading rates (shown in

Chapter 6, section 6.3.2) are all within ± 4 mL of the model predicted NaOH

consumption for the BAAP soil.

The amount of phosphorous needed by bacteria varies depending on the type of

bacteria. For these bacteria, it is assumed that the phosphorous requirement is one-fifth

of the nitrogen requirement [2]. Table 7.6 presents the required phosphorous

concentration in the reactor for all soils and solids loading rates. For each soil and solids

loading rate, the amount of DNT (μmol) added into the reactors is shown (taken from

Table 5.1, Chapter 5). The total DNT used to predict the amount of biomass produced

(μM) using the stoichiometry from Chapter 2, Equation 2.12. From the biomass, the

amount of nitrogen required can be calculated from chemical formula for the bacteria

shown in Chapter 2, Equation 2.12. There is no experimental data for phosphorous

concentrations, but the medium for the reactor contained 20 mM phosphorous for part of

the VAAP 5% solids loading test, but was switched to 1 mM phosphorous for all other

solids loading rates. These calculations show that the phosphorous requirement by the

bacteria is equal to or exceeds the phosphorous supplied by the media for BAAP soil with

solid loading rates of 20%, 30%, and 40% and VAAP soil for solid loading rates of 20%

and 30%.

Table 7.6. Model predicted nutrient and sodium hydroxide requirements

Soil	Solids Loading	Total DNT (mmol)	Biomass Predicted (μM)	Nitrogen Requirement (mM)	Phosphorous Requirement (mM)	12.5 N NaOH (mL)
BAAP	5%	172	1,179	1.18	0.24	22.4
	10%	344	2,358	2.36	0.47	44.8
	20%	688	4,716	4.72	0.94	89.7
	30%	1,032	7,073	7.07	1.41	134.5
	40%	1,375	9,431	9.43	1.89	179.4
VAAP	5%	209	1,436	1.44	0.29	27.3
	20%	838	5,744	5.74	1.15	109.2
	30%	1,257	8,616	8.62	1.72	163.9

7.4.0. Discussion

The objective of developing a model to mathematically represent the partitioning

and biodegradation of DNT in the bioslurry reactor was to better understand the

processes occurring in the reactor, and to aid in the operation of a full-scale reactor

system. In this study, the model proved to be most useful in the interpretation of the pilot

scale results. After the previous study was completed, the factor that controlled the

degradation of DNT was unknown. The model allowed for interpretation of the

experimental data, which showed that k, the maximum substrate utilization, was the

controlling factor for DNT degradation in the reactor.

The model also lead to two very important observations in the behavior of the

microbes in the reactor. During the test of BAAP soil at a solids loading rate of 5%, there

was an increase in the rate of DNT degradation, which was indicated by the experimental

data becoming better described by a higher value of k (Figure 7.2). This increase in the

degradation rate can be explained only by a population shift of the bacteria. The reactors

were inoculated with *Burkholderia cepacia* JS872 (2,4-DNT degrading strain) and *B.*

cepacia JS850 and *Hydrogenophaga palleronii* JS863 (2,6-DNT degrading strains), but it

has been shown that there are indigenous bacteria present in the soil that are DNT-

degraders. It is feasible that the indigenous population out competed the bacteria added

to the reactor, and these bacteria were capable of utilizing DNT at a faster rate.

The second observation in the behavior of the microbes was the tendency for the

rate of DNT degradation to slow after approximately half of the DNT was degraded in

tests with BAAP soil (20%, 30%, 40%) and VAAP soil (20%, 30%). The slowing of the

rate of DNT degradation was caused by a nutrient limitation. In all the test cases

mentioned above, the amount of phosphorous needed by the bacteria in the reactors was

at or above the amount of phosphorous supplied by the nutrient medium. This type of

nutrient limitation would allow the bacteria to degrade DNT at a high rate in the

beginning of a test because the phosphorous is in excess, but once the phosphorous

becomes limiting the DNT degradation rate slows.

The varying degradation rate shown in the experimental results can have a large

effect on the soil throughput to the reactor. The experimental data shows that for BAAP

soil with a solids loading rate of 30% the throughput of soil to the reactor is

approximately 13 kg soil per day. This is characteristic of a k value of 2.5 μmol

DNT/μmol X-d. At the same solids loading rate for the same soil, if the bacteria were degrading at a fast rate (k=10 μmol DNT/μmol X-d), the model predicts that approximately 42 kg of soil could be remediated per day.

The model introduced in this work could also be a useful tool to aid in the operation of a full-scale system. In this capacity, the model would be most useful as a diagnostics tool to perform "what if " tests. This type of test would allow for the investigation of different soils and different DNT concentrations in the reactor to determine the effect on the system without having to run the reactor itself. The model predictions of the "what if" tests can be coupled with the stoichiometry to calculate the required NaOH and oxygen consumption rates and can be used to calculate the soil throughput to the reactors.

The model should not be used to determine when to refeed the reactors (end a cycle). This type of prediction is better made using experimental data, such as nitrite production, as suggested in Chapter 6. The nitrite production can be directly related to DNT degraded using stoichiometry. The model predicts the end of a cycle when there is approximately 99% removal of DNT from the reactor, which is a time dependent calculation based on rate of DNT degradation. This rate of degradation varies depending on the bacterial behavior, which cannot be predicted by the model.

The model developed for this work has proven to be a useful tool for analyzing data for the biodegradation of 2,4-DNT in a bioslurry reactor. It is capable of predicting amounts of nitrite and biomass produced, and it is capable of detecting important changes in biological activity in the reactors. The model can also be used as an diagnostic tool for

the operation of a full-scale system, where it can be used to predict changes in the

operation of the reactor when input DNT concentrations are changed.

References

1. Heinze, L., M. Brosius, and U. Wiesmann, Biological Degradation of 2,4-Dinitrotoluene in a Continuous Bioreactor and Kinetic Studies. *Acta Hydrochim. Hydrobio.*, 1995. **23**(6): p. 254-263.

2. Rittmann, B.E. and P.L. McCarty, *Environmental Biotechnology: Principles and Applications*. 2001, New York: McGraw-Hill.

CHAPTER EIGHT

CONCLUSIONS

The following conclusions have been drawn from this study:

• The use of a soil washing procedure for contaminated soil prior to treatment in the bioslurry reactors was an effective method for retaining DNT and fine soil particles, while removing large soil particles that would clog the reactor.

• Direct measurement of 2,4-DNT concentrations in the reactors gives a non-representative analysis of DNT levels. Instead, monitoring nitrite production or NaOH consumption and applying biological stoichiometry is the best method for determining 2,4-DNT levels and assessing nutrient and electron acceptor requirements.

• Direct measurement of 2,6-DNT concentrations is the only method for monitoring the reactor performance in the second reactor, due to low concentrations of 2,6-DNT.

• The partition coefficients for 2,4-DNT for BAAP soil and VAAP soil were 7.27 L/kg and 3.52 L/kg, respectively.

• The maximum substrate utilization, k, is the only biological kinetic parameter that controls the rate of DNT degradation in the reactors.

• During the test of BAAP soil at a solids loading rate of 5%, there was a population shift of the bacteria in the reactor, which lead to higher DNT degradation rates.

• Higher degradation rates were slowed by phosphorous limitation in the tests with higher solids loading rates i.e., BAAP 20%, 30% and 40% and VAAPP 20% and 30%.

- The model developed can be used to aid full-scale processes by providing a

  diagnostics tool to analyze slurry reactor performance including the treatability of

  DNT-contaminated soils, and to aid in preliminary cost estimation.

CHAPTER NINE

FURTHER RESEARCH

Previous work has shown that soil contaminated with high concentrations of 2,4-DNT and 2,6-DNT can be treated with an aerobic bioslurry reactor. This work has contributed to the understanding of the processes occurring in these reactors, but there are still questions to answer. The microbial ecology of the contaminated soils is still poorly understood. Understanding the indigenous DNT-degrading strains in the contaminated soil can lead to the prediction of population shifts that could occur during reactor operation. Also, the study of these strains could lead to the discovery of bacteria with high maximum substrate utilization rates, which controls the rate of DNT degradation in the reactors.

In this study, monitoring the second reactor proved to be a difficult task. Low concentrations of 2,6-DNT and carry over of high nitrite concentrations from the first reactor did not allow for the use of surrogate monitoring parameters. Since the use of nitrite production and NaOH consumption to determine reactor performance do not extend to this reactor, a better method for collection of 2,6-DNT data is needed to assure accurate predictions of reactor performance from direct 2,6-DNT measurements.

The model developed for this study allowed for the interpretation of experimental data from the previous work. The analysis of model results proved there was a phosphorous limitation in the reactors at high solids loading rates. The model could be adjusted to use equations for a dual substrate limitation, with both DNT and phosphorous being limiting, to help predict when phosphorous limitations would occur.

APPENDIX I

This appendix contains the scripts for the model used in this research. The title of each program is listed at the top of each page.

BAAP Soil Program

```
%BAAP soil program
clear;
clf;
global total masssoil kd masscry ttemp2 n ytemp2 cycle ttemp ytemp3 m cycle

input1;

if loadrate == 5
    masssoil = 0.49;
elseif loadrate == 10
    masssoil = 0.91;
elseif loadrate == 20
    masssoil = 1.82;
elseif loadrate == 30
    masssoil = 2.73;
else
    masssoil = 3.64;
end


kd=7.27;   %L/kg
masscry=total-(1500*70+1500*kd*masssoil);
soil=total/(70/kd+masssoil);
aqueous=soil/kd;
cyclelen=2;
y0=[777,total,0,aqueous];
tspan=[0 cyclelen];
m=0;
n=0;
t=zeros(1,1);
t(length(t))=0;
r=0;
s=0;
y=zeros(1,4);
t=zeros(1,1);

for cycle=1:5
  if masscry > 0
   aqueous=1500;
   crystal;

   total=ytemp(j,2);
   y0=[ytemp(j,1),ytemp(j,2),ytemp(j,3),ytemp(j,4)];
   tspan=[ttemp(j), ttemp(j)+cyclelen];

  if cycle == 1
```

```
   y=ytemp(1:(j-1),:);
   t=ttemp(1:(j-1));
else
   y=[y' ytemp(1:(j-1),:)']';
   t=[t' ttemp(1:(j-1))']';
end


  while total>2000
s=s+1;
[ttemp2,ytemp2]=ode15s('nocrystals',tspan,y0);
dnt=ytemp2(1,2);

    while dnt>(total-10)
      n=n+1;
      dnt=ytemp2(n,2);
    end
    if s==1
       y=[y' ytemp2(1:n,:)']';
       t=[t' ttemp2(1:n)']';
    else
       y=[y' ytemp2(2:n,:)']';
       t=[t' ttemp2(2:n)']';
    end
      [a,b]=size(y);
      deg=aqueous*70-y(a,4)*70;
      total=total-deg;
      soil=total/(70/kd+masssoil);
      aqueous=soil/kd;
      y0=[y(a,1),total,y(a,3),aqueous];
      tspan=[t(a),t(a)+cyclelen];
      n=0;
        end
    m=1;
else
    while total>2000
      r=r+1;
      [ttemp3,ytemp3]=ode15s('nocrystals',tspan,y0);
      dnt2=ytemp3(1,2);
      while dnt2>=(total-10)
        m=m+1;
        dnt2=ytemp3(m,2);
      end

          if r==1
          y=[y' ytemp3(1:m,:)'] ;
```

```
            t=[t' ttemp3(1:m)']';
          else
          y=[y' ytemp3(2:m,:)']';
          t=[t' ttemp3(2:m)']';
        end
        [a,b]=size(y);
        deg=aqueous*70-y(a,4)*70;
        total=total-deg;
        soil=total/(70/kd+masssoil);
        aqueous=soil/kd;
        y0=[y(a,1),total,y(a,3),aqueous];
        tspan=[t(a),t(a)+cyclelen];
        m=0;
    end
      n=1;
end
  input2;
  masscry=total-(1500*70+1500*kd*masssoil);
  soil=total/(70/kd+masssoil);
  aqueous=soil/kd;
  y0=[y(a,1)*0.1,total,y(a,3)*0.1,aqueous];
  tspan = [t(a),t(a)+cyclelen];

end
plot(t,y);
```

VAAP Soil Program

```
%VAAP soil program
clear;
clf;
global total masssoil kd masscry ttemp2 n ytemp2 cycle ttemp ytemp3 m cycle

input1;

if loadrate == 5
  masssoil = 2.8;
elseif loadrate == 20
  masssoil = 11.2;
else
  masssoil = 17.5;
end

kd=3.52;    %L/kg
asscry=total-(1500*70+1500*kd*masssoil);
soil=total/(70/kd+masssoil);
aqueous=soil/kd;
cyclelen=2;
y0=[154,total,0,aqueous];
tspan=[0 cyclelen];
m=0;
n=0;
t=zeros(1,1);
t(length(t))=0;
r=0;
s=0;
y=zeros(1,4);
t=zeros(1,1);

for cycle=1:7
  if masscry > 0
   aqueous=1500;
   crystal;

   total=ytemp(j,2);
   y0=[ytemp(j,1),ytemp(j,2),ytemp(j,3),ytemp(j,4)];
   tspan=[ttemp(j), ttemp(j)+cyclelen];

  if cycle == 1
    y=ytemp(1:(j-1),:);
    t=ttemp(1:(j-1));
  else
```

```
   y=[y' ytemp(1:(j-1),:)']';
   t=[t' ttemp(1:(j-1))']';
end


   while total>2000
   s=s+1;
   [ttemp2,ytemp2]=ode15s('nocrystals',tspan,y0);
   dnt=ytemp2(1,2);

      while dnt>(total-10)
        n=n+1;
        dnt=ytemp2(n,2);
      end
      if s==1
         y=[y' ytemp2(1:n,:)']';
         t=[t' ttemp2(1:n)']';
      else
         y=[y' ytemp2(2:n,:)']';
         t=[t' ttemp2(2:n)']';
      end
      [a,b]=size(y);
      deg=aqueous*70-y(a,4)*70;
      total=total-deg;
      soil=total/(70/kd+masssoil);
      aqueous=soil/kd;
      y0=[y(a,1),total,y(a,3),aqueous];
      tspan=[t(a),t(a)+cyclelen];
      n=0;
        end
   m=1;
else
   while total>2000
     r=r+1;
     [ttemp3,ytemp3]=ode15s('nocrystals',tspan,y0);
     dnt2=ytemp3(1,2);
     while dnt2>=(total-10)
       m=m+1;
       dnt2=ytemp3(m,2);
     end


        if r==1
        y=[y' ytemp3(1:m,:)']';
        t=[t' ttemp3(1:m)']';
        else
        y=[y' ytemp3(2:m,:)']';
```

```
            t=[t' ttemp3(2:m)']';
          end
          [a,b]=size(y);
          deg=aqueous*70-y(a,4)*70;
          total=total-deg;
          soil=total/(70/kd+masssoil);
          aqueous=soil/kd;
          y0=[y(a,1),total,y(a,3),aqueous];
          tspan=[t(a),t(a)+cyclelen];
          m=0;
      end
        n=1;
  end
  input2;
  masscry=total-(1500*70+1500*kd*masssoil);
  soil=total/(70/kd+masssoil);
  aqueous=soil/kd;
  y0=[y(a,1)*0.1,total,y(a,3)*0.1,aqueous];
  tspan = [t(a),t(a)+cyclelen];

end
plot(t,y);
```

Crystal

```
global kd masssoil total masscry ttemp2 n ytemp2 cycle ttemp ytemp m

Y=0.48;      %umol X/umol DNT (from stoichiometry)
Ks=10;       %umol DNT/L
k=4.92;      %umol DNT/(umol X*d)
b=0.1;       %l/d
Yn=1.63;     %umol NO2/umol DNT
Vw=70;       %L
S=1500;      %umol DNT/L (solubility)

%y(1) is X(umolX/L)
%y(2) is M(total DNT, umol)
%y(3) is N(umolNO2/L)

j=0;
t1=0+t(length(t));

if cycle==1
   x0=500;
   tstop=log((masscry*Y/Vw+x0)/x0)/(Y*k*S/(Ks+S)-b);
else
   x0=y(length(y),1)*0.1;
   tstop=log(((masscry*Y)/Vw+x0)/x0)/(Y*k*S/(Ks+S)-b);
   tstop=tstop+t(length(t));
end

while t1<=tstop
   if cycle==1
      x=x0*exp((Y*k*S/(Ks+S)-b)*t1);
      no2=Yn*(x-x0)/Y;
   else
      x=x0*exp((Y*k*S/(Ks+S)-b)*(t1-t(length(t))));
      no2=Yn*(x-x0)/Y+y(length(y),3)*0.1;
   end
   totalnew=total-(x-x0)/Y*70;
   j=j+1;
   ytemp(j,1)=x;
   ytemp(j,2)=totalnew;
   ytemp(j,3)=no2;
   ytemp(j,4)=S;
   ttemp(j,1)=t1;
   t1=t1+0.005;
end
```

Nocrystals

```
function yprime=nocrystals(t,y)

global masssoil kd total

Y=0.48;     %umol X/umol DNT (from stoichiometry)
Ks=10;      %umol DNT/L
k=4.92;     %umol DNT/(umol X*d)
b=0.1;      %l/d
Yn=1.63;    %umol NO2/umol DNT
Vw=70;      %L

%y(1) is X(umolX/L)
%y(2) is M(total mass,umol)
%y(3) is N(umolNO2/L)
%y(4) is S(umolDNT/L)

yprime=zeros(4,1);
yprime(1)=[Y*k*y(1)*y(4)/(Ks+y(4))-b*y(1)];
yprime(2)=[(-(k*y(1)*y(2))/(kd*masssoil+Vw))/(Ks+y(2)/(kd*masssoil+Vw))*Vw];
yprime(3)=[Yn*k*y(1)*y(4)/(Ks+y(4))];
yprime(4)=[-k*y(1)*y(4)/(Ks+y(4))];
```

Input Files

```
%input1
loadrate=5;
total=209423;




%input2
global cycle total

if cycle==1
   total=209423;
elseif cycle==2
   total=209423;
elseif cycle==3
   total=209423;
elseif cycle==4
   total=209423;
elseif cycle==5
   total=209423;
elseif cycle==6
   total=209423;
elseif cycle==7
   total=209423;
elseif cycle==8
   total=209423;
elseif cycle==9
   total=209423;
else
   total=209423;
end
```

APPENDIX II

This appendix contains the experimental data for determining the partition

coefficients for 2,4-DNT and 2,6-DNT.

Determination of 2,4-DNT and 2,6-DNT concentration on BAAP soil

2,4-DNT Calibration Curve	y=490199x-940556	2,4-DNT Extraction Efficiency	0.948
2,6-DNT Calibration Curve	y=450447x+1850557	2,6-DNT Extraction Efficiency	1

Volume CAN (ml)	0.4
Soil Sample Volume (ml)	0.3
Volume Medium in Reactors (ml)	200

Resuspend Volume (mL)	3.0
Soil Volume from Slurry (ml)	30

2,4-DNT

	Soil Mass/Volume (g/ml)	Mass of Soil (g)	Area	Average Area	Concentration (uM)	Concentration (ug/g)	Concentration (efficiency)	Concentration (uM/kg)
Slurry 1	0.229	0.069	6293970	11670535	25.73	27.30	28.80	158.237
			7452978					
			2368007					
			10627548					
			9410035					
			338706671					
Slurry 2	0.208	0.063	12110421	11100649	24.56	28.61	30.18	165.832
			9664661					
			121192508					
			13050667					
			9527590					
			10058049					
Slurry 3	0.207	0.062	11190868	10278014	22.89	26.87	28.35	155.749
			108400077					
			121147094					
			10490131					
			8335635					
			8664277					

	Soil Mass/Volume (g/ml)	Mass of Soil (g)	Area	Average Area	Concentration (uM)	Concentration (ug/g)	Concentration (efficiency)	Concentration (uM/kg)
Slurry 4	0.230	0.069	9416636	13030662	28.50	30.11	31.77	174.540
			10565935					
			12127397					
			13400259					
			18108668					
			14565075					

2,6-DNT

	Soil Mass/Volume (g/ml)	Mass of Soil (g)	Area	Average Area	Concentration (uM)	Concentration (ug/g)	Concentration (Corrected for efficiency)	Concentration (uM/kg)
Slurry 1	0.229	0.069	9656434	4301574	5.44	5.77	5.77	31.728
			4465866					
			9249941					
			3165178					
			5388301					
			2208726					
Slurry 2	0.208	0.063	3530380	3345538	3.32	3.87	3.87	21.241
			2669085					
			3309696					
			3341762					
			2409541					
			4812765					

	Soil Mass/Volume (g/ml)	Mass of Soil (g)	Area	Average Area	Concentration (uM)	Concentration (ug/g)	Concentration (Corrected for efficiency)	Concentration (uM/kg)
Slurry 3	0.207	0.062	3029699	3871324	4.49	5.27	5.27	28.943
			7075711					
			4066105					
			3362271					
			3022994					
			2671164					
Slurry 4	0.230	0.069	3077314	3563783	3.80	4.02	4.02	22.081
			2336120					
			3629121					
			4468012					
			3797446					
			4074686					

Determination of 2,4-DNT and 2,6-DNT concentration in aqueous phase for BAAP soil

2,4-DNT Calibration Curve	y=490199x-940556	
2,6-DNT Calibration Curve	y=450447x+1850557	

MW 2,4 and 2,6 DNT	182
Density DCM (g/ml)	1.325
Denisty aqueous (g/ml)	1.00

2,4-DNT

	Mass Aqueous (g)	Mass DCM (g)	Area	Average Area	Concentration (uM) (DCM)	Concentration (uM) (Aq)	Kd (L/kg)	Average Kd (L/kg)	Stdev
Slurry 1	27.0723	3.55	105716498 108009154	106862826	219.92	21.76	7.27	7.53	0.20
Slurry 2	27.5639	3.8162	1036613420 101707200	1026660310	211.34	22.08	7.51		
Slurry 3	26.7156	3.9762	84480432 92895762	88688097	182.84	20.54	7.58		
Slurry4	26.8244	3.8165	102718571 100814201	101766386	209.52	22.50	7.76		

2,6-DNT

	Mass Aqueous (g)	Mass DCM (g)	Area	Average Area	Concentration (uM) (DCM)	Concentration (uM) (Aq)	Kd (L/kg)	Average Kd (L/kg)	Stdev
Slurry 1	27.0723	3.55	46048214 47449271	46748743	99.67	9.86	3.22	2.82	0.57
Slurry 2	27.5639	3.8162	41627274 40812389	41219832	87.40	9.13	2.33		

	Mass Aqueous (g)	Mass DCM (g)	Area	Average Area	Concentration (uM) (DCM)	Concentration (uM) (Aq)	Kd (L/kg)	Average Kd (L/kg)	Stdev
Slurry 3	26.7156	3.9762	34305207 37543152	35924180	75.64	8.50	3.41		
Slurry4	26.8244	3.8165	40804837 42059323	41432080	87.87	9.44	2.34		

Determination of 2,4-DNT and 2,6-DNT concentration on VAAP soil

2,4-DNT Calibration Curve	y=490199x-940556	2,4-DNT Extraction Efficiency 0.923
2,6-DNT Calibration Curve	y=450447x+1850557	2,6-DNT Extraction Efficiency 1.000

Volume CAN (ml)	0.4
Soil Sample Volume (ml)	0.3
Volume Medium in Reactors (ml)	200

2,4-DNT

	Soil Mass/Volume (g/ml)	Mass of Soil (g)	Area	Average Area	Concentration (uM)	Concentration (ug/g)	Concentration (efficiency)	Concentration (uM/kg)
Slurry 1	0.150	0.045	22167264	26779347	56.55	91.54	99.18	544.948
			26207544					
			25488540					
			27093271					
			298503348					
			29869115					
Slurry 2	0.143	0.043	27095026	25618977	54.18	91.82	99.47	546.565
			25044806					
			27453475					
			27101087					
			22379290					
			24640175					

	Soil Mass/Volume (g/ml)	Mass of Soil (g)	Area	Average Area	Concentration (uM)	Concentration (ug/g)	Concentration (Corrected for efficiency)	Concentration (uM/kg)
Slurry 3	0.147	0.044	211108250	22789911	48.41	79.66	86.31	474.217
			23896330					
			23132655					
			22231061					
			23855833					
			22515337					
Slurry 4	0.148	0.044	23005943	232234628	49.32	80.99	87.75	482.123
			21398818					
			25713032					
			20200579					
			25859754					
			23229644					

2,6-DNT

	Soil Mass/Volume (g/ml)	Mass of Soil (g)	Area	Average Area	Concentration (uM)	Concentration (ug/g)	Concentration (Corrected for efficiency)	Concentration (uM/kg)
Slurry 1	0.150	0.045	139982620	18008060	35.87	58.07	58.07	319.057
			173558643					
			17291306					
			179907585					
			20664237					
			20843971					

	Soil Mass/Volume (g/ml)	Mass of Soil (g)	Area	Average Area	Concentration (uM)	Concentration (ug/g)	Concentration (Corrected for efficiency)	Concentration (uM/kg)
Slurry 2	0.143	0.043	19309899	19612366	39.43	66.82	66.82	367.146
			17947180					
			20340614					
			19370052					
			20022138					
			20684311					
Slurry 3	0.147	0.044	15210167	16538165	32.61	53.66	53.66	294.817
			17234380					
			17202262					
			16185377					
			16854727					
			16542077					
Slurry 4	0.148	0.044	175227 25	171835 29	34.04	55.90	55.90	307.146
			15753527					
			18329544					
			15552071					
			18760252					
			17183055					

Determination of 2,4-DNT and 2,6-DNT concentration in aqueous phase for VAAP soil

2,4-DNT Calibration Curve	y=490199x-940556
2,6-DNT Calibration Curve	y=450447x+1850557

MW 2,4 and 2,6 DNT	182
Density DCM (g/ml)	1.325
Denisty aqueous (g/ml)	1.00

2,4-DNT

	Mass Aqueous (g)	Mass DCM (g)	Area	Average Area	Concentration (uM) (DCM)	Concentration (uM) (Aq)	Kd (L/kg)	Average Kd (L/kg)	Stdev
Slurry 1	11.4291	1.8311	605969663 618658577	612314120	1251.03	151.27	3.60	3.52	0.39
Slurry 2	9.5975	1.9002	500837694 387327444	444082569	907.84	135.65	4.03		
Slurry 3	10.5092	1.8804	543056959 553976932	548516946	1120.89	151.37	3.13		
Slurry4	11.1481	2.2849	462069013 462926380	462497697	945.41	146.24	3.30		

2,6-DNT

	Mass Aqueous (g)	Mass DCM (g)	Area	Average Area	Concentration (uM) (DCM)	Concentration (uM) (Aq)	Kd (L/kg)	Average Kd (L/kg)	Stdev
Slurry 1	11.4291	1.8311	426111584 435941443	431026514	952.78	115.21	2.77	2.91	0.45
Slurry 2	9.5975	1.9002	350701982 272366331	311534157	687.50	102.73	3.57		
Slurry 3	10.5092	1.8804	382743736 389228099	385985918	852.79	115.16	2.56		
Slurry4	11.1481	2.2849	328586313 329943199	329264756	726.87	112.44	2.73		